MODIFIED POLYETHYLENE GLYCOL AS A POTENTIAL MATERIAL FOR CO_2 CAPTURE

MAHSA SADEGH POUR

FACULTY OF ENGINEERING

UNIVERSITY OF MALAYA

KUALA LUMPUR

2019

MODIFIED POLYETHYLENE GLYCOL AS A POTENTIAL MATERIAL FOR CO_2 CAPTURE

MAHSA SADEGH POUR

THESIS SUBMITTED IN FULFILMENT OF THE REQUIREMENTS FOR THE DEGREE OF DOCTOR OF PHLOSOPHY

FACULTY OF ENGINEERING

UNIVERSITY OF MALAYA

KUALA LUMPUR

2019

UNIVERSITY OF MALAYA

ORIGINAL LITERARY WORK DECLARATION

Name of Candidate: Mahsa Sadegh pour

Matric No: KHA130027

Name of Degree: Doctor of Philosophy

Title of Project Paper/Research Report/Dissertation/Thesis ("this Work"):

MODIFIED POLYETHYLENE GLYCOL AS A POTENTIAL MATERIAL FOR CO_2 CAPTURE

Field of Study: Purification & Separation Processes

I do solemnly and sincerely declare that:

(1) I am the sole author/writer of this Work;
(2) This Work is original;
(3) Any use of any work in which copyright exists was done by way of fair dealing and for permitted purposes and any excerpt or extract from, or reference to or reproduction of any copyright work has been disclosed expressly and sufficiently and the title of the Work and its authorship have been acknowledged in this Work;
(4) I do not have any actual knowledge nor do I ought reasonably to know that the making of this work constitutes an infringement of any copyright work;
(5) I hereby assign all and every rights in the copyright to this Work to the University of Malaya ("UM"), who henceforth shall be owner of the copyright in this Work and that any reproduction or use in any form or by any means whatsoever is prohibited without the written consent of UM having been first had and obtained;
(6) I am fully aware that if in the course of making this Work I have infringed any copyright whether intentionally or otherwise, I may be subject to legal action or any other action as may be determined by UM.

Candidate's Signature Date:

Subscribed and solemnly declared before,

Witness's Signature Date:

Name:

Designation:

MODIFIED POLYETHYLENE GLYCOL AS A POTENTIAL MATERIAL FOR CO_2 CAPTURE

ABSTRACT

Carbon dioxide gas from the utilization of fossil fuel is one of the most significant contributors to greenhouse effect. Absorption process by various solvents is one of the common techniques to capture CO_2. Poly ionic liquids (PILs) have shown to be potential solvent for CO_2 absorption. Thus, in this work new PILs were synthesized and later used for CO_2 absorption process. Two types of water soluble PILs polyethylene glycol-di choline chloride (PEG-$(ChCl)_2$) and polyethylene glycol-di imidazolium iodide (PEG-$(mImidI)_2$) were synthesized. The synthesis was performed through modification of two molecular weights of poly ethylene glycol (PEG); 400 and 600, to be used as solvents for CO_2 capture. The synthesized polymers were characterized using ^{1}H-NMR and FT-IR. Presence of choline chloride and methyl imidazolium iodide in the final product were confirmed with ^{1}H-NMR spectra. Moreover, the thermal stability of the prepared polymers were defined by thermal gravimetric analysis and the results showed that the synthesized polymers have high thermal stability. Viscosity and densities of aqueous solutions of modified polymers were also measured. Furthermore, CO_2 absorption using the modified poly ionic liquids was conducted at pressures ranging from 10 to 13 bars and temperatures ranging from 30 to 70 ºC. PEG 400-$(ChCl)_2$, PEG 600-$(ChCl)_2$, PEG 400-$(mImidI)_2$ and PEG 600-$(mImidI)_2$ with a concentration of 0.03 M showed CO_2 loading of 16.33, 15.53, 18.89 and 18.38 mol CO_2/mol PIL respectively. These results showed 20% increase for PEG (400-600)-$(ChCl)_2$ and up to 30% for PEG (400-600)-$(mImidI)_2$ as compared to unmodified PEGs. In order to study on the concentration impact, three different concentration of PEG 400-$(mImidI)_2$ from 0.03 M to 0.1 M were used for CO_2 absorption at pressure ranging from 5 to 13 bar and constant temperature. Henry's constants were also determined and the values obtained at temperature 30 ˚C were 30.11, 28.89, 24.02 and 24.38 for PEG 400-$(ChCl)_2$, PEG 600-$(ChCl)_2$, PEG 400-$(mImidI)_2$ and PEG 600-$(mImidI)_2$, respectively. Enthalpy of the absorption were also obtained and reported. The linear CO_2 absorption and decreasing trend

for values of heat of absorption confirms the presence of physical CO_2 absorption mechanism for the synthesized PILs. In addition, pressure and temperature swing techniques were used to investigate recyclability and regeneration of aqueous polymers and the result showed the synthesized PILs showed great stability on theirs sorption capacity after three cycles of regeneration with only 15% reduction in CO_2 loading capacity.

Keywords: Poly ionic liquids, Polyethylene glycol, Choline chloride, Methyl imidazole, CO_2 absorption.

POLIETILENA GLIKOL YANG DIUBAHSUAI SEBAGAI BAHAN BERPOTENSI BAGI PEMERANGKAPAN GAS KARBON DIOKSIDA

ABSTRAK

Gas karbon dioksida (CO_2) yang terhasil daripada penggunaan bahan api fosil merupakan salah satu penyumbang utama kepada kesan rumah hijau. Proses penyerapan oleh pelbagai pelarut merupakan salah satu teknik yang lazim digunakan untuk memerangkap CO_2. Cecair poli ionik (PILs) telah menunjukkan potensi sebagai pelarut bagi penyerapan CO_2. Maka, di dalam kajian ini, PILs baharu telah disintesis dan kemudiannya digunakan bagi proses penyerapan CO_2. Dua jenis cecair PILs larut air iaitu polietilena glikol-kolina klorida (PEG-$(ChCl)_2$) dan polietilena glikol-imidazol iodida (PEG-$(mImidI)_2$) telah disintesis. Proses sintesis telah dijalankan melalui pengubahsuaian polietilena glikol (PEG) dengan dua jisim molekul iaitu 400 dan 600, untuk digunakan sebagai pelarut bagi memerangkap CO_2. Polimer yang disintesis dicirikan menggunakan ^{1}H-NMR dan FT-IR. Kehadiran kolina klorida dan metil imidazol iodida di dalam produk akhir telah disahkan dengan menggunakan spektrum ^{1}H-NMR. Selain itu, kestabilan terma bagi setiap polimer yang disediakan telah dikenalpasti melalui analisis gravimetri terma dan keputusan menunjukkan bahawa polimer yang disintesis mempunyai kestabilan terma yang tinggi. Kelikatan dan ketumpatan larutan akueus polimer yang diubahsuai juga diukur. Seterusnya, penyerapan CO_2 menggunakan PILs yang diubahsuai telah dijalankan pada julat tekanan di antara 10 hingga 13 bar dan julat suhu di antara 30 hingga 70ºC. PEG 400-$(ChCl)_2$, PEG 600-$(ChCl)_2$, PEG 400-$(mImidI)_2$ dan PEG 600-$(mImidI)_2$ dengan kepekatan 0.03M menunjukkan muatan CO_2, masing-masing sebanyak 16.33, 15.53, 18.89 dan 18.38. Keputusan ini menunjukkan peningkatan sebanyak 25% bagi PEG (400-600)-$(ChCl)_2$ dan sehingga 30% bagi PEG(400-600)-$(mImidI)_2$ berbanding PEGs yang tidak diubahsuai. Bagi mengkaji kesan ke atas kepekatan, PEG 400-$(mImidI)_2$ dengan tiga kepekatan berbeza di antara 0.03M hingga 0.01M telah digunakan bagi penyerapan CO_2 pada julat tekanan di antara 5 hingga 13 bar dan suhu malar. Pemalar Henry juga telah ditentukan dan nilai yang diperolehi pada suhu 30ºC adalah 30.11, 28.89, 24.02 dan 24.38, masing-masing bagi PEG 400-$(ChCl)_2$, PEG 600-$(ChCl)_2$, PEG 400-$(mImidI)_2$ dan PEG 600-$(mImidI)_2$. Entalpi penyerapan juga telah

diperolehi dan dilaporkan. Garis lurus bagi penyerapan CO_2 dan pola penurunan nilai haba penyerapan mengesahkan kehadiran mekanisma fizikal penyerapan CO_2 bagi PILs yang disintesis. Sebagai tambahan, teknik hayunan tekanan dan suhu telah digunakan bagi mengkaji kebolehkitar dan penjanaan semula polimer akueus. Keputusan menunjukkan bahawa PILs yang disintesis memaparkan kestabilan yang tinggi ke atas kapasiti serapan selepas 3 kitaran penjanaan semula dengan hanya pengurangan sebanyak 15% di dalam kapasiti muatan CO_2.

Kata kunci: Cecair Poli Ionik, Polietilena glikol, Kolina klorida, Metil imidazol, penyerapan CO_2.

ACKNOWLEDGEMENTS

First and foremost, I would like to express my grateful sincere gratitude and respect to my research supervisors, Prof. Dr. Mohamed Kheireddine Aroua and Assoc. Prof. Ir. Dr. Rozita for their advice, guidance, supervision and constructive comments during the long way of my PhD.

My appreciation goes to my labmates for their continuous support, encouragement and sharing.

I would also like to acknowledge the Ministry of Education (MOE) for their generous financial support under High Impact Research (HIR) grant allocation which aided me in the completion of my study. Thank you to the administrative staffs in the Department of Chemical Engineering, Faculty of Engineering for all the continuous assistance during my study.

I would like to express my heartfelt to my parents Laya and Jalil whose prayers is the secret of my success. My beloved siblings; Shiva, Neda, Mohammad and Sepideh, for their assistance and care toward completing this project.

TABLE OF CONTENTS

LIST OF FIGURES

LIST OF TABLES

LIST OF SYMBOLS AND ABBREVIATION

LIST OF SYMBOLS

V_{EC}	:	Volume of the equilibrium cell
$V_{EC.\,t}$	:	Total volume of the equilibrium cell
V_L	:	Volume of existing solution
V_{GR}	:	Volume of of the gas reservoir
$P_{GR,\,1}$	:	Initial pressure of the gas reservoir
$P_{GR,\,1}$	:	Final pressure of the gas reservoir
$P_{EC,\,1}$	:	Initial pressure of the equilibrium cell
$P_{EC,\,2}$	:	Final pressure of the equilibrium cell
K_H	:	Henry's constants
ρ	:	Density
η	:	Viscosity
ΔH	:	Enthalpy

LIST OF ABBREVIATIONS

IPCC	:	Intergovernmental panel on climate change
CCS	:	CO_2 capture and storage
PIL	:	Polymeric ionic liquid
IL	:	Ionic liquid

DMF	:	Dimethylformamide
DMSO	:	Dimethyl sulfoxide
RTIL	:	Room temperature ionic liquid
AIBN	:	Azobisisobutyronitrile
ATRP	:	Atom transfer radical polymerization
PEG	:	Poly ethylene glycol
DSC	:	Differential scanning calometric
Tg	:	Glass transition temperature
TGA	:	Thermo gravimetric analysis
SPME	:	Solid-phase microextraction
NMP	:	1-methy-2-pyrrolidinone
GTA	:	Glycerol triacetate
FT-IR	:	Fourier-transform infrared spectroscopy
NMR	:	Proton nuclear magnetic resonance
THF	:	Tetrahydrofuran
TLC	:	Thin layer chromatography
DCM	:	Dichloromethane
PCV	:	Pressure control valve

CHAPTER 1: INTRODUCTION

1.1 Background of the Study

Rapid economic growth has resulted in today's increasing demand for energy. A strong impact of this is a major rise in the use of fossil fuels (mainly coal and natural gas) which has become the main energy source since industrial revolution in the year 1750. Moreover, it is important to mention that the scientific community predicts that by the year 2030, the energy usage will increase by almost 50%, and this is when the fossil fuels will continue to supply most of the energy demands (Leung, Caramanna, & Maroto-Valer, 2014; Olivier, Bouwman, Van der Maas, & Berdowski, 1994). This huge utilization of fossil fuels has become a major concern because of their destructive impact on environment mostly related to the emission of carbon dioxide (CO_2). CO_2 which is generated through the combustion of fossil fuels (coal, petroleum and natural gas) is regarded as one of the most significant contributors to the greenhouse effect. The presence of CO_2 is a major concern due to its harmful impacts on the environment, mainly the effect of the increase in global temperature which is generally referred as global warming. The global warming will affect the environment with considerable signs such as melting of the polar ice caps, changing of sea levels and drastic changes in weather patterns. 1.9 °C increase in world's temperature by the year 2100 was predicted by the Intergovernmental panel on climate change (IPCC) (Wang, Lang, & Fan, 2013). Furthermore, the global emission of CO_2 in 2011 was 33.4 billion tonnes which is considerably more than two decades ago with 48% increase. Without urgent mitigation policies for climate change and environmental problems, it is predicted that the greenhouse gas (GHG) emission by 2030 will rise by 25-90% (Nakicenovi, Alcamo, Davis, & Vries, 2000).

Predicted harmful problems catalysed the approaches to mitigate global climate change including techniques to reduce CO_2 emission. Various methods are considered to alleviate global warming and many measures are taken in to consideration to reduce the CO_2 emissions such as the use of efficient devices to increase energy efficiency. The use of less carbon fuels including hydrogen, renewable energies (solar, bioenergy and hydropower) and natural gas and finally CO_2 capture and storage (CCS) systems. It seems impossible to use a single method to meet the IPCC target which is 50-58% CO_2 reduction by 2050 from 2000 levels. Among the above listed strategies, CCS can be more efficient and it is based on sequestration technologies which can reduce CO_2 emissions up to 90% (Change, 2015; Leung, 2014). Main steps in CO_2 sequestration technologies are; capturing, transporting and storage; First step is capturing CO_2 from different sources like industrial flue gas and natural gas streams, then sending purified CO_2 to the storage and finally storing the CO_2 gas in managed conditions to geological forms (Fahrenkamp-Uppenbrink, 2015).

CO_2 which is formed during combustion process is directly needed to deal with. There are three main CO_2 capture processes, namely, post-combustion, pre-combustion and oxy fuel combustion. Post-combustion is defined as the process which removes CO_2 from the flue gas after combustion has occurred. In pre-combustion the fuel is pretreated under low oxygen level to form a syngas. Syngas mostly includes CO and H_2 and there is no other pollutant gases. In oxy fuel combustion, oxygen is used for combustion. Using oxygen instead of air decreases the amount of nitrogen in gas and the main gases after combustion are CO_2, SO_2 and water (Farzaneh, McLellan, & Ishihara, 2016; Leung, 2014). Among the above methods, post-combustion is preferred because of its ease of application in

systems and also its cost which is relatively cheaper than two other technologies mentioned.

There are several methods in the post-combustion technology which can be applied for CO_2 capture namely: absorption process (chemical, physical) which includes using liquid sorbent to capture CO_2 from flue gas, adsorption process which uses a solid sorbent to capture CO_2 on its surface, membrane technology which includes using membrane to separate CO_2 from other components of the flue gas and cryogenic distillation method which is separation of gas using distillation at a very low temperature and high pressure. The cryogenic distillation method produces high purity gases but is energy-intensive (Yang, Fan, Gupta, Slimane, Bland, & Wright, 2008).

Amine-based absorption is undoubtedly the most common method for CO_2 capture because of their reactivity with CO_2, low price and ease of preparation. However, this method involves several difficulties related to their corrosive nature, poor thermal stability, high volatility and high energy demand for regeneration (Z. Liang, Fu, Idem, & Tontiwachwuthikul, 2016; Yang, Fan, Gupta, Slimane, Bland, & Wright, 2008).

Therefore, the development of a highly efficient liquid sorbent is urgently needed. Another highly researched solvents for CO_2 capture is ionic liquids (ILs). The unique characteristics of ionic liquids (ILs) represented by wide liquid range, negligible vapor pressure, high thermal stability, flexible characteristics and above all, high CO_2 solubility makes them the ideal alternatives for CO_2 absorption. However, a notable disadvantage of ionic liquids is their high viscosity and low CO_2 capacity (J. Tang, Tang, Sun, Radosz, & Shen, 2005c). Despite that, this shortcoming can be fixed by choosing appropriate cations and anions. Ionic liquids can be covalently bonded to make polymeric ionic liquids (PILs). These compounds demonstrate better performance in CO_2 capture (Hasib-ur-Rahman, Siaj, & Larachi, 2010; Hirao, Ito, & Ohno, 2000; Lutz, 2008; G.-J. Zhang,

2014; Zhao, Dong, & Zhang, 2012) Recently, it has been found that PILs, which are monomer-generated polymers with ionic liquid moieties, showed higher CO_2 sorption and desorption potential as compared to ionic liquids at room temperature (Blasig, Tang, Hu, Shen, & Radosz, 2007; Hirao, 2000; Lu, Yan, & Texter, 2009; Alexander, Shaplov, Marcilla, & Mecerreyes, 2015; Uchytil, Schauer, Petrychkovych, Setnickova, & Suen, 2011). Studies have also shown that CO_2 sorption by poly ionic liquids requires much less time to attain an equilibrium state, compared to room temperature ionic liquids (Tang, Tang, Sun, & Radosz, 2005). It is also reported that among the solvents for CO_2 capture poly ethylene glycol (PEG) 300 is the best because of the high CO_2 solubility and high stability, low solvent loss, and low desorption energy (Mirzaei, Shamiri, & Aroua, 2015).

There are two main methods for synthesizing PILs. These are; direct polymerization of IL monomers and chemical modification of existing polymers (Sadeghpour, Yusoff, & Aroua; Yuan & Antonietti, 2011). These synthesized PILs and their modified derivatives with green solvents (binary mixtures or grafted ones) can be a good candidate for CO_2 capture (Amooghin, 2010; Aschenbrenner & Styring, 2010; Car, Stropnik, Yave, & Peinemann, 2008).

1.2 Problem Statement

Currently, CO_2 emission from the gas streams is one of the most significant issues which causes greenhouse effect. Environmental aspects are the main motivation for research on energy efficient processes. Existence of CO_2 in a gas stream reduces the quality and calorific value of the product. Furthermore, this phenomenon may result in corrosive gas streams. Consequently, efficient materials are needed to remove CO_2 from gas streams. The most common sorbents for CO_2 capture are amine-based solvents which have considerable disadvantages like toxicity, corrosiveness and high energy

consumption for regeneration. Another potential solvents such as ILs have limitations namely low capacity and high viscosity as well as having low and less CO_2 uptake as compared to their poly ionic liquids. Moreover, ionic liquids are expensive and direct polymerization of them would be costly, thus grafting of ionic liquids to existing polymer might be a good candidate for CO_2 capture. By adding ILs to polymers, it is possible to have high CO_2 capacity sorbents with a lower cost. The main aim and novelty of this study is to synthesis novel materials with new method as potential sorbents for CO_2 capture. The solubility study of CO_2 in the synthesized materials were conducted. Henry's constant were also determined. Henry's constant plays a vital role in environmental chemistry. The knowledge of K_H value of a gas at a given temperature can be helpful in calculating the solubility at the specific temperature.

1.3 Scope and Research Objectives

In this work, modification of polymer by grafting an existing polymer using methyl imidazole/choline chloride were carried out. PILs can be prepared by the choice of cations which has great effect on the solubility of the final PIL. Ammonium and imidazolium cations were selected in terms of cation. Imidazolium is selected because of its impact on CO_2 sorption and also ease of synthesis. In addition, choline chloride is chosen as cholinium-based ammonium salt because of its high impact on CO_2 sorption. In this work, choline chloride and methyl-imidazole were used.

In terms of back-bone, poly ethylene glycol (PEG) which showed a high solubility of carbon dioxide was chosen. Polyethylene glycol could be an excellent choice, because this material is environmentally friendly, inexpensive, nontoxic and suitable for chemical reactions. In addition, polyethylene glycol and its derivatives are known to be thermally stable and recyclable. Moreover, the advantages of nontoxicity, high stability, low solvent

loss and low desorption energy of PEG may outweigh its lower absorption capacity compared to the amine-based solvents and making it a potentially advantageous solvent for industrial carbon dioxide absorption processes.

In order to modify PEG, tosylation method was used because of its convenience and efficiency. In tosylation method, the conversion of alcohols to tosylates occurs, using tosyl chloride by replacing an -OH group which will be converted to the good leaving group.

To the best of our knowledge, no work has been reported on the modification of polyethylene glycol with choline chloride/methyl imidazolium iodide. Therefore, using the choline chloride as an ammonium salt and methyl imidazole for the modification of PEG which has substantial CO_2 solubility would make good potential poly ionic liquids for CO_2 capture.

The modified PILs were characterized by FT-IR, ^{1}H-NMR. Thermal stabilities of the polymers were tested by thermo gravimetric analysis (TGA). Furthermore, densities and viscosities of modified polymers were also determined. The synthesized polymers were then applied as solvents in the form of aqueous solutions for CO_2 absorption.

Therefore the objectives of this work are as follows:

i. To synthesize new poly ionic liquids with choline chloride/methyl-imidazole as cation and poly ethylene glycol as backbone and then to determine the physical properties of the synthesized PILs such as viscosity, density and thermal stability.

ii. To determine the CO_2 solubility in PEG (400-600)-$(ChCl)_2$/PEG (400-600)-$(mImidI)_2$ at various pressures (10-13 bar) and temperatures (30-70 ˚C).

iii. To obtain the Henry's constant (H) and heat of absorption for CO_2 capture of the synthesized PILs.

iv. To investigate the regeneration and recyclability of the synthesized PILs as CO_2 absorption solvent.

1.4 Thesis Outlines

This thesis contains five chapters. The current chapter is an introduction that describes the background and the scope of the research which include the objectives and problem statement.

Chapter two presents the literature review of various topics related to absorption by various solvents in particular poly ionic liquids.

Chapter three presents the materials and complete procedures of the modification and synthesis steps of PILs and application of prepared PILs for CO_2 capture.

Chapter four presents the results and discussion of synthesis and characterization of PILs and also application of synthesized PILs for CO_2 capture.

Chapter five presents the conclusion, research contribution and suggestions for future work.

CHAPTER 2: LITERATURE REVIEW

2.1 Introduction

This chapter presents an overview of research studies conducted on PILs for CO_2 capture technology which mainly focuses on detailed review of PILs synthesis, modification and their application as membranes, absorbents and adsorbents. The effect of PILs' structure on CO_2 capture is also discussed. In addition, the thermal properties of PILs and the effect of temperature and pressure on the CO_2 sorption are also detailed.

Recently, carbon dioxide capture using various CO_2 capture technologies has continued to gain considerable attention due to the need to reduce carbon emissions from the generated flue gas. CO_2 generation through the combustion of fossil fuels (coal, petroleum and natural gas) is regarded as one of the most significant contributors to greenhouse effect. The presence of CO_2 in a gas stream reduces the quality and calorific value of the product as well as resulting in corrosive gas stream as it mentioned earlier in the previous chapter. Therefore, the suitable techniques to remove CO_2 from gas streams have become a major research endeavor in the scientific world (Aziz, Yusoff, & Aroua, 2012; Feng, 2010; Muhammad Hasib-ur-Rahman, Siaj, & Larachi, 2012; Raeissi & Peters, 2008; Soosaiprakasam & Veawab, 2008).

The traditional methods of CO_2 capture, involving absorption by aqueous amine solutions and their mixtures, are the most utilized technology for CO_2 capture. It can be said that using amine as CO_2 capture solvents are the only commercially available method in the absorption techniques. Nevertheless, this method have major limitations which are associated with the high energy consumption through solvent regeneration, insufficient CO_2 sorption, corrosiveness, poor thermal stability and high solvent losses (Liang , 2016).

There are various methods which have been applied in industries to remove CO_2 from flue gas, namely: absorption, adsorption, cryogenic, membrane, and biological fixation (Choi, Seo, Jang, Jung, & Oh, 2009; Li , 2011). The absorption process is generally used for treatment of gas streams in chemical industries.

2.1.1 Comparison of Various Solvents for CO_2 Absorption

The conventional method for CO_2 absorption is using aqueous alkanolamine solutions as solvents. However, these solvents and their mixtures cause some problems such as: corrosion in systems which may impose additional cost, difficulty in regeneration and recycling process because of amines degradation at high temperatures and high solvent loss because of volatile property of alkanolamines (Feng , 2010). The most reputed amine based absorbent is monoethanolamine (MEA), a primary amine, which has high affinity to CO_2 and above all, has a lower cost of production. Despite the mentioned benefits this solvent suffers from some limitations such as low CO_2 capacity and corrosion problems (Liang , 2015; Rochelle, Bishnoi, Chi, Dang, & Santos, 2001). Another promising solvent for CO_2 capture is ammonia (NH_3) which has higher CO_2 capacity compared to MEA. However, there are some limitations like its low CO_2 sorption rate and high volatility.

To get sorbents with better features, blending of a various solvents is considered as another method to improve CO_2 sorption (Hagewiesche, Ashour, Al-Ghawas, & Sandall, 1995; Zhu, Fang, Lv, Wang, & Luo, 2011). By doing this, it is possible to have mixtures with combination of good properties of different solvents. For example, different kind of mixtures was studied such as diethanolamine (DEA)- N-methyldiethanolamine (MDEA), MEA–MDEA and 2-amino-2-methyl-1-propanol (AMP)- piperazine (PZ). Results were reported to be good and close to commercial level for PZ–potassium carbonate (K_2CO_3).

For instance, by adding 2 mass% piperazine to 28 mass% AMP, the enhancement factor is increased to 45.1 (Samanta & Bandyopadhyay, 2009; Sema , 2012).

The modification of amines structure could give great impact on their CO_2 capture properties. For instance by modification of MEA and formation of AMP, it showed higher CO_2 sorption than MEA (Chakraborty, Astarita, & Bischoff, 1986). Therefore, modification of amines structure could resulted in more desirable sorbents (Liang, 2016; Robinson, McCluskey, & Attalla, 2011)

Another well-researched potential solvent for CO_2 capture are ILs. ILs are defined as liquid organic salts at temperature less than 100 ºC. ILs have shown considerable properties like wide liquid range, negligible vapor pressure, high thermal stability, flexible characteristics and generally have high CO_2 solubility (Hasib-ur-Rahman, Siaj, & Larachi, 2010). These characteristics make them the ideal alternatives for CO_2 absorption. Imidazolium based ILs were the most common ILs tested for CO_2 capture since they were physical absorbents and their regeneration process have low energy consumption (Cadena, 2004). However, due to low capacity for CO_2 absorption with imidazolium sorbents, other sorbents i.e., task special ILs with functionalizing imidazolium cations with amine moiety were proposed to improve CO_2 absorption capacity. For example, modified 3-n-butyl-3-methylimidazolium tetrafluoroborate ([3Amim][BF_4]) showed better CO_2 capacity after functionalization (Gurkan, 2010; Sánchez, Meindersma, & De Haan, 2007).

Other ionic liquid, 1-butyl-3-methylimidazolium hexafluorophosphate ([bmim][PF_6]), was also studied, and it was reported that CO_2 was considerably soluble in this ionic liquid. (Blanchard, Hancu, Beckman, & Brennecke, 1999). In another study, the (2-hydroxyethyl)-tri methyl ammonium (S)-2-pyrrolidine-carboxylic acid salt ([Choline][Pro]) and a mixture of [Choline][Pro]/PEG 200 were used for CO_2 capture and

the results showed that the PEG 200 has extremely good impact on CO_2 absorption (Li, 2008).

It is also found that polyethylene glycol 300 is an effective sorbent for CO_2 capture (Mirzaei , 2015). As mentioned earlier although MEA has higher CO_2 capacity as compared to PEG, PEG has great properties such as high stability, low solvent loss, good regeneration and many more advantages which are mentioned previously. These properties make PEG a great candidate for CO_2 capture.

Polymeric ionic liquids (PILs) which are covalently bonded ILs show higher and faster CO_2 uptake as compared to their origin ILs. PILs, which are monomer-generated polymers with ionic liquid moieties, showed better CO_2 sorption and desorption potential as compared to ionic liquids at room temperature (Blasig, 2007; Chi, Hong, Jung, Kang, Kang, & Kim, 2013; Hirao, Ito, & Ohno, 2000; Lu, 2009; Alexander S. Shaplov, 2015; Uchytil, 2011). Previous studies have also shown that CO_2 sorption by poly ionic liquids requires much less time to attain an equilibrium state, as compared to room temperature ionic liquids (Tang, Sun, & Radosz, 2005).

The advantages and disadvantages of previous technologies compared to this work are shown in Table 2.1. In the next section synthesis of PILs and their application as CO_2 sorbent in different systems such as membrane, absorption and adsorption will be discussed in detail.

Table 2.1: Comparison on various technologies

Technologies	Advantages	Disadvantages	Ref
Amin based solvents	High CO_2 solubility	Toxicity Corrosiveness High energy consumption for regeneration	(Liliana, Tomé, Mecerreyes, Freire, Rebelo, & Marrucho, 2013a)
Ionic liquids	Environment friendly negligible vapor pressure	Low capacity High viscosity Less CO_2 uptake as compared to their poly ionic liquids, High cost	(Ahmady, Hashim, & Aroua, 2011a)
Poly ionic liquids	High CO_2 solubility Fast CO_2 solubility Environment friendly negligible vapor pressure	Sometimes synthesis steps may have difficulties	(Bhavsar, Kumbharkar, & Kharul, 2012a)

2.2 Synthesis and Polymerization of PILs for CO_2 Capture

ILs can be covalently bonded or existing polymer can be modified to produce PILs. PILs include a minimum of one ionic center similar to ILs. Most PILs contain cations, namely imidazolium, pyrrolidinium, pyridinium, ammonium, or phosphonium. These cations may either be bonded to the main polymer or exist as free opposite ions. In addition, a fine cation-anion mix enables PILs to be used as a tailor-made solvent successfully (González-Álvarez , 2012; Alexander S Shaplov , 2011). There are two main methods to synthesize PILs. These are direct polymerization of IL monomers and chemical modification of existing polymers (Yuan & Antonietti, 2011). PILs have considerably higher CO_2 sorption rate than ionic liquids and exhibit several times more CO_2 absorption than ionic liquid monomers. By varying the cations and anions the solubility of CO_2 can be optimized in PILs (An, Wu, Li, & Zhu, 2007; González-Álvarez, 2013; Pont, Marcilla, De Meatza, Grande, & Mecerreyes, 2009; Tang, Sun, & Plancher, 2005; Yuan, Mecerreyes, & Antonietti, 2013).

In the direct polymerization of PILs for CO_2 capture, the corresponding IL is mostly dissolved in dimethyl formamide (DMF), dimethyl sulfoxide (DMSO), and acetonitrile. ILs are soluble in DMF, DMSO and acetonitrile, but normally insoluble in water, dichloromethane, and toluene (Salamone, Israel, Taylor, & Snider, 1973).

PILs can also be synthesized by the reaction of two reactants instead of direct polymerization of monomers. For example, the synthesis of poly (1-ethyl-4-vinylpyridinium bromide) poly (ViEtPy+Br-), can be carried out by reacting 4-vinylpyridine with ethyl bromide instead of using a monomer quaternary salt. In an experiment, this procedure obtained 25.6 g of poly (ViEtPy+Br-), which constitutes 63% of the product (Marcilla , 2005).

2.2.1 PILs for Membrane Absorption (Permeability and Solubility)

Membrane process is utilized to separate certain materials, especially CO_2, from gas streams in different systems. The process can be divided into two categories, namely, the gas separation membrane and the gas absorption membrane (Luis, Van Gerven, & Van der Bruggen, 2012; Simons, 2010; Yu, Yang, Yan, & Tu; Zhang, Qu , Sha, Wang, & Yang, 2015). In the gas separation membrane, the preferential permeation of the membrane allows the constituents of the mixture to diffuse through the membrane (Alothman, Unsal, Habila, Tuzen, & Soylak, 2015; Hall, 2015). The most important aspect of the design of these membranes is their selectivity and permeability (Fu, Sanders, Kulkarni, Wenz, & Koros, 2015; Swaidan, Ghanem, & Pinnau, 2015; Liliana, Tomé, Gouveia, Freire, Mecerreyes, & Marrucho, 2015). As for the gas absorption membrane, it works as a base of micro porous solid membrane between the gas and liquid flows. Here, the CO_2 is diffused across the membrane and is then recovered by the liquid absorbent. Overall, the absorption system in membrane gave better removal results as compared to the separation systems membrane (Brunetti, Scura, Barbieri, & Drioli, 2010; Gupta, Coyle, & Thambimuthu, 2003; Meisen & Shuai, 1997; Mondal, Balsora, & Varshney, 2012).

The current CO_2 separation membrane schemes mainly employ polymeric membranes given the fact that, in terms of cost, they are relatively cheaper. They are also mechanically stable at high pressures and easily conform to both flat and hollow fibers. However, polymeric membranes commonly have problems associated with either low permeability or low selectivity (Bahukudumbi & Ford, 2006; Bai & Ho, 2008; Y. Zhang, Sunarso, Liu, & Wang, 2013). Generally, there is a reverse relationship between permeability and selectivity. Robeson plot is a general metric that shows gas separation membrane performance. These common charts assess the progress in the field of membrane science by plotting the optimal separation selectivity for a gas pair (e.g.,

CO_2/N_2) in a polymer membrane against the permeability of the more permeable gas (i.e., CO_2) (Freeman, 1999; Robeson, 1991, 2008).

Room temperature ionic liquids (RTILs) can be polymerized through photo polymerization. A variety of PILs can be synthesized to be used as membrane. Here, the monomers are polymerized and converted into polymer films that are used as membranes for CO_2 capture (Bara, Lessmann, Gabriel, Hatakeyama, Noble, & Gin, 2007). For example, P[VBTMA][BF_4] and P[VBMI][BF_4] polymers are usually synthesized from their corresponding monomers by means of free radical polymerization, which is initiated by azobisisobutyronitrile (AIBN) with dimethyl form amide (DMF) as the solvent (Blasig, 2007). In this technique, ammonium based membrane was reported to give the highest solubility reaching 170 cm^3 (STP)/cm^3.

Radical polymerization is commonly used for direct polymerization of PILs. These poly (RTIL) membranes have the capability to dissolve about twice the amount of CO_2 compared to their analogues (Tang, Ding, Radosz, & Shen, 2005; Tang, Tang, Sun, & Radosz, 2005; Xiong, Wang, Wang, & Wang, 2011).

Grafting is another way to prepare the polymers which gives high CO_2 loading capacity, where a compound is prepared by grafting a material with special properties to a known material in order to achieve a novel structure. Grafting makes it possible to synthesize a new and special structure with tailor-made properties. Permeability and solubility of PILs can be improved by grafting and by adding ILs.

In one study, synthesis of graft copolymers was afforded through the process of atom transfer radical polymerization (ATRP). Among them, was poly (vinyl chloride) (PVC), which was acting as the main chains and PIL as the side chains. PVC and 1-methy-2-pyrrolidinone (NMP) were added into a round flask together with varying amounts of EBI

[Tf_2N], which resulted in the formation of a PVC-g-PEBI [Tf_2N] polymer. PVC:IL ratios of 1:3 and 1:5 were used and up to 33% and 65% of graft polymers were attained respectively (Chi, Hong, Jung, Kang, Kang, & Kim, 2013). The gas permeability and selectivity across pristine PVC, PVC-g-PIL, and PVC-g-PIL/IL composite membranes were then computed based on a CO_2/N_2 gas mixture at 35 °C. The permeability of CO_2 and N_2 through the pristine PVC membrane was 1.7 Barrer and 0.06 Barrer respectively, and the selectivity for CO_2/N_2 was 28.7. After grafting PVC with 33 wt% PIL, the CO_2 permeability increased to 7.5 Barrer. However, the selectivity dropped slightly to 25.0. Furthermore, as PIL's composition increased to 65 wt%, the CO_2 level of permeability rose to 17.9 Barrer. CO_2 permeability of the PVC-g-PIL graft copolymer membranes was also found to be higher than the pristine PVC by almost tenfold, indicating that PIL showed good permeability performance for CO_2. When 15 wt% of IL was added to the PVC-g-PIL composite membrane, the CO_2 permeability was further increased by almost 7.7 fold to 137.6 Barrer, which consequently decreased the selectivity to 20.2 (Chi, Hong, Jung, Kang, Kang, & Kim, 2013).

It is also mentioned in the literature that some chemicals like polyethylene glycol (PEG) can improve the performance of PILs for CO_2 capture (Hu, Tang, Blasig, Shen, & Radosz, 2006). PEG cause reduction in the hardness of the prepared polymers. Thus, it may have a positive impact on CO_2 permeability. Moreover, increasing PEG chain length causes enhanced permeability and solubility of CO_2. Grafted PILs are prepared by grafting two types of PEG (PEG2000 and PEG400) via free radical polymerization in order to provide CO_2-selective membranes with thermal, chemical, and mechanical stability. The technique involved grafting of PEG onto ionic polymers, poly [p-vinyl benzyl trimethyl ammonium tetrafluoroborate] (P[VBTMA][BF_4]) and poly [2-(methylacryloyloxy)ethyl-trimethyl ammonium tetrafluoroborate] (P[MATMA][BF_4]). The results indicated that PEG2000 appeared to be more effective in comparison with

PEG 475. Moreover, the membranes generated from the grafted polymers onto PEG were found to be less brittle in comparison with those of P[VBTMA][BF_4] and P[MATMA][BF_4] (Hu, Tang, Blasig, Shen, & Radosz, 2006). With regards to CO_2 permeability of the two grafted PILs, the PEG2000, P[MATMA][BF_4] showed 120 Barrer which was twice the permeability of P[VBTMA][BF_4].

As mentioned earlier, addition of IL can increase CO_2 solubility. By adding IL to PIL, a composite with high CO_2 permeability can be produced. Studies have been carried out on a number of PIL–IL composite membranes using poly (diallyldimethyl ammonium), bis (tri fluoro methyl sulfonyl) imide, and poly ([pyr11][NTf_2]), by adding varying amounts of 1-Butyl-1-methyl pyrrolidinium bis (trifluoromethylsulfonyl) imide ([pyr_{14}][NTf_2]) in order to improve the performance of the CO_2 separation. These polymers are easily prepared given the fact that the starting material is a commercially available polymer, with the PIL being generated through metathesis (Liliana, Tomé, Mecerreyes, Freire, Rebelo, & Marrucho, 2013). This was obtained by dissolving the poly ([pyr11][NTf_2]) into acetone (12% (w/v), followed by the addition of varying amounts of IL to obtain a range of percentages of ILs in the polymer matrix. In order to attain transparent and free standing membranes, each individual solution was casted into petri dishes (Liliana, Tomé, 2013). Gas permeability was measured for CO_2, N_2 and CH_4 whereas perm-selectivity was obtained for CO_2/N_2 and CO_2/CH_4. The addition of the IL to PIL increased the perm-selectivity for CO_2/N_2. However, it gave a reverse result for CO_2/CH_4. Furthermore, plotting on Robeson plot showed that the performance of pyrrolidinium based composite was still below the Robeson upper bond. The highest perm-selectivity was for PIL-20IL (20% IL) with the amount of 32.0±0.7 for CO_2/N_2 (Liliana, Tomé, 2013). It was also demonstrated that the addition of free IL to PIL membranes enhanced the CO_2/N_2 perm-selectivity. Moreover, for this composite membrane, the measured CO_2/N_2 perm-selectivity was higher than pure PIL and pure IL

(Liliana, Tomé, 2013). This procedure was found to be more convenient compared to the method employed in the preparation of imidazolium-based PILs (Bara, Gin, & Noble, 2008; Carlisle, Nicodemus, Gin, & Noble, 2012; P. Li, Pramoda, & Chung, 2011). Moreover, the monomeric unit containing the pyrrolidinium functionality exhibited lower toxicity compared to the imidazolium parts (Petkovic, Seddon, Rebelo, & Pereira, 2011).

The incorporation of RTIL to poly (RTIL) was reported to increase the chain mobility, thus, increasing the CO_2 permeability and CO_2/N_2 permeability selectivity of poly (RTIL)-RTIL composites (Orme, Klaehn, Harrup, Luther, Peterson, & Stewart, 2006). The permeability and selectivity were measured for three different polymer systems. Based on Robeson plot, the permeability for imidazolium ionene with the Tf_2N counterion (polymer 2) was better than imidazolium ionene with the bromide counterion (polymer 1). However, the selectivity was reversed. Furthermore, when comparing between polymer 2 and polymer 2–RTIL, results showed improvement in the permeability of CO_2, CH_4, and N_2 reaching 360%, 430%, and 380%, respectively, when using polymer 2–RTIL composite film, while there was no significant change in the CO_2/CH_4 selectivity. It was also shown that addition of RTIL to the polymer matrix lowered its resistance to gas diffusion and eventually increased CO_2 diffusivity.

Furthermore, adding IL to the PILs can increase CO_2 permeability and CO_2/N_2 perm-selectivity to above Robeson upper bond 2008. The pyrrolidinium-based polymers containing different cyano-functionalized counter-anions were synthesized and different amounts of IL were added to their film. Results showed that IL can boost both CO_2 permeability and CO_2/N_2 perm-selectivity (Liliana, Tomé, Isik, Freire, Mecerreyes, & Marrucho, 2015).

Another technique for improving the properties of polymers is blending (Reijerkerk, Knoef, Nijmeijer, & Wessling, 2010). Polymer blending is increasingly being employed

in the design of novel materials (Hosseini, Teoh, & Chung, 2008). Due to its convenience, blending has become an ideal method to obtain a polymeric membrane with high mechanical properties and enhanced formation ability. Moreover, blending can improve the performance of membrane in gas absorption (Hamouda, Nguyen, Langevin, & Roudesli, 2010). For instance, a blended membrane can be prepared as a CO_2 philic membrane. It was reported that the poly (amid-12-b-ethylene oxide) (Pebax1074) was found to gain superior properties with higher tendency towards CO_2 when glycerol triacetate was added. A CO_2 philic membrane showed a relatively high permeability of 1800 Barrer (Feng , 2013). Blending IL's with compatible polymers has been identified as a suitable alternative method for the preparation of IL-containing membranes. However, the mechanical properties of the blended membrane seem to be of low quality (Carlisle, Bara, Lafrate, Gin, & Noble, 2010; Chen, Choi, Salas-de la Cruz, Winey, & Elabd, 2009; Hong, Park, Ko, & Baek, 2009; Hudiono, Carlisle, LaFrate, Gin, & Noble, 2011; Jansen, Friess, Clarizia, Schauer, & Izak, 2010). In one study, a polymer based imidazolium ionene was synthesized and blended with 20 wt% [C_6mim][Tf_2N]. The polymer imidazolium ionene and IL along with DMSO were added and homogenized through mixing and heating to generate composite films (Camper, Bara, Gin, & Noble, 2008; Carlisle, 2010). In another study, three RTIL based imidazoliums were synthesized and then polymerized by UV polymerization for the preparation of membranes. The RTILs were poly([veim][dca]), poly([vbim][dca]), and poly([vhim][dca]); while the three kinds of RTILs, namely [emim][dca], [emim][BF_4], and [emim][$B(CN)_4$] were blended with the P(RTIL)s in order to prepare P(RTIL)-(RTIL) the composites. The increase in N-alkyl groups in the poly (RTIL)s resulted in an increase in the CO_2 permeability and the best separation performance was achieved by the poly([vbim][dca])–[emim][$B(CN)_4$] (1:2) and poly([vbim][dca])–[emim][dca] (1:2) composite membranes (Li, Paul, &

Chung, 2012; Scovazzo, 2009). Blending caused the CO_2 philic to be increased, and the blended membranes seemed to show better quality and higher performance.

Table 2.2 shows PILs that were synthesized as membranes via free radical polymerization or atom transfer radical polymerization as well as those that were prepared by polymer blending method.

From Table 2.2, comparing CO_2 solubility of the two PILs, namely P[VBTMA][BF_4] and P[VBMI][BF_4], it showed that the ammonium based PIL has better solubility. As for the CO_2 permeability for grafted PIL, it was 17.9 Barrer, which was ten times higher than the 1.7 Barrer achieved by a pristine PVC membrane. It was observed that adding IL to PIL, increased the permeability, for example for (Poly ([vbim][dca])–[emim][$B(CN)_4$] (1: 2)) the permeability reached its highest values of 340.1 ± 0.3 as compared to pure Poly([vbim][dca]) and other PIL-IL mixtures. Moreover, by adding glycerol triacetate (GTA) to Poly (amid-12-b-ethylene oxide), the CO_2 permeability increased from 135 to 1800 Barrer. In terms of anions, the PIL with the [Tf_2N] anion showed higher permeability than the PIL with the bromide anion. Furthermore, the PIL-IL mixture with the [Tf_2N] anion showed higher permeability in comparison with both pure PILs.

The poly (RTIL)s as well as the poly (RTIL)–RTIL composites which exhibit longer N-alkyl groups were reported to show superior chain flexibility. As such, there was an increasing trend of CO_2 permeability across the films in the order of poly([veim][dca]) < poly([vbim][dca]) < poly([vhim][dca]). A similar trend was also observed for diffusivity/diffusivity selectivity. Specifically, the diffusivity selectivity was found to be within the range of 0.94 –1.26 across the films. Poly (RTIL) membranes have shown permeability exceeding Robeson upper bond. Perm-selectivity was constant for CO_2/N_2 and CO_2/CH_4 even with increased permeability values due to the lengthening in alkyl chain. The Oligo (ethylene glycol), OEG functionalized have shown the same

permeability as poly (RTLs) with n-alkyl groups. However, they showed increased perm-selectivity for CO_2/N_2, which have exceeded the Robeson plot upper bond (Bara, & Gabriel, 2008; Bara, & Gin, 2008; Bara, Hatakeyama, & Gabriel, 2008; Bara, Hatakeyama, Gin, & Noble, 2008; Bara , 2007; Bara, Noble, & Gin, 2009).

It's important to mention that the thickness has impact on diffusivity and the ideal permeability. Which can be estimated using related equations (Bara, & Gin, 2008; Bara, 2007; Carlisle, 2012; Li, 2011; Liliana, Tomé, 2013).

In general, composite films containing poly imidazolium ionene and RTIL showed similar behavior to some of the neat poly (RTIL) membranes. However, their permeability were different than other poly (RTIL)-RTIL composite films (Bara, Hatakeyama, & Gin, 2008; Carlisle, 2010). Moreover, the contribution of RTIL in the poly (RTIL) membrane considerably enhanced permeability without causing any significant reduction in CO_2 selectivity (Bara, Hatakeyama, & Gin, 2008; Bara , 2009; Carlisle, 2010). The selectivity of poly (RTIL)-RTIL composites is related to solubility selectivity. The more CO_2-N_2 solubility selectivity for free RTILs, the more CO_2-N_2 gas pair selectivity for poly (RTIL)-(RTIL) (Li, 2012; Li , 2011). Consequently, the addition of IL to PIL and the addition of PIL to polymers, even for long chains in alkyls, resulted in higher mobility and increased diffusivity while decreasing selectivity.

Table 2.2: PILs synthesized as membrane

Polymer Name	Synthesis Method	Apply As	CO_2 Loading		Findings	Ref
			Permeability (Barrer)	CO_2 Solubility [cm^3 (STP)/cm^3]		
P[VBTMA][BF_4]	Free radical polymerization	Membrane		170	Ammonium ionic polymer is much higher than an imidazolium ionic polymer.	(Blasig , 2007)
P[VBMI][BF_4]	Free radical polymerization	Membrane		149		(Blasig , 2007)
(PVC-g-PEBI [Tf_2N]) polymer	Atom transfer radical polymerization (ATRP)	Membrane	17.9		Permeability of PVC-g-PIL membrane with 65wt% of PIL at 35 °C, is ten times higher than pristine PVC membrane. The CO_2 permeability will increase to 137.6 by adding 13% of IL into PVC-g-PIL.	(Chi, 2013)
grafting Polyethylene glycol (PEG) on to (P[MATMA][BF_4])	Free radical polymerization	Membrane	120	5.25	CO_2 permeability for P[MATMA][BF_4]-g-PEG 2000 is twice higher than P[VBTMA][BF4]-g-PEG2000.	(Hu, 2006)
grafting Polyethylene glycol (PEG) on to (P[VBTMA][BF_4])	Free radical polymerizations	Membrane	60	4.41		
PIL–IL composite membranes poly ([pyr_{11}][NTf_2]) by addition of different amount of ([pyr_{14}][NTf_2])		PIL–IL composite membranes			Addition of IL to PIL increased the permselectivity for CO_2/N_2. Robeson plot showed that pyrrolidinium composite is still below the Robeson upper bond.	(Liliana & Tomé , 2013)

Table 2.2: Continued

Polymer Name	Synthesis Method	Apply As	CO_2 Loading		Findings	Ref
			Permeability (Barrer)	CO_2 Solubility [cm^3 (STP)/cm^3]		
A CO_2 philic membrane Pebax 1074/GTA80	polymer blending method	Blended membrane	1800 Barrer		With the increase of GTA from 0 to 80 wt%,CO_2 permeability increases from ~135 to ~1800 Barrer	(Feng, 2013)
Polymer 1 is an imidazolium ionene with the bromide counterion		Composite membrane	0.13 ± 0.02	0.45 ± 0.09 cm^3 (STP)cm^{-3}-atm^{-1}		(Carlisle, 2010)
Polymer 2 is an imidazolium ionene with the bromide counterion		Composite membrane	5.3 ± 0.1	0.79 ± 0.05 cm^3 (STP)cm^{-3}-atm^{-1}		(Carlisle, 2010)
Blended composite film, polymer 2 is an imidazolium ionene with the bromide counterion	Blending	Composite membrane	19 ± 1	1.2 ± 0.1 cm^3 (STP)cm^{-3}-atm^{-1}	Selectivity has slight decrease	(Carlisle, 2010)
Poly([veim][dca])			0.09 ± 0.03	6.43		(Li, Paul, & Chung, 2012)
Poly([vhim][dca])			33.50 ± 0.03	14.24		(Li , 2012)

Table 2.2: Continued

Polymer Name	Synthesis Method	Apply As	CO_2 Loading		Findings	Ref
			Permeability (Barrer)	CO_2 Solubility [cm^3 (STP)/cm^3]		
Poly([vhim][dca])			33.50 ± 0.03	14.24		(Li , 2012)
Poly([vbim][dca])			4.24 ± 0.07	9.59		(Li , 2012)
Poly([veim][dca])–[emim][dca] (1 : 1)			62.1 ± 1.0	13.80		(Li , 2012)
Poly([vbim][dca])–[emim][dca] (1 : 1)			118.8 ± 0.3	15.34		(Li , 2012)
Poly([vhim][dca])–[emim][dca] (1 : 1)			138.0 ± 0.2	17.86		(Li , 2012)
Poly([veim][dca])–[emim][BF_4] (1 : 1)			36.0 ± 0.1	13.85		(Li , 2012)
Poly([vbim][dca])–[emim][BF_4] (1 : 1)			74.8 ± 0.1	15.96		(Li , 2012)
Poly([vhim][dca])–[emim][BF_4] (1 : 1)			89.7 ± 0.5	17.38		(Li , 2012)
Poly([veim][dca])–[emim][$B(CN)_4$] (1 : 1)			99.8 ± 0.5	21.93		(Li , 2012)
Poly([vbim][dca])–[emim][$B(CN)_4$] (1 : 1)			184.7 ± 0.3	23.62		(Li , 2012)
Poly([vhim][dca])–[emim][$B(CN)_4$] (1:1)			230.0 ± 1.5	26.20		(Li , 2012)
Poly([vbim][dca])–[emim][dca] (1: 2)			272.9±1.1			(Li , 2012)

Table 2.2: **Continued**

Polymer Name	Synthesis Method	Apply As	CO_2 Loading		Findings	Ref
			Permeability (Barrer)	CO_2 Solubility [cm^3 (STP)/cm^3]		
Poly([vbim][dca])–[emim][$B(CN)_4$] (1 :2)			340±0.3			(Li , 2012)
Poly([Pyr_{11}][$C(CN)_3$])s–60 ILC($CN)_3$	Blending	Composite membrane	439.3 ± 0.		Overcomes the Robeson 2008 upper bound with CO_2/N_2 64.4 Permselectivity	(Liliana, Tomé, 2015)
Poly([Pyr_{11}][$N(CN)_2$]-20 [C_2mim][$N(CN)_2$]			3.79±0.03			(Liliana, Tomé, 2015)
Poly([Pyr_{11}][$C(CN)_3$])-20[C_2mim][$C(CN)_3$]			8.03±0.04			(Liliana, Tomé, 2015)
			143.0±0.1			(Liliana, Tomé, 2015)

Table 2.2: **Continued**

Polymer Name	Synthesis Method	Apply As	CO_2 Loading		Findings	Ref
			Permeability (Barrer)	CO_2 Solubility [cm^3 (STP)/cm^3]		
poly([ViEtIm][NTf_2])	Free radical polymerization	Composite membrane	14.9±0.12			(Liliana, Tomé, 2015)
Poly([ViEtPy][NTf_2])	Free radical polymerization	Composite membrane	20.4±0.07			(Liliana, Tomé, 2015)
Poly([Pyr_{11}][NTf_2])	Free radical polymerization	Composite membrane	11.5±0.09			(Liliana, Tomé, 2015)
Poly([EMTMA][NTf_2])	Free radical polymerization	Composite membrane	9.44±0.13			(Liliana, Tomé, 2015)
Poly([EMCh][NTf_2])	Free radical polymerization	Composite membrane	3.66±0.01			(Liliana, Tomé, 2015)

2.2.2 PILs as Absorbent

It has been reported that the absorption of CO_2 by polymers was twice higher than in ionic liquids (Hu, 2006; Tang, Tang, Sun, & Plancher, 2005). In recent years, studies have found that the mere transformation of ionic liquids into polymeric forms considerably improves CO_2 sorption capacity in comparison to pure ionic liquids. While, the polymer provides a high rate of CO_2 sorption and desorption, the process is also completely reversible. As such, these polymers show high prospects as potential sorbents for CO_2 separation.

Anions have effect on PILs' features. It was observed that PILs containing BF_4^- anion has the highest CO_2 uptake in comparison to other anions. With AIBN and DMF as the initiator and the solvent, respectively, a series of poly ionic liquids can be synthesized using free radical polymerization (Tang, Shen, Radosz, & Sun, 2009; Tang, Sun, Tang, Radosz, & Shen, 2005; Tang, Tang, Sun, & Radosz, 2005c). PILs can also be directly synthesized from their associated monomers by free radical polymerization.

Table 2.3 summarizes the various PILs synthesized for absorption. In one study, two PILs were synthesized by free radical polymerization, namely poly [1-(para-vinyl benzyl) pyridinium tetrafluoroborate] P[VBP][BF_4] and poly [1-(para-vinyl benzyl) triethyl phosphonium tetrafluoroborate] P[VBTEP][BF_4]. Their CO_2 sorption was compared with various other PILs (Tang, Shen, Radosz, & Sun, 2009). In another study, the polymers poly [1-(4-vinylbenzyl)-3-butylimidazolium tetrafluoroborate] P[VBIT], poly [(1-(4-vinylbenzyl)- 3-butylimidazolium hexa fluoro phosphate] P[VBIH] and poly [2-(1-butylimidazolium-3-yl) ethyl methacrylate tetrafluoroborate] P[BIMT] were also synthesized and their CO_2 absorption capacity is shown in Figure 2.1 (Tang, & Sun, 2005). Also, in a different investigation, a series of imidazolium based polymers, namely Poly [1-(p-Vinyl benzyl)-3-butyl-imidazolium tetra fluoro borate] P[VBBI][BF_4], Poly

[1-(p-vinyl benzyl)-3-butyl-imidazolium hexafluoro phosphate] P[VBBI][PF_6], Poly [1-(p-Vinyl benzyl)-3-butyl-imidazolium benzoic sulphimide] P[VBBI][Sac], Poly [1-(p-Vinyl benzyl)- 3-butyl-imidazolium trifluoro methane sulfonamide] P[VBBI][Tf_2N], Poly [1-[2-(Methacryloyloxy)ethyl]-3-butyl-imidazolium tetra fluoro borate] P[MABI][BF_4], and Poly [1-(p-vinyl benzyl)-3-methyl-imidazolium tetra fluoro borate] P[VBMI][BF_4], all of which were made from their monomers and were tested as CO_2 absorbents (Tang, Tang, Sun, & Radosz, 2005). Comparing all this mentioned work, P[MABI][BF_4] showed slightly higher CO_2 absorption than the others.

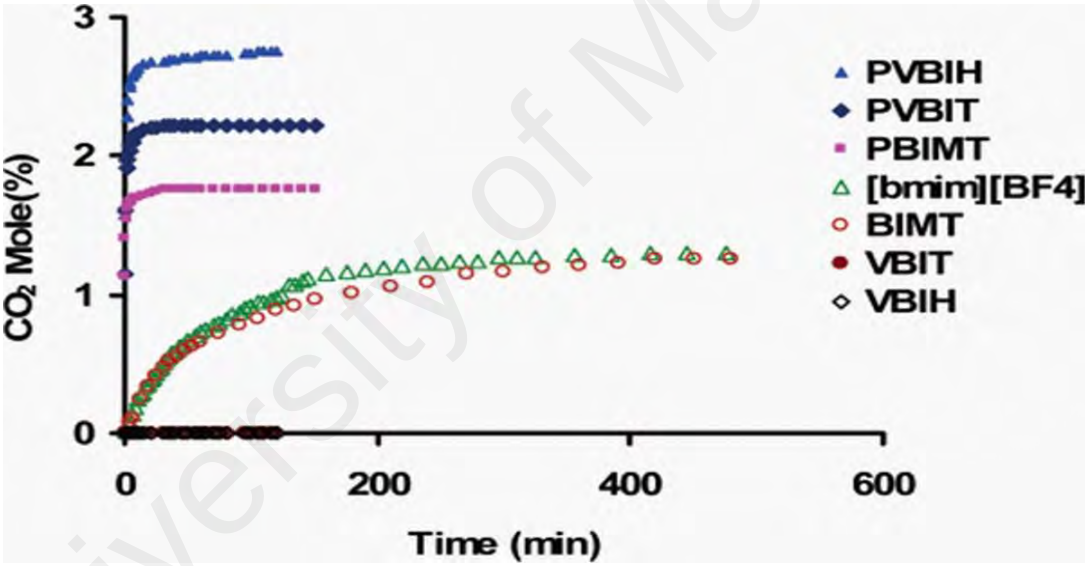

Figure 2.1: CO_2 absorption of the polymers (PVBIT, PVBIH, PBIMT), corresponding monomers (VBIT, VBIH, BIMT), and an ionic liquid [bmim][BF_4] as a function of time (592.3 mmHg CO_2, 22 ˚C). Reprinted with permission from (Tang, & Sun, 2005). Copyright (2005) American Chemical Society (Tang, & Sun, 2005).

In another study (Tang, Tang, Sun, & Plancher, 2005), PILs were synthesized from their associated monomers and then compared with ionic liquids at room temperature [bmim][BF_4]. In this scenario, the polymers demonstrated CO_2 absorption of up to 10.22

mol% for (P[VBTMA][BF_4]), 7.99 mol% for (P[MATMA][BF_4]), 2.27 mol% for (P[VBBI][BF_4]), P[VBBI][Tf_2N]) and 1.80 mol% for (P[MABI][BF_4]) with reference to their monomer units. On the other hand, the ionic liquid [bmim][BF_4] which experienced similar conditions at room temperature only absorbed 1.34 mol% of CO_2. The [MABI][BF_4] monomer, which is basically a liquid at room temperature, demonstrated a similar CO_2 absorption behavior as [bmim][BF_4]. Thus, it can be argued that the mere transformation of ionic liquids into a polymeric format considerably improves the CO_2 sorption potential. These CO_2 sorption capacities are also substantially greater than other polymer solids such as polymethacrylates, polystyrene, and polycarbonates (Budzien, McCoy, Weinkauf, LaViolette, & Peterson, 1998; Kato, Tsujita, Yoshimizu, Kinoshita, & Higgins, 1997; Mogri & Paul, 2001; Tang, Tang, Sun, & Plancher, 2005). The sorption rates of these polymers were very high and took only a few minutes to reach their 95% sorption capacities. In contrast, for room temperature ionic liquids [MABI][BF_4] and [bmim][BF_4], it took them more than 400 min to reach equilibrium. This fast CO_2 sorption is the main feature of the poly (ionic liquids). In addition, the monomers of ([VBTMA][BF_4], [MATMA][BF_4], and [VBBI][BF_4]) showed no CO_2 sorption, due to their crystalline structures.

Some polymers cannot be synthesized from their direct monomers. For instance poly[(1-butyl imidazolium-3) methyl ethylene oxide tetrafluoroborate] P[BIEO][BF_4] was synthesized by a poly ethylene oxide back bone using poly (epichlorohydrin) as shown in Figure 2.2 (Tang, Tang, Sun, & Radosz, 2005). In this experiment, aluminum isopropoxide, degassed THF, and epichlorohydrin was added to the flask using degassed syringes. After the reaction, the poly (epichlorohydrin) was precipitated. Poly (epichlorohydrin) was then dissolved in DMF, followed by the addition of N-butyl imidazole to the DMF solution. Then, anhydrous ethyl ether was added to the filtrate to

precipitate the P[BIEO][BF_4]. This synthesized PIL gave 1.06 mol% CO_2 (Tang, Tang, Sun, & Radosz, 2005).

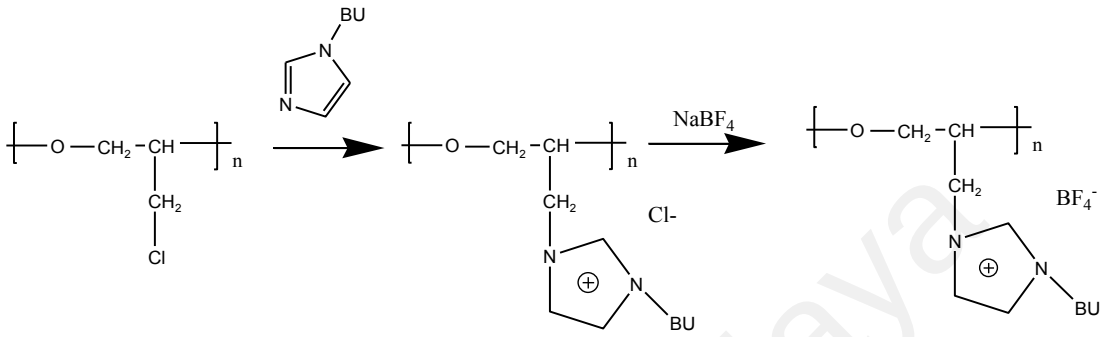

Figure 2.2: Synthesis of P[BIEO][BF_4]. Adapted from (Tang, Tang, Sun, & Radosz, 2005). Adapted from (Tang, Tang, Sun, & Radosz, 2005) with permission of john Wiley and sons.

It is also possible to prepare ionic liquid monomers from the exchange reaction of anions, coupled with concurrent polymerization of their monomers by free radicals. Some of these polymers are poly[p-vinyl benzyl trimethyl ammonium tetrafluoro borate] (P[VBTMA] [BF_4]), poly [2-(methacryloyloxy)ethyl tri methyl ammonium tetrafluoro borate] (P[MATMA][BF_4]), poly [1-(p-vinyl benzyl)- 3-butyl imidazolium tetrafluoroborate](P[VBBI][BF_4]), bis(trifluoro methyl sulfonyl)imide (P[VBBI][Tf_2N]), and poly[1-(2-methacryloyloxy)ethyl-3-butylimidazoliumtetrafluoroborate] P[MABI][BF_4]). The ionic liquid monomers, AIBN, and DMF were charged into a reaction tube. The tube was then tightly sealed and degassed. The tube, together with its contents, was then submerged in an oil bath for six hours at 60 °C, for the polymer to precipitate. The precipitated polymer was then allowed to dry in a vacuum at a controlled temperature of 60 °C, As a result, the yield for each polymer was determined in a separate reaction as follows: 75% P[VBBI][BF_4], 68% P[VBBI][Tf_2N], 70% P[MABI][BF_4],

90% P[MATMA][BF_4], and 95% P[VBTMA][BF_4] (Tang, Tang, Sun, & Radosz, 2005). The study reported that the ammonium cation with a short alkyl group as well as the BF_4 anion favored CO_2 sorption in PILs. As such, Poly [1-(pvinylbenzyl) trimethylammonium tetrafluoroborate] P[VBTMA][BF_4] gave the highest CO_2 absorption. There was a considerable increase in CO_2 sorption when the pressure was increased. For example, [VBTMA][BF_4] absorbed 44.8 mol% of CO_2 (in terms of its monomer units) at 12 atm. The CO_2 sorption of P[VBTMA][BF_4] as a function of pressure is shown in Figure 2.3 (Tang, Tang, Sun, & Radosz, 2005). It was indicated that the presence of PIL in the absorption process could cause a considerable increase in CO_2 absorption. Similar findings were also reported for PILs based on polyurethane where the best performance was achieved with 75.7 mol% CO_2 at 20 bar (Magalhaes , 2014).

It is also worth mentioning that the desorption of the poly (ionic liquid)s is faster than ILs. The polymers released CO_2 in less than 15 min under vacuum. No change in sorption/desorption kinetics and sorption capacity was observed after four cycles of sorption/desorption experiments. This indicates that the sorption/desorption was totally reversible. Also, no gain in weight was registered when the polymers were in contact with N_2 or O_2 under identical conditions. However, It should be noted that the presence of moisture may result in a slight decrease in CO_2 absorption potential. For example, P[VBTMA][BF_4] in its wet form with 13.8 mol% water content showed a decrease in absorption potential of 7.9 mol% CO_2 below the dry form P[VBTMA][BF_4] (Tang, Tang, Sun, & Radosz, 2005). Nevertheless, poly ionic liquids appear to be a novel polymer material with advanced CO_2 absorption potential.

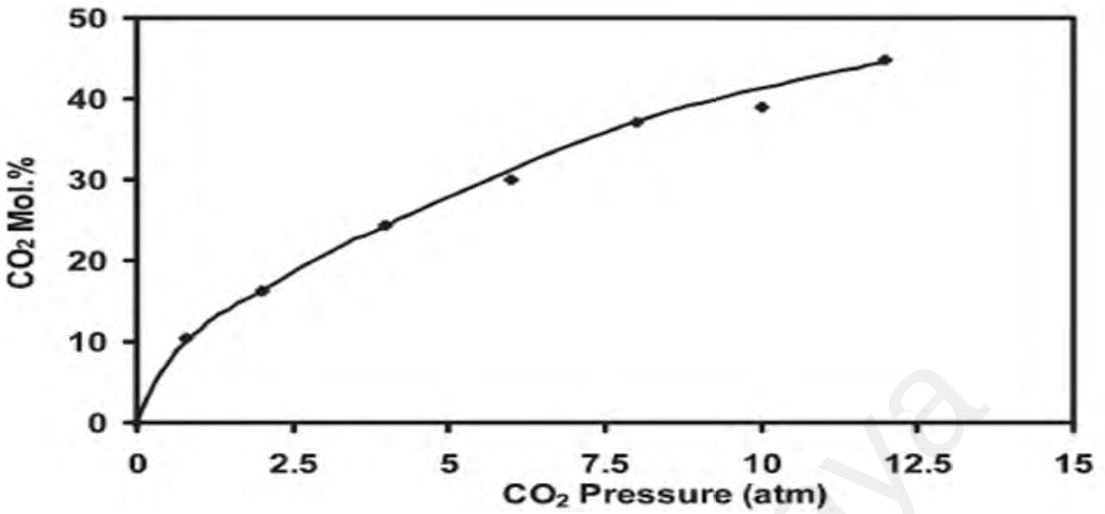

Figure 2.3: CO_2 sorption capacities of P[VBTMA][BF_4] at different CO_2 pressures (22 °C). (Tang, Tang, Sun, & Radosz, 2005). Reproduced from (Tang, Tang, Sun, & Radosz, 2005) with permission of The Royal Society of Chemistry.

Table 2.3: PILs synthesized as absorbent

Polymer	Reactant	Method	CO_2 absorption (cm^3/cm^3)	Ref
P[VBTEA][BF_4]			5.90	(Tang, 2009)
P[VBTEP][BF_4]		Free radical polymerization	4.77	(Tang, 2009)
P[VBP][BF_4]		Free radical polymerization	5.62	(Tang, 2009)
P[VBMI][BF_4]			3.99	(Tang, 2009)
P[VBTMA][BF_4]			10.68 An ammonium cation with short alkyl group, BF_4 anion, and polystyrene backbone was found to favor CO_2 sorption in PILs	(Tang, 2009)
P[VBTMA][PF_6]			8.95	(Tang, 2009)
P[VBTMA][Tf_2N]			2.59	(Tang, 2009)
P[MATMA][BF_4]			8.13	(Tang, 2009)

Table 2.3: Continued

Polymer	Reactant	Method	CO_2 absorption (cm^3/cm^3)	Ref
P[BIMT]	corresponding monomers	Free radical polymerization	1.77 mol% P[VBIH]> P[VBIT]> P[BIMT]	(Tang, & Sun, 2005)
P[VBIH]			2.75 mol%	(Tang, & Sun, 2005)
P[VBIT]			2.22 mol%	(Tang, & Sun, 2005)
P[VBBI][BF_4]			2.27 mol%	(Tang, Tang, Sun, & Radosz, 2005)
P[VBBI][Tf_2N],	corresponding monomers	Free radical polymerization	2.23 mol%	(Tang, Tang, Sun, & Radosz, 2005)

Table 2.3: Continued

Polymer	Reactant	Method	CO_2 absorption (cm^3/cm^3)	Ref
P[VBBI][PF_6],			2.8 mol%	(Tang, Tang, Sun, & Radosz, 2005)
P[VBBI][Sac]			1.55 mol%	(Tang, Tang, Sun, & Radosz, 2005)
P[MABI][BF_4]			1.78 mol%	(Tang, Tang, Sun, & Radosz, 2005)
P[VBMI][BF_4]			3.0 mol% (at 0.078 MPa and 22 ºC)	(Yu, 2014)

Table 2.3: Continued

Polymer	Reactant	Method	CO_2 absorption (cm^3/cm^3)	Ref
P[VBMI][BF_4]			3.05 mol%	(Tang, Tang, Sun, & Radosz, 2005)
P[BIEO][BF_4]	poly (epichlorohydrin), N-butyl imidazole		1.06 mol%	(Tang, Tang, Sun, & Radosz, 2005)
PUA-02a			75.7 mol% at 20 atm	(Magalhae, 2014)
P[VBBI][Tf_2N]	corresponding monomers	Free radical polymerization	2.27 mol%	(Tang, Tang, Sun, & Plancher, 2005)

Table 2.3: Continued

Polymer	Reactant	Method	CO_2 absorption (cm^3/cm^3)	Ref
P[MABI][BF_4]			1.8 mol%	(Tang, Tang, Sun, & Plancher, 2005)
P[MATMA][BF_4]			7.99 mol%	(Tang, Tang, Sun, & Plancher, 2005)
P[VBTMA][BF_4]			10.22 mol%	(Tang, Tang, Sun, & Plancher, 2005)

Table 2.3: Continued

Polymer	Reactant	Method	CO_2 absorption (cm^3/cm^3)	Ref
P[VBTMA][BF_4]			44.8 mol% at 12 atm	(Tang, Tang, Sun, & Plancher, 2005)
P[VBTMA][PF_6]			10.6	(Yu, 2014)
P[VBTMA][BF_4]			10.2 mol%	(Yu, 2014)
P[VBTEA][BF_4]			4.8 mol%	(Yu, 2014)
P[MATMA][BF_4]			7.9 mol%	(Yu, 2014)
P[VBTMA][Sac]			2.7 mol%	(Yu, 2014)
P[VBTMA][Tf_2N]			2.8 mol%	(Yu, 2014)

2.2.3 PILs as Adsorbents

Adsorption is the process of eliminating one or more components of a mixture using a solid surface. In other words, it refers to the adhesive behavior of an atom, ion, or molecule emanating from gases, liquids, or dissolved solids to a surface. The procedure depends on substantial intermolecular forces between the adsorbent and solid surfaces. In CO_2 capture, the CO_2 is attracted to the adsorbent and adheres to the adsorbent's surface (Meisen & Shuai, 1997; Mondal, 2012). It is necessary to note that not much work has been reported pertaining to the adsorption of CO_2 using PILs.

In a previous study (Yu, 2014) CO_2 adsorption isotherm of two PILs, P[VBTEA][PF_6] and MBA-cross-linked-P[VBTEA][PF_6] was obtained by means of an Autosorb iQ-MP

by Quantachrome. Adsorption isotherm for both PILs at 25 °C is shown in Figure 2.4 (Yu, 2014). It is observed that by increasing the pressure, the CO_2 mass fraction in the PILs increased. Based on Figure 2.4 the maximum adsorption readings of P[VBTEA][PF_6] and MBA-cross-linked-P[VBTEA][PF_6] were 10.36 and 14.04 mg/g respectively, under maximum pressure of Autosorb-iQ-MP at 25 °C. Other studies (Bhavsar, Kumbharkar, & Kharul, 2012; Blasig, 2007; Tang, 2005; Tang, Radosz, & Shen, 2008; Yu, 2014) also reported that, MBA-cross-linked-P [VBTEA][PF_6] showed better adsorption efficiency with up to 1.38 wt% higher than certain PILs such as P[VBTMA][PF_6] and 1-allyl-3-methylimidazolium (Blasig, Tang, Hu, Shen, & Radosz, 2007; Tang, 2005; Tang, Tang, Sun, & Radosz, 2005).

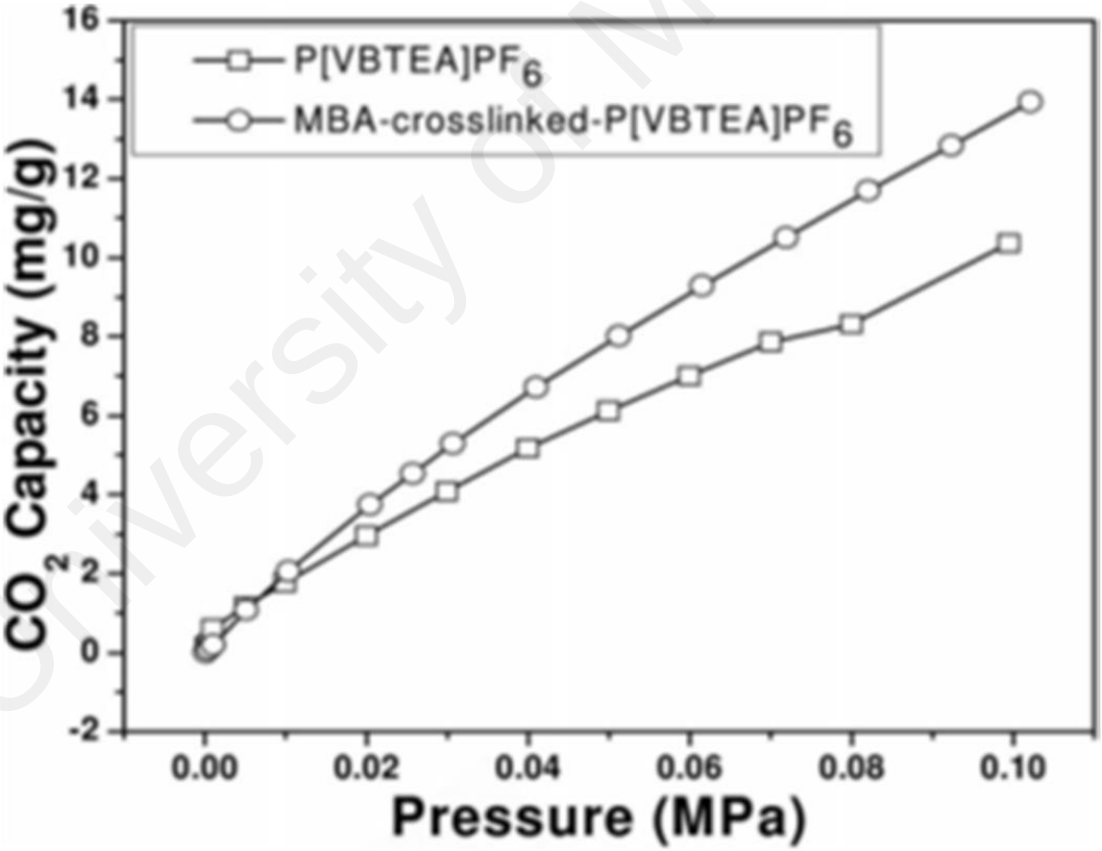

Figure 2.4: Sorption isotherm of P[VBTEA][PF_6] and MBA-cross-linked-P[VBTEA][PF_6]. Reproduced from (Yu, 2014) with permission of the John Wiley and Sons.

Terafluoroborate and acrylonitrile PILs were reported to act as a suitable sorbent coatings for solid-phase microextraction (SPME). Poly (1-vinyl-3- hexyl imidazolium) bis [(tri fluoro methyl) sulfonyl] imide [poly (VHIM- NTf_2)] and Poly (1-vinyl-3- hexyl imidazolium) taurate [poly (VHIM-taurate)] were initially synthesized from their associated monomer (VHIM-Br) by free radical polymerization using AIBN as an initiator and anion exchange. Poly (VHIM-taurate) was then generated by adding an equimolar amount of taurine. Results showed that the poly(VHIM-NTf_2) fiber possessed superior CO_2/CH_4 and CO_2/N_2 selectivity compared to [poly (VHIM-taurate)] and the commercial carboxen fiber (Zhao, & Anderson, 2010).

Crosslinking and modification were reported to have positive impact on CO_2 sorption (Samadi, Kemmerlin, & Husson, 2010; Yu., 2014). In one investigation, a new poly (ionic liquid) of N, N-methylene bis acryl amide (MBA) was cross-linked with poly (4-vinylbenzyltriethylammonium hexafluorophosphate) (MBA-cross-linked-P [VBTEA][PF_6]) through radical solution polymerization and then it was studied extensively for CO_2 sorption. This new cross-linked polymer showed better adsorption characteristics compared to P[VBTEA][PF_6] (Yu , 2014). In another work, the adsorption isotherms of CO_2 and N_2 were computed based on PIL nanolayers grafted from cellulose substrates. The readings showed that CO_2 adsorption only occurred with PIL-modified substrates and no CO_2 uptake was recorded for the unmodified cellulose (Samadi, 2010).

In another report, a mesoporous poly (ionic liquid) was prepared from the 3-(4-vinylbenzyl)-1-vinylimidazolium chloride monomer and this mesoporous PIL showed considerably faster CO_2 adsorption than its nonporous counterpart (Wilke, Yuan, Antonietti, & Weber, 2012). As a result, the mesoporous PIL showed higher CO_2 adsorption than the monomeric species. In addition, CO_2 adsorption in gas pair selectivity for [NTf_2] was double the taurate anion.

Studies have also indicated that the CO_2 potential increased in an ATRP-modified substrate with up to 12 hours of polymerization, but there was no noticeable change beyond this period of time. In general, studies involving a single gas indicated that PIL-modified substrates show higher selectivity for CO_2 compared to N_2, whereas for CO_2, the values registered are relatively modest based on per mass of PIL. (Li , 2008; Samadi, 2010; Su, Lu, Kuo, & Zeng, 2010). Table 2.4 summarizes PILs as adsorbents.

Table 2.4: PILs synthesized as adsorbent

Polymer	Method	Adsorption (mg/g)	selectivity CO_2/N_2	selectivity CO_2/CH_4	Ref
[poly (VHIM- NTf_2)]	Free radical polymerization		8.03	6.44	(Zhao, & Anderson, 2010)
poly(VHIM-taurate)			3.34	2.95	(Zhao, & Anderson, 2010)
(MBA-cross-linked-P [VBTEA][PF_6])	Free radical polymerization s	14.04 mg/g (at 0.2 MPa and 25°C)			(Yu, 2014)
P[VBTEA][PF_6]	Free radical polymerization s	10.36			(Bara, Hatakeyama, & Gin, 2008)
Poly 3-(4- vinylbenzyl)-1-vinylimidazolium tetra fluoro borate	based on hard-templating of silica nanoparticles	0.46 mmol/g		Mp (~0.46 $mmol \cdot g^{-1}$)/monomeric species (~0.02 mmol·g−1).	(Wilke , 2012)

2.3 Modified Polymers for CO_2 Capture

Modification of existing polymers could show significant impact on their CO_2 sorption. An organic polymer was modified with amine and the results showed excellent improvement on CO_2 capture (Li, Yang, Zhu, Hu, & Liu, 2017). In another study by modifying the porous of MCM-41 with poly ethylene imine, it showed a good effect on the adsorption of CO_2 by poly ethylene imine (Xu, Song, Andresen, Miller, & Scaroni, 2002). Moreover, surface modification and supported polymeric sorbents showed a considerable impact on CO_2 capture. For instance, a surface modified poly vinylidene fluoride has good CO_2 absorption capacity after modification (Filburn, Helble, & Weiss, 2005; Xu, 2002).

2.4 Effect of Pressure and Temperature on PILs CO_2 Capture

It was indicated that increasing pressure caused the CO_2 sorption to increase. The CO_2 sorption of P-[VBTMA][BF_4] as a function of pressure is shown in Figure 2.3 (Tang, Tang, Sun, & Plancher, 2005). For example from the Figure 2.3, the CO_2 absorption of P[VBTMA][BF_4] is 44.8 mol% at 12 atm of CO_2 pressure, which is much greater than that of the room temperature ionic liquids (Cadena , 2004; Tang, Tang, Sun, & Plancher, 2005).

The impact of the temperature as a CO_2 adsorption factor on the PIL-modified substrate was investigated in another study (Samadi, 2010). As expected, the increase of temperature decreases CO_2 solubility, absorption and adsorption in PILs. As shown in Table 2.4 A, B, and C, for poly [$(META)^+ BF_4^-$], increasing the pressure, caused CO_2 adsorption to increase, while the impact of temperature is reversed (Samadi, 2010). In another work, using poly[(p-vinyl benzyl)trimethyl ammonium hexa fluoro phosphate] P([VBTMA][PF_6]) as absorbent exhibited decreased CO_2 absorption levels under

increasing temperatures (Supasitmongkol & Styring, 2010). For a polymer grafted to PEG (P[VBTMA][BF_4]-g-PEG2000), the CO_2 solubility decreases with increasing temperature, but there was an increase in permeability and diffusivity of CO_2 (Hu, 2006b). Furthermore, for poly[(p-vinyl benzyl) trimethyl ammonium hexa fluoro phosphate] P([VBTMA][PF_6]), increasing the temperature caused a decrease in CO_2 absorption levels (Supasitmongkol & Styring, 2010).

Table 2.4: Effect of temperature on PIL poly[$(META)^+$ [BF_4^-] CO_2 adsorption (A) BF_4^- 20 ˚C, (B) BF_4^- 40 ˚C, (C) BF_4^- 60 ˚C (Samadi, 2010).

(A)		(B)		(C)	
P/bar	**Q(g CO_2/g PIL)**	**P/bar**	**Q(g CO_2/g PIL)**	**P/bar**	**Q(g CO_2/g PIL)**
~0.5	~0.04	~0.5	~0.02	~1.0	~0.01
~1.0	~0.08	~1.0	~0.04	~1.3	~0.02
~1.4	~0.09	~1.4	~0.06	~1.7	~0.025
~2.0	~0.15	~2.0	~0.10	~2.0	~0.07
~0.5	~0.04	~0.5	~0.02	~1.0	~0.01

2.5 Effect of PILs Structure on CO_2 Capture

The change and modification in different parts of the polymer chains can have a significant effect on CO_2 capture. There are three main structure changes that were reported to affect the performance of PILs. They are cation, anion and backbone.

2.5.1 Effect of Cations

Choice of cation is of great importance in the structure of PIL for CO_2 capture. It has a significant impact on PILs features (Zulfiqar, Sarwar, & Mecerreyes, 2015). Research has been carried out on the sorption of CO_2 using PILs (P[VBTEA][BF_4], P[VBTEP][BF_4], P[VBP][BF_4], and P[VBMI][BF_4]) which were comprised of different cations but similar anion (BF_4) and polystyrene backbone as shown in Figure 2.5 (Tang , 2009). The CO_2 sorption potentials (mL(STP)/mL) of the PILs were reported in the order of P[VBTEA][BF_4] > P[VBP][BF_4] > P[VBTEP][BF_4] > P[VBMI][BF_4] (Tang, 2009).

Large substituents for the imidazolium cation were suggested to block the CO_2 sorption (Tang, Tang, Sun, & Radosz, 2005). For instance, P[VBMI][BF_4], comprising of a methyl substituent on the imidazolium cation, was found to depict higher CO_2 sorption potential (3.05 mol%) as compared to P[VBBI][BF_4] (2.27 mol%) with a butyl group (Tang, Tang, Sun, & Radosz, 2005). To prove the importance of cations in the sorption process, a comparison of the solubility between biphenyl, a polysulfide (PSF), with PILs was carried out. Here, the CO_2 solubility of P[VBTMA][BF_4] was found to be higher than that of PSF, while the CO_2 solubility levels of P[VBMI][BF_4] were lower than those for PSF. This phenomenon suggested that the type of cation has a significant impact on CO_2 sorption (Blasig, Tang, Hu, Shen, & Radosz, 2007). Although cations are known to play a weak role in the ILs (Anthony, Anderson, Maginn, & Brennecke, 2005; Cadena, 2004), their influence on CO_2 sorption by PILs is considerable. For example, the ammonium-based PILs exhibit higher CO_2 sorption compared to the imidazolium-based PILs. In addition, it was indicate that the cations of PILs can also play a pivotal role in CO_2 membrane separation. The influence of polycation variation on CO_2 permeability and diffusivity was reported and considerable CO_2 permselectivities were obtained using tetra-alkyl ammonium-based PILs like pyrrolidinium, ammonium and cholinium in comparison to imidazolium and pyridinium. The highest amount was 43.0±1.1 by using

cholinium. However, for single CO_2 permeability, PIL with pyridinium cation showed 20.4±0.07 Barrer (Liliana & Tomé , 2015).

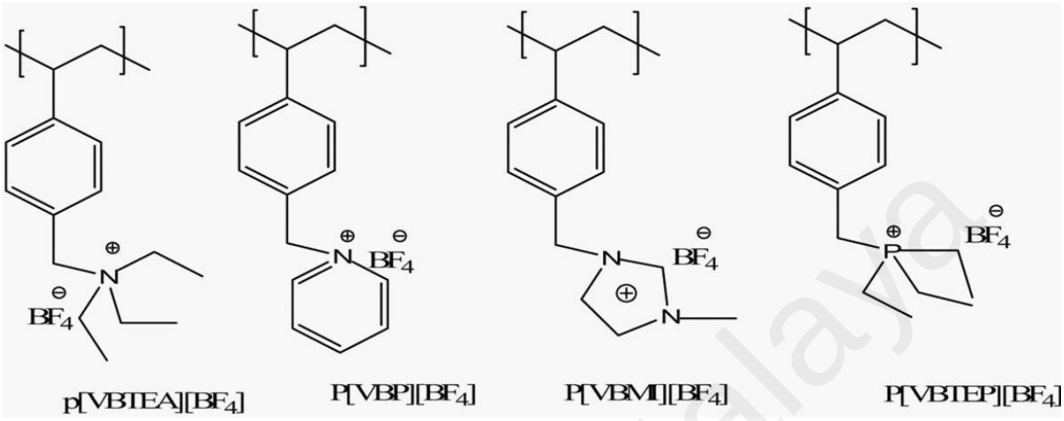

Figure 2.5: Structures of the poly (ionic liquid)s (Tang, 2009). Adapted with permission from (Tang, 2009) Copyright (2009) American Chemical Society (Tang, 2009).

2.5.2 Effect of Anions

The anions have an impact on the characteristics of ionic fluids such as solubility, viscosity, and thermal stability. As such, the characteristics of the PILs are also expected to have some dependence on the type and status of the counter-anion (Marcilla, 2005). The effect of anions on CO_2 sorption shows different results for PILs compared to ionic liquids. For instance, despite the fact that the Tf_2N^- anion performs well with ILs, its performance was reported to be much less efficient in PILs (J. Tang, Tang, Sun, Radosz, & Shen, 2005b). Similar findings were reported for trimethylammonium-based PIL when it was employed as CO_2 adsorption sorbents (Samadi, 2010). The studies on PIL-RTIL composite membranes showed that the anion had minimal impact on the CO_2 permeability (Bara, & Gin, 2008). In this work, three different anions, BF_4^-, $CH_3SO_3^-$, and $CF_3SO_3^-$ in poly [$(META)^+$ BF_4^-], poly[$(META)^+CH_3SO_3^-$], and

poly[(META)$^{+}CF_3SO_3^{-}$] respectively, were compared for their CO_2 sorbent capacity and the results showed that all these anions had low impact on CO_2 solubility (Bara, & Gin, 2008; Samadi, 2010).

Although fluorine atoms do not have a direct effect on CO_2 sorption, their presence in the anions was reported to enhance the CO_2 sorption (Tang, Shen, Radosz, & Sun, 2009). However, Tf_2N ions in comparison to other fluorinated ions have lower CO_2 sorption. The CO_2 sorption was investigated for PILs with the same ammonium cation and polystyrene backbone but different anions, namely P[VBTMA][BF_4], P[VBTMA][PF_6], and P[VBTMA][Tf_2N]. The results showed that their CO_2 sorption capacities followed the order P[VBTMA][BF_4] > P[VBTMA][PF_6] >> P[VBTMA][Tf_2N] (Tang, Shen, Radosz, & Sun, 2009). In another study, PILs of aromatic backbone with various anions were compared for their CO_2 sorption and the results showed that the sorption of the acetate anion was in the order of Ac> BF_4 > Tf_2N (Kumbharkar, Bhavsar, & Kharul, 2014).

The effect of changing the anion on CO_2 sorption capacity was investigated for Poly [1-(p-Vinyl benzyl) -3-butyl-imidazolium (Tang, Tang, Sun, & Radosz, 2005c). The results showed that the CO_2 sorption capacities for P[VBBI][PF_6], P[VBBI][BF_4], P[VBBI][Tf_2N] and P[VBBI] [Sac] were 2.80 mol% , 2.27 mol%, 2.23 mol%, and 1.55 mol%, respectively. Here, the poly ionic liquid with PF_6^{-} anions ([PVBBI][PF_6]) was found to have the highest sorption potential. The fact that the poly ionic liquid comprising of Sac^{-} anions may take up 1.55 mol% of CO_2 indicates that the CO_2 sorption behavior of the poly ionic liquids is not totally depended on fluorine atoms but its presence in the anions improves the CO_2 sorption (Cadena, 2004; Tang, Tang, Sun, & Radosz, 2005c).

2.5.3 Effect of Backbones

CO_2 sorption in PILs with different backbones has been studied by various researchers (Cadena, 2004). In one investigation, the styrene backbone was reported to demonstrate higher CO_2 sorption (Tang, 2009). This study, compared between Poly [1-(para-vinyl benzyl)-tri ethyl ammonium [tetrafluoroborate] (P[VBTMA][BF_4]) and poly[2-(methacryloyloxy)ethyl]trimethyl ammonium tetrafluoroborate (P[MATMA][BF_4]) having similar anions and cations but different backbones. All these PILs were obtained from direct polymerization of their monomers. The outcome showed that the CO_2 sorption of P[VBTMA][BF_4] exhibited a higher CO_2 sorption potential compared to P[MATMA][BF_4] in CO_2 absorption system (Tang, 2009).

In another work, the CO_2 absorption of PILs with different backbones were investigated and the results showed that the CO_2 sorption of Poly[1-(p-Vinylbenzyl)-3-butyl-imidazoliumtetrafluoroborate] (P[VBBI][BF_4]), Poly [1- [2-(Methacryloyloxy)ethyl]-3-butyl-imidazoliumtetrafluoroborate] (P[MABI][BF_4]) and Poly[(1-butylimidazolium-3) methyl ethylene oxide tetrafluoroborate] (P[BIEO] [BF_4]) are 2.27% mol, 1.78% mol and 1.06% mol respectively. P[VBBI][BF_4] with polystyrene backbone showed good CO_2 sorption potential compared to P[MABI][BF_4] and P[BIEO] [BF_4] (Tang, Tang, Sun, & Radosz, 2005c).

2.6 Thermal Properties of PILs

2.6.1 Glass Transition Temperature of PILs

It is very important to know that the glass transition temperature (T_g) of PILs, since T_g is the lowest temperature at which configuration of the polymer starts to change. Most of

the research reported on PILs for CO_2 capture also determined the T_g of the PILs. The majority of the reported T_g were measured using a differential scanning calometric (DSC) instrument. Table 2.5 summarizes the T_g for PILs which are related to CO_2 capture either via absorption or membrane (Tang, Tang, Sun, & Radosz, 2005c; Tang, Tang, Sun, & Plancher, 2005b; J. Tang, Tang, Sun, Radosz, & Shen, 2005a). From Table 2.5, it is clear that the lowest T_g point belongs to the Tf_2N included polymer.

Studies (Tang, Tang, Sun, & Radosz, 2005c) showed that the anion variation has a strong influence on T_g. In one study, it was reported that Tf_2N^- and Sac^- can strongly decrease the T_g, due to the plasticization of anions. Moreover, different backbones have different effects on T_g. Butyl group plasticization may decrease while being on imidazolium units as compared to methyl group, causing a decrease in T_g. The polymers with poly (1-butyl-3-vinylbenzylimidazolium)(P[VBBI]) back bone, were investigated and the following trend was reported for T_g: P[VBBI][Tf_2N] (3 °C) < P[VBBI][Sac] (40 °C) < P[VBBI][BF_4] (78 °C) < P[VBBI][PF_6] (85 °C). Investigations on PILs by a BF_4^- anion and different backbones were also performed. The T_g trend was found as follows; P[BIEO][BF_4] (33 °C) < P [MABI][BF_4] (54 °C) < P[VBBI][BF_4] (78 °C) < P[VBMI][BF4] (110 °C). The P[BIEO] [BF_4] with a more flexible structure had the lowest T_g. In addition, the polymer with a methyl group had a higher value of T_g (110 °C) compared to P[VBBI][BF_4]. This phenomenon was mainly due to the effect of the loss of the plasticization of the butyl group on the imidazolium units (Tang, Tang, Sun, & Radosz, 2005c).

In another work, the effect of Tf_2N was also studied where the Tf_2N ion was found to lower the T_g point. The glass transition temperatures were measured for PILs and the T_g obtained were 215 °C for (P[VBTMA][BF_4]), 166 °C for (P[MATMA][BF_4]), 86 °C for

(P[VBBI][BF_4]), 30 °C for (P[VBBI]n[Tf_2N]), and 69 °C for (P[MABI][BF_4]) (Tang, Tang, Sun, & Plancher, 2005a).

Newly made poly(RTIL)s including poly([veim][dca]), poly([vbim][dca]), and poly([vhim][dca]) showed higher T_g compared to the [emim][dca]. By increasing the alkyl chain in poly (RTIL), T_g decreased from 29 °C to -37 °C (Li , 2012b). Furthermore, when RTILs ([emim][dca], [emim][BF_4] or [emim][$B(CN)_4$]) was added to poly (RTIL), the value of T_g decreased with the following trend: poly([veim][dca])–RTIL > poly([vbim][dca])–RTIL > poly([vhim][dca])–RTIL. It is worth mentioning that the Tg for [emim][dca], [emim][BF_4] and [emim][$B(CN)_4$] were −104 °C, −92 °C, and −82 °C, respectively. Based on these results, it can be concluded that the lowest T_g RTIL with the longer poly (RTIL) alkyl chain will result in a lower T_g for the composite (Li, 2012b).

From Table 2.5 it can be seen that the structure of the PILs has significant impact on T_g. For instance, the anion [Tf_2N^-] and also the addition of IL to PILs can decrease the T_g point. In general, there is no significant relation between CO_2 capture performance and T_g point. However, P[VBTMA][BF_4] with the highest T_g shows the highest CO_2 sorption among the reported PILs.

It is also worth mentioning that CO_2 sorption causes a plasticization effect on PILs, which results in reduction of T_g points. Studies (Blasig, Tang, Hu, Shen, & Radosz,, 2007a) were conducted on the effect of CO_2 absorption on T_g for ammonium P[VBTMA][BF_4] and imidazolium P[VBMI][BF_4] polymers and it was found that CO_2 absorption resulted in reduction of Tg points for both polymers. The glass temperature were decreased from 236 °C to 221 °C and from 116 °C to 86 °C for P[VBTMA][BF_4] and P[VBMI][BF_4], respectively (Blasig, Tang, Hu, Shen, & Radosz, 2007a).

Table 2.5: PILs T_g in different cases and their comparison

Poly ionic liquid	T_g	Effects
PILs with same backbone		
P [VBBI][Tf_2N]	3 °C	[Tf_2N^-] can strongly decrease the T_g
P [VBBI][Sac]	40 °C	
P [VBBI][BF_4]	78 °C	
P [VBBI][PF_6]	85 °C	
Investigation on PILs by [BF_4^-] anion and different backbone		
P [BIEO][BF_4]	33 °C	The more flexible structure has the lowest T_g
P [MABI][BF_4]	54 °C	
P [VBBI][BF_4]	78 °C	
P [VBMI][BF_4]	110 °C	Methyl group has highest T_g point
Investigation on effect of [Tf_2N] anion		
(P[VBTMA][BF_4])	215 °C	
(P[MATMA][BF_4])	166 °C	
(P[VBBI][BF_4])	86 °C	
(P[VBBI]n[Tf_2N])	30 °C	[Tf_2N^-] can strongly decrease the T_g
(P[MABI][BF_4])	69 °C	

Table 2.5: Continued

Poly ionic liquid	T_g	Effects
The amount of T_g decreased for all poly (RTL)-RTL		By adding RTL to P(RTL) the T_g decreased
Poly([veim][dca])	29 °C	
Poly([veim][dca])–[emim][dca] (1 : 1)	-96 °C	
Poly([veim][dca])–[emim][BF_4] (1 : 1)	-65 °C	
Poly([veim][dca])–[emim][$B(CN)_4$] (1 : 1)	-68 °C	
Poly([vbim][dca])	-27 °C	
Poly([vbim][dca])–[emim][dca] (1 : 1)	-98 °C	
Poly([vbim][dca])–[emim][BF_4] (1 : 1)	-74 °C	
Poly([vbim][dca])–[emim][$B(CN)_4$] (1 : 1)	-70 °C	
Poly([vhim][dca])	-37 °C	
Poly([vhim][dca])–[emim][dca] (1 : 1)	-101 °C	
Poly([vhim][dca])–[emim][BF_4] (1 : 1)	-80 °C	
Poly([vhim][dca])-[emim][$B(CN)_4$] (1 : 1)	-73 °C	
[emim][dca]	-104 °C	
[emim][BF_4]	-92 °C	
[emim][$B(CN)_4$]	-82 °C	
CO_2 absorption caused a reduction on T_g		
P[VBTMA][BF_4]	236 °C	Decreased to 221 °C
P[VBMI][BF_4]	116 °C	Decreased to 86 °C

2.6.2 Thermal Stability and Degradation of PILs

PILs are generally known to have high thermal stability. However, their stability is limited by their chemical structure and backbone. Moreover, the thermal stability of PILs is related to their IL species. In certain conditions, PILs will depolymerize or degrade, nevertheless their IL species can survive (Yuan, Mecerreyes, & Antonietti, 2013). Most of the reported work employed thermo gravimetric analysis (TGA) to determine the thermal stability of polymers in specific samples (Isik, 2013). Thermal analysis was performed for MBA-cross-linked- P[VBTEA][PF_6] using a SETSYS evolution 18 thermo gravimetric analyzer (TGA) under nitrogen at a heating rate of 10 °C/min as shown in Figure 2.6. The loss in weight occurred at around 300 °C which proved good thermal stability of the PIL (Yu, 2014).

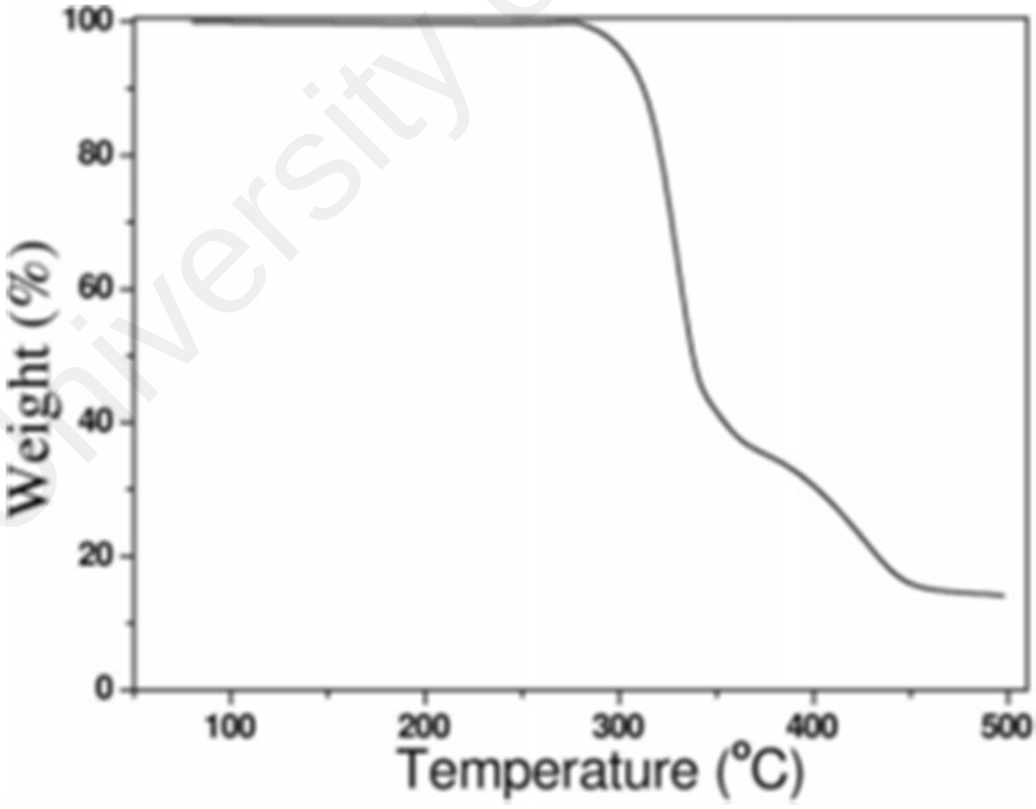

Figure 2.6: TGA curve of P[VBTEA][PF_6]. (Yu, 2014). Reproduced from (Yu , 2014) with permission of the John Wiley and Sons.

2.7 Henry's law and its impact on CO_2 loading

Henry's law is a gas law that states that the amount of dissolved gas in a liquid is proportional to its partial pressure above the liquid. In another word, Henry's law is frequently used to explain the gas solubility in liquid Equation 2-1 (J. Li, Ye, Chen, & Qi, 2012).

$$H_{(T,P)} = \lim_{x1 \to 0} f/x \cong p/x \qquad (2\text{-}1)$$

Where in Equation 2-1, H is the Henry's constant, X is the mole fraction of dissolved gas in the sorbent, f is the fugacity of vapor in the liquid phase and p is the pressure of the gas.

Henry's constants were calculated for $[C_2mim][ES]$, $[C_2mim][Tf_2N]$, $[C_4mim][Tf_2N]$, [VBTMA][PF_6] and P[[VBTMA][PF_6] and the amounts were reported to be 13.45, 10.42, 9.51, 6.59 and 1.41 respectively. Based on the equation it can be said that the lower henrys constant is belong to ionic liquids with higher CO_2 loading (Supasitmongkol & Styring, 2010). Poly ionic liquids were shown to have lower henry constant as compared to ionic liquids, for instance the reported henry constant for P[[VBTMA][PF_6]] is 1.41 in the same study.

Henry's constant for PEG with molecular weights of 150, 200, 300, and 400 were measured and the obtained amounts were 18.6, 16.9, 15.7 and 15.6, respectively. It showed that the henry's constant decreases with increasing the CO_2 loading (Li , 2012).

2.8 Heat of absorption for CO_2 absorption

The Heat of absorption is simply defined as the amount of heat absorbed or released by the reaction. The Heat of absorption were obtained for [C_2mim][ES], [C_2mim][Tf_2N], [C_4mim][Tf_2N], [C_4mpy][Tf_2N], [C_6mpy][Tf_2N], [P_{66614}][Tf_2N] and [C_6mim][OTf]. The values were -8.65, -9.36, -9.70, -9.41, -9.80, -9.16 and -8.89 (ΔH_{abs}/kJ mol^{-1} CO_2), respectively. Values confirmed that the absorbed CO_2 mechanism were physical CO_2 absorption (Supasitmongkol & Styring, 2010). The heat of absorption for PEG with molecular weights of 150, 200, 300, and 400 were obtained and reported to be -13.77, -12.40, -12.66 and -11.18 (kJ mol^{-1}). The values indicated the strength of interaction between the CO_2 and PEG in the liquid (Li, 2012; Zhijun, Haifeng, & Zhang, 2012).

2.9 Conclusion

This chapter discussed the status of the development and application of various absorbents in particular PILs for CO_2 capture. Modified polymers and their modification impact on their CO_2 capture were discussed. Moreover, various solvents impact on CO_2 capture were detailed. PILs can be prepared via various methods such as the direct polymerization of monomers, grafting or modification and blending. In general based on reviews PILs and their presence in the final polymer as polymerized monomers or modified polymers were reported to be more effective for CO_2 capture in comparison with ILs. PILs have the capability to be used as membranes, absorbents, and adsorbents, whereas ILs are mostly used as absorbents in CO_2 capture. Comparing between these three applications, membrane and absorption gave better performance than adsorption. In general, for membrane and absorption applications PEG 200 showed a superior CO_2 sorption compared to other reported sorbents and the CO_2 loading of ammonium type ionic polymers was found to be much effective that other types. Furthermore, the effect

of structure was discussed and cation effect was seemed to be more significant as compared with the anion and backbone. In terms of cation effect, ammonium-based PILs showed superior CO_2 capture. The structures of PILs and modifying chemicals as sorbents must be well understood through the implementation of further experiments as CO_2 sorbents.

CHAPTER 3: METHODOLOGY

3.1 Introduction

This chapter provides details of the materials involved, PILs synthesis, experimental techniques and data analysis used throughout the course of this work.

As mentioned earlier in the previous chapter, there are two main methods to get a new poly ionic liquid; direct polymerization of ionic liquid and modification of existing polymer. The aim of this work was to modify poly ethylene glycol to obtain poly ionic liquids with high capacity for CO_2 capture at low cost. Low molecular weight PEG (200 g/mol) is a good sorbent with high affinity to CO_2. However, low molecular weight PEG is expensive, thus, polyethylene glycol with molecular weight of 400 g/mol and 600 g/mol were used in this study. The price of poly ethylene glycol 200 is RM409/kg which is double the price of polyethylene with higher molecular weight (Sigma Aldrich Co 2018). Poly ionic liquids with cations like ammonium and imidazolium have remarkable CO_2 sorption. Hence, to produce this types of PILs, choline chloride as a cholinium based ammonium and methyl imidazole were used as based materials for cation. Furthermore, poly ethylene glycol shows a good affinity to CO_2 thus, this material was also selected to be used as polymers which serve as the back-bone in this study. Two step synthesis for PEG (400-600)-$(ChCl)_2$ and three step synthesis for PEG (400-600)-$(mImidI)_2$ were conducted. The first step was tosylation process and the method was similar for both modified PEGs. For the second step, PEG (400-600)-$(ChCl)_2$ was used to replace tosylate (Ts) in tosylated PEGs with choline chloride. Second step of synthesis for PEG (400-600)-$(mImidI)_2$ was replacing tosylate with iodide. For this tosylate intermediate were treated with sodium iodide (NaI). The final step was adding methyl imidazole to PEGs structure. To achieve the final product, PEG (400-600)-iodide were reacted with methyl

imidazole. After all the synthesis steps were carried out, characterization with FT-IR and NMR were followed. To obtain the physical properties for synthesized PILs, only PILs with 0.03 M concentration was selected as this concentration gave the best CO_2 loading. Modified PEGs as new PILs were later applied for CO_2 capture at high pressure reactor and various temperatures. Since water is used as part of solvent, it is not necessary to calculate the amount of water in synthesized PILs. Only the final concentration of PILs were measured. Figure 3.1 shows the flowchart of the overall processes used in synthesizing the poly ionic liquids for CO_2 capture.

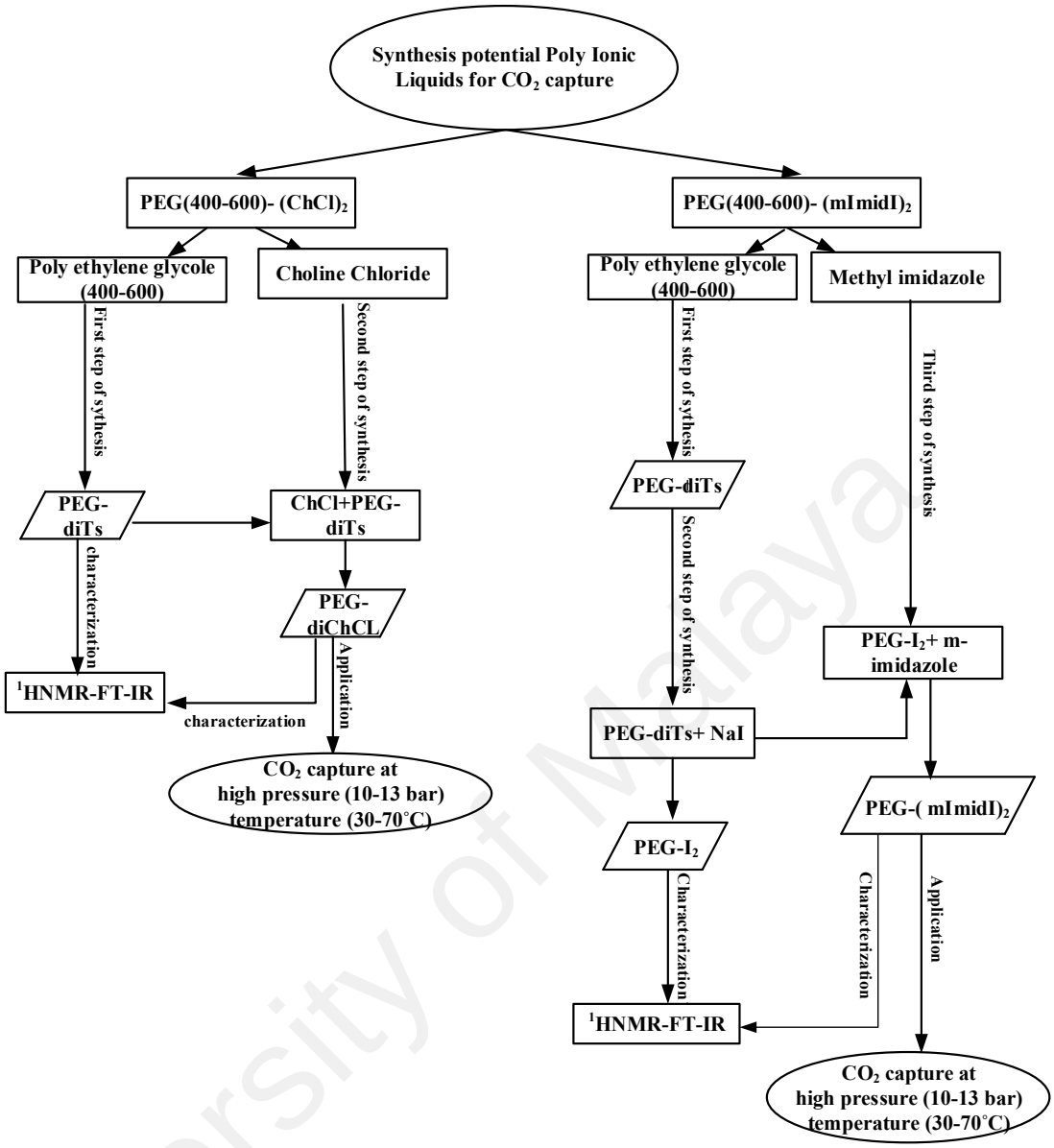

Figure 3.1: Flowchart of modification of polyethylene glycol with choline chloride/imidazole and application

3.2 Materials

The CO_2 gas used in the experiments (99.99% purity) was purchased from the Linde Group. Choline chloride and methyl imidazole (98% purity) as shown in Figure 3.2 and Figure 3.3, respectively were purchased from Sigma-Aldrich. PEG (400) and PEG (600) as shown in Figure 3.4, sodium iodide, sodium hydride, 4-toluenesulfonyl chloride

(TsCl), tetrahydrofuran (THF) and dimethylformamide (DMF) were obtained from Merck Co. Deuterated solvents for NMR were obtained from Aldrich.

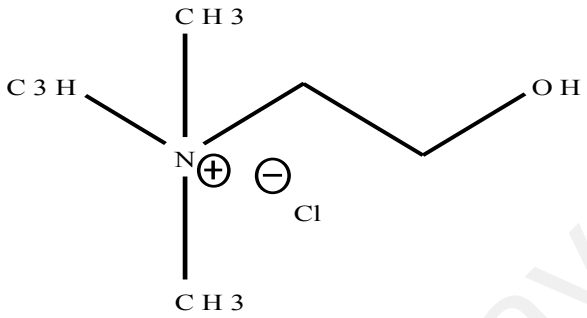

Figure 3.2: Choline chloride structure with molecular weight of 139.62 g·mol^{-1}

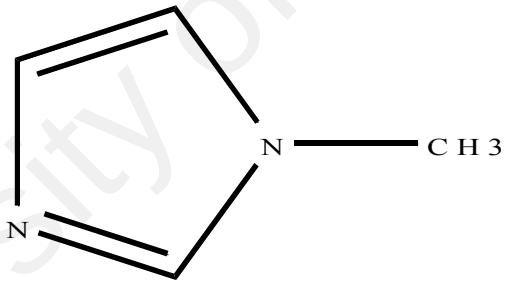

Figure 3.3: Methyl imidazole structure with molecular weight of 82.1 g·mol^{-1}

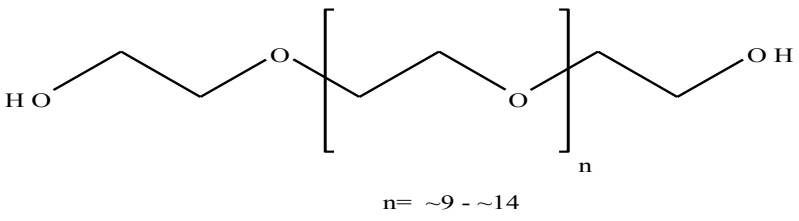

Figure 3.4: Poly ethylene glycol structure with molecular weight of 400 and 600 g·mol^{-1}

3.3 Experimental

In this work, two types of PILs were synthesized for CO_2 capture. These PILs are known as polyethylene glycol (400-600)-di choline chloride (PEG (400-600)-$(ChCl)_2$) and polyethylene glycol (400-600)-di methyl imidazolium iodide (PEG (400-600)-$(mImidI)_2$). The first step was tosylation process and the method was similar for both modified PEGs. This synthesis is an established procedure using the very famous tosylation method (Weber, Czaplewska, Baumgaertel, Altuntas, Gottschaldt, Hoogenboom, & Schubert, 2012). After the tosylation process has taken place, another step synthesis was carried out to modify polyethylene glycol with choline chloride. This is to achieve polyethylene glycol (400-600)-di choline chloride (PEG (400-600)-$(ChCl)_2$). Two more step syntheses were performed to get polyethylene glycol (400-600)-di methyl imidazolium iodide (PEG (400-600)-$(mImidI)_2$. The obtained percentage yields of products were calculated using the following Equation 3-1:

$$\% \text{ yield} = (\text{experimental yield}/\text{theoretical yield}) \times 100 \quad (3\text{-}1)$$

3.3.1 Tosylation Process

The substitution reactions of alcohols are not as easy to accomplish as those of alkyl halides. Halide ions are very weak bases and hence, they are good leaving groups. Hydroxide, on the other hand is a strong base and is not a good leaving group. Before the substitution or elimination reactions can be done on alcohols, the OH must first be converted into a good leaving group. Tosylation which is a well-known method was used for modification because of its convenience and efficiency (Kabalka, Varma, Varma, Srivastava, & Knapp Jr, 1986; Ouchi, 1990; Petersen, Yin, Kokkoli, & Hillmyer, 2010). This method includes converting alcohols to tosylates using tosyl chloride by replacing

an -OH group which will be transformed to the good leaving group (Petersen, 2010). Figure 3.5 shows the polyethylene glycol (400-600)-di Ts (PEG (400-600)-$(Ts)_2$) as an intermediate product. Thin layer chromatography (TLC) was used to indicate the conversion of starting materials. TLC is a well-known method which distinguishes materials based on their polarity. Tosylate is nonpolar and PEG- di tosylate is polar. Hence, it is a fast and an absolute way to make sure the starting materials are converted to the first step product. In addition, to convert Ts intermediate to iodide intermediate, enough treatment of tosyl derivative with sodium iodide in acetone is needed, which results in replacement of tosyl by iodine only in the primary position (Low & White, 1943).

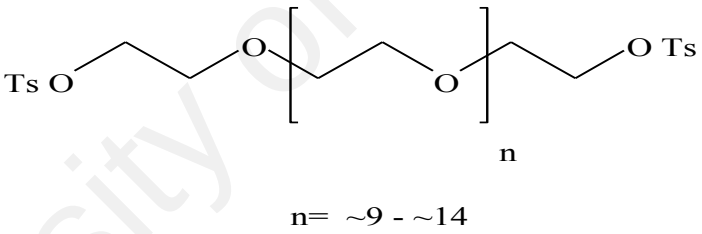

Figure 3.5: Polyethylene glycol (400-600)-di tosylate

3.3.2 Synthesis of PEG (400-600)-di tosylate

PEG (400-600)-di tosylate was synthesized from 4-toluenesulfonyl chloride (TsCl) and polyethylene glycol (400-600) in the presence of sodium hydroxide (NaOH). Tetrahydrofuran (THF) was used as a solvent in this reaction.

3.3.2.1 Synthesis of PEG 400-di tosylate

For the production of PEG 400-$(OTs)_2$, based on the structure of product, the amount of materials calculated per mmol, PEG 400 (1.78 ml, 5 mmol) and sodium hydroxide (0.44 g, 11 mmol) were added to 50 ml THF in a 100-mL flask equipped with a magnetic stir bar and was stirred for one (1) hour, followed by the addition of TsCl (2.86 g, 15 mmol). The mixture was stirred overnight at room temperature. After that, conversion of the starting materials was indicated with thin layer chromatography (TLC). Purification of the product involved five stages; Reaction solvent mixture was initially filtered to remove the excess solid material, then, the evaporation of the reaction solvent was carried out in vacuum, followed by liquid extraction using dichloromethane (DCM) and water. The product which was in DCM phase was then evaporated to remove the DCM. The product, a yellowish liquid, was later washed with n-hexane to remove the unreacted TsCl.

3.3.2.2 Synthesis of PEG 600-di tosylate

To synthesize PEG 600-$(OTs)_2$ starting materials including, PEG 600 (1.77 ml, 3.33 mmol) sodium hydroxide (0.29 g, 7.33 mmol) and 50 ml THF were placed in a round bottom flask equipped with magnetic stir bar and was stirred continuously. After one (1) hour, TsCl (1.90 g, 9.99 mmol) was added to the reaction flask. The reaction was carried out overnight at room condition. Completion of the reaction was confirmed with TLC. Then, the purification steps were carried out to obtain PEG 600-di tosylate. Initially, the reaction solvent was filtered off and the evaporation was conducted to remove all the solvent completely. Liquid extraction was carried out by DCM and water to extract unreacted materials from the product. DCM containing product was vacuumed to remove

DCM. Finally, the unreacted TsCl was washed and removed with n-hexane and a yellowish liquid was collected as a PEG 600-di tosylate.

3.3.3 General Procedure for Synthesis of PEG (400-600)-di choline chloride

The second and the final step of synthesis PEG (400-600)-di choline chloride is to replace tosylate with choline chloride as a final product. The reaction was conducted at room temperature in a stirrer containing flask overnight. Figure 3.6 shows the general procedure for synthesis of PEG (400-600)-di choline chloride. The tosylate of PEG (400-600)-di tosylate were replaced by choline chloride to obtain the final product. NaH as a strong base was used and the reaction was carried out using DMF as a solvent which resulted in high dissolution of the starting materials.

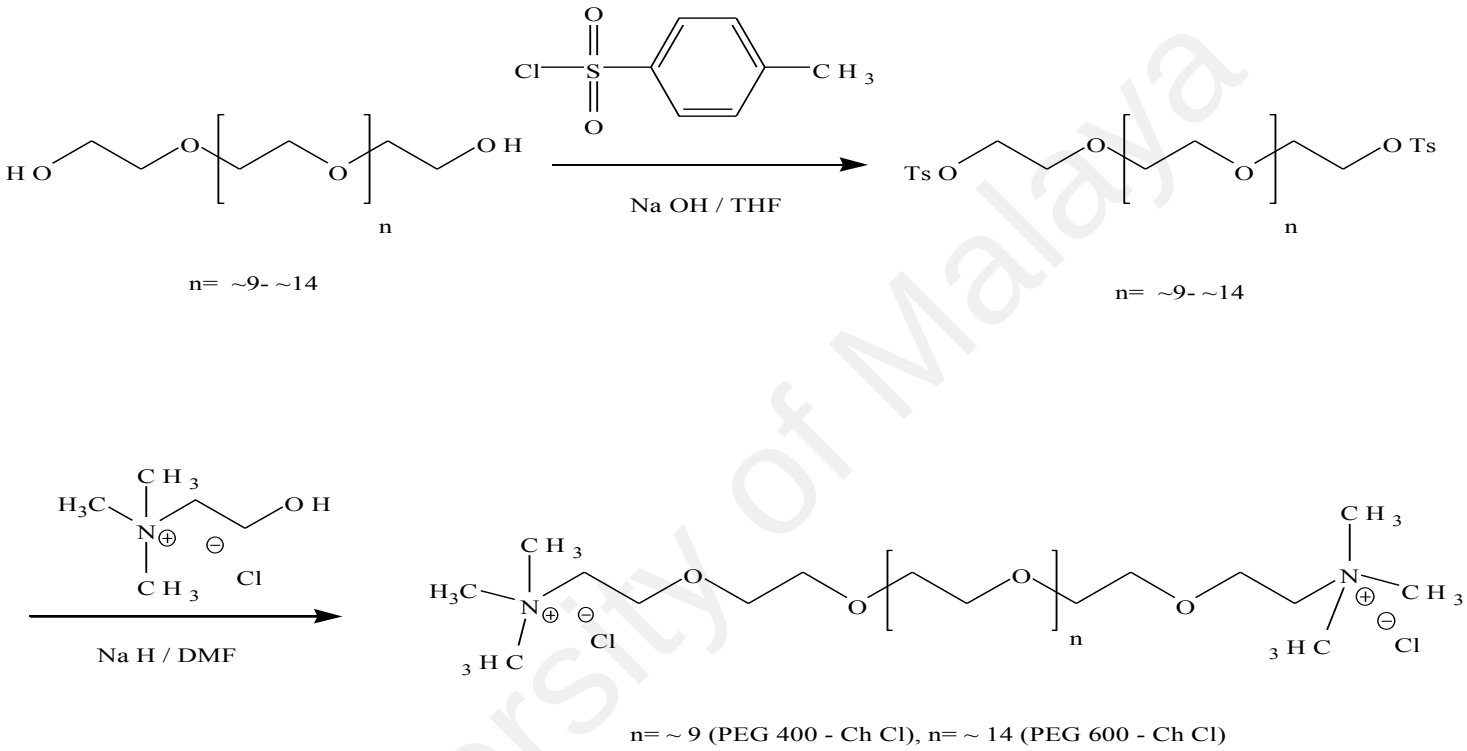

Figure 3.6: General procedure for synthesis of PEG (400-600)-di choline chloride

3.3.4 Synthesis of PEG 400-di choline chloride

To synthesize the PEG 400-di choline chloride, choline chloride (0.43 g, 3.08 mmol) and sodium hydride (0.083 g, 3.48 mmol) were added to 50 ml DMF and mixed thoroughly. After one hour, the reaction was followed by adding PEG 400-$(OTs)_2$ (1.0 g, 1.34 mmol) to the mixture. The reaction was continued while stirring overnight. After all the residue was removed by filtration, the solvent was evaporated to remove the DMF completely. The product was in the form of highly viscous yellow colour liquid.

3.3.5 Synthesis of PEG 600- di choline chloride

The synthesis procedure of PEG 600-$(ChCl)_2$ was identical to PEG 400-$(ChCl)_2$, with the only difference being the amount of choline chloride (0.34 g, 2.43 mmol) and the amount of sodium hydride (0.066 g, 2.75 mmol). Firstly, all choline chloride, sodium hydride and 50 ml DMF were placed in the reaction flask and was stirred vigorously for one (1) hour, this was followed by the addition PEG 600-$(OTs)_2$ (1.0 g, 1.058 mmol) to the mixtures. The reaction was carried out overnight. After filtration and solvent evaporation, the highly viscous liquid was obtained as a product.

3.4 General Procedure for Synthesis of PEG (400-600)-di methyl imidazolium iodide

Two-step synthesis were accomplished to get PEG (400-600)-di methyl imidazolium iodide from the PEG tosylated derivative, involving iodination process and addition of methyl imidazole to PEG (400-600)-di iodide.

3.4.1 Synthesis of PEG (400-600)-di iodide

To attain the PEG (400-600)-di iodide, the tosylate derivative which was synthesized previously were iodinated by the treatment with NaI dissolved in acetone under stirring condition. Figure 3.7 shows the structure of PEG (400-600)-di iodide.

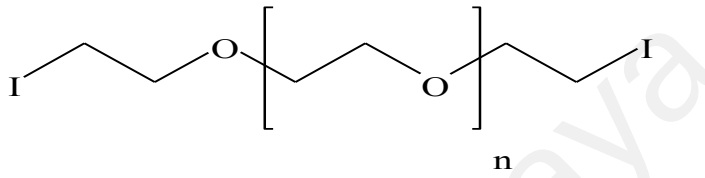

n= ~ 9 (PEG 400-d i I), n= ~ 14 (PEG 600-d i I)

Figure 3.7: PEG (400-600)-di iodide structure

3.4.1.1 Synthesis of PEG 400-di iodide

PEG 400- $(OTs)_2$ (5 g, 6.9 mmol) was dissolved in acetone (50 mL) in a 100-mL round bottom flask equipped with a stirring bar. The mixture was treated by sodium iodide (8.2 g, 55 mmol) for 8 hours. The completion of reaction was confirmed by TLC. The organic solvent was evaporated. The residue was taken up in DCM and washed by water; afterwards, sodium thiosulfate solution was added in to remove the excess iodine. Lastly, the solution was washed with brine to remove the organic phase. DCM was extracted and dried over $MgSO_4$. Finally, after the evaporation the clean yellow liquid (PEG 400- di iodide) was obtained.

3.4.1.2 Synthesis of PEG 600-di iodide

First PEG 600- $(OTs)_2$ (4 g, 4.3 mmol) was treated by sodium iodide (5 g, 34 mmol) in acetone (50mL) under stirring condition for 8 hours. The procedure was identical to

PEG 400-di iodide synthesis. TLC was also used to confirm the reaction. The purification of product requires seven stages. Firstly, the acetone was removed by vacuum and then, DCM and water extraction were carried out. For further purification, sodium thiosulfate solution and brine treatment were followed respectively. Next, DCM was first dried with $MgSO_4$ and then, vacuumed for complete removal of it. Finally, the yellowish viscous liquid product was obtained.

3.4.2 Synthesis of PEG (400-600)-di methyl imidazolium iodide

The final step of synthesis for PEG (400-600)-di methyl imidazolium iodide was reacting the methyl imidazole with PEG (400-600)-di iodide. The reactions were carried out under reflux condition for 12 hours. The total reaction procedure is shown in Figure 3.8.

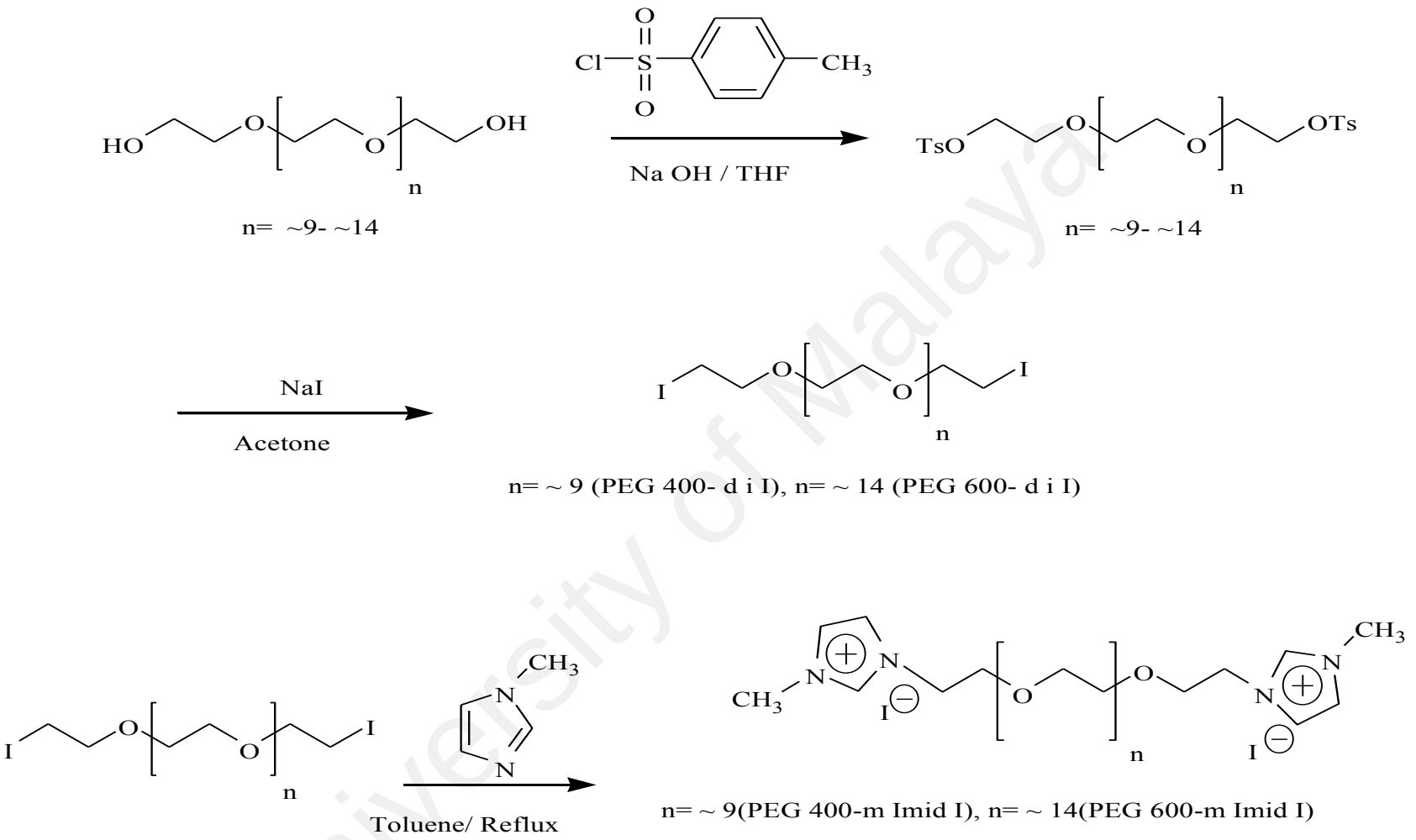

Figure 3.8: The total reaction procedure for PEG (400-600)-di methyl imidazolium iodide

3.4.2.1 Synthesis of PEG 400-(mImidI)$_2$

For the synthesis of PEG 400-(mImidI)$_2$, the PEG (400)-di iodide (3.8 g, 5.6 mmol) and 1-methyl imidazole (0.9 g, 11 mmol) were reacted in 40 mL toluene. The reaction was carried out under reflux condition for 12 hours. The completion of the reaction was confirmed by ionic liquid layer observation. The organic layer was then separated and the residue was washed with 10 mL toluene for 3 times. The pure PEG 400-(mImidI)$_2$ was obtained after the evaporation of toluene under vacuum at low pressure.

3.4.2.2 Synthesis of PEG 600-(mImidI)$_2$

Synthesis procedures, for PEG 600-(mImidI)$_2$ are the same as PEG 400- (mImidI)$_2$ except that the amount of reactants and solvent were different. PEG 600- di iodide (2.95 g, 3.5 mmol) and 1-methyl imidazole (0.58 g, 7.1 mmol) were reacted in 20 mL toluene for 12 hours.

3.5 Polymer Characterization

Fourier transform infrared spectroscopy (FT-IR) (Bruker Tensor 27 FT-IR & OPUS device) at the range of 500-3500 cm^{-1} was used to characterize the PILs. The characterization was also performed by proton nuclear magnetic resonance (^{1}H-NMR) using ($CDCl_3$, DMSO-d_6 and CD_3OD) solution (6% wt) and 5mm NMR tubes at ambient temperature in a Varian Spectrometer 400 MHz (7.05 T of magnetic) and a Bruker Spectrometer 400 MHz (9.4 T of magnetic).

3.6 Physical Properties

The physical properties of aqueous PILs i.e., density and viscosity were performed. Density were carried out using Mettler Toledo density meter instrument. The apparatus was precise within 1.0 $x10^{-4}$ g cm^{-3}, and the measurement uncertainty was estimated to be better than 0.001 g cm^{-3}. Viscosity were performed using Brookfield LV DV-II+pro extra viscometer with the accuracy of less than 3%. The density and viscosity were measured at different temperatures ranging from 25 ºC to 80 ºC for aqueous PILs (0.03 M).

3.7 Thermal Gravimetric Analysis (TGA)

Thermo or thermal gravimetric analysis (TGA) is considered as the common samples testing which defines changes in weight to a temperature program in a controlled atmosphere. TGA is a process which involves heating a sample to a high enough temperature until the components in the sample decompose. The TGA analyzer involves a high-accurate balance with a platinum pan which is loaded with sample that is heated and cooled during the experiment. The atmosphere may be supplied with an inert gas to prevent oxidation or other undesired reactions. In this work, TGA (Q500 SDT model) was used to assess the thermal stability of synthesized PILs. Thermal stability was also investigated using TGAQ500 SDT model. TGA was performed with sample weight: ~10 mg, between 25 $^{\circ}$C to 400 $^{\circ}$C for 30 min, and heating ramp rate of 15 $^{\circ}$C min^{-1} in a nitrogen atmosphere.

3.8 Solubility of CO_2 at Various Pressure and Temperatures in Synthesized PILs

Table 3.1 and Table 3.2 show the concentration of aqueous solutions of PEG (400-600)-di choline chloride and PEG (400-600)-di methyl imidazolium iodide used for CO_2 capture at various pressures and temperatures.

Table 3.1: PEG (400-600)-di choline chloride at various temperatures and pressures for CO_2 capture

PIL	mol/L	T/°C	P/bar
PEG 400-di choline chloride	0.03 M	30, 50, 70°C	9.8
			10.3
			13.4
PEG 600-di choline chloride	0.03 M	30, 50, 70°C	9.8
			10.3
			13.4

Table 3.2: PEG (400-600)-di methyl imidazolium iodide at various temperatures and pressures for CO_2 capture

PIL	mol/L	T/°C	P/bar
PEG 400-di methyl imidazolium iodide	0.03 M	30, 50, 70°C	9.8
			10.3
			13.4
	0.055 M, 0.1 M	30°C	5
			9.8
			10.3
			13.4
PEG 600-di methyl imidazolium iodide	0.03 M	30, 50, 70°C	9.8
			10.3
			13.4
			10.3
			13.4

3.9 CO_2 Absorption Using PEG (400-600)-di choline chloride and PEG (400-600)-di methyl imidazolium iodide

The set-up as shown in Figure 3.9 was used to perform the CO_2 capture experiment. A stirred stainless steel equilibrium cell reactor was used for CO_2 absorption. The cell was equipped with a welded stirrer assemble, a thermocouple, an inlet gas tube and air vent tube. The thermocouple had the accuracy of ± 0.1 K. Firstly, to remove the air from the gas reservoir, sufficient flow of CO_2 was purged throughout the operation system. Then, before the gas reservoir tank was heated and pressurized, it was loaded with purified CO_2 from the storage tank.

After adding 20 ml sample into the equilibrium cell, it was closed tightly. The gas reservoir was pressurized to the desired pressure. Throughout the experiment, the temperature was kept constant at desired temperature and the solvent was stirred continuously. The total CO_2 pressure was regulated using PCV (pressure control valve). CO_2 gas was fed from the gas reservoir vessel to the reaction cell through an automated pressure control valve during the CO_2 absorption process. Following the contact of CO_2 with the solutions, the total systems' pressure dropped gradually, and equilibrium was considered reached after the pressure in the cell reactor remained constant for at least half an hour. The initial and final pressure of CO_2 in the gas reservoir and in the reaction cell were used to calculate the amount of CO_2 absorbed by the aqueous solutions of PEG (400-600)- $(ChCl)_2$ and PEG (400-600)-$(mImidI)_2$. The pressure and temperature of the equilibrium cell were reported as the equilibrium conditions for CO_2 loading data.

The absorption experiment was conducted with a fixed concentration of synthesized PILs of 0.03 M at a pressure range of 10 to 13 bar and a temperature ranging from 30 $^{\circ}$C to 70 $^{\circ}$C. In addition, for the study on concentration impact on CO_2 sorption, another experiment has been designed in higher concentration for PEG 400-$(mImidI)_2$ 0.055 M and 0.1 M at pressure range of 5-13 bar at room temperature. The set-up was designed to have accurate absorption measurements with low consumption of samples (20 ml).

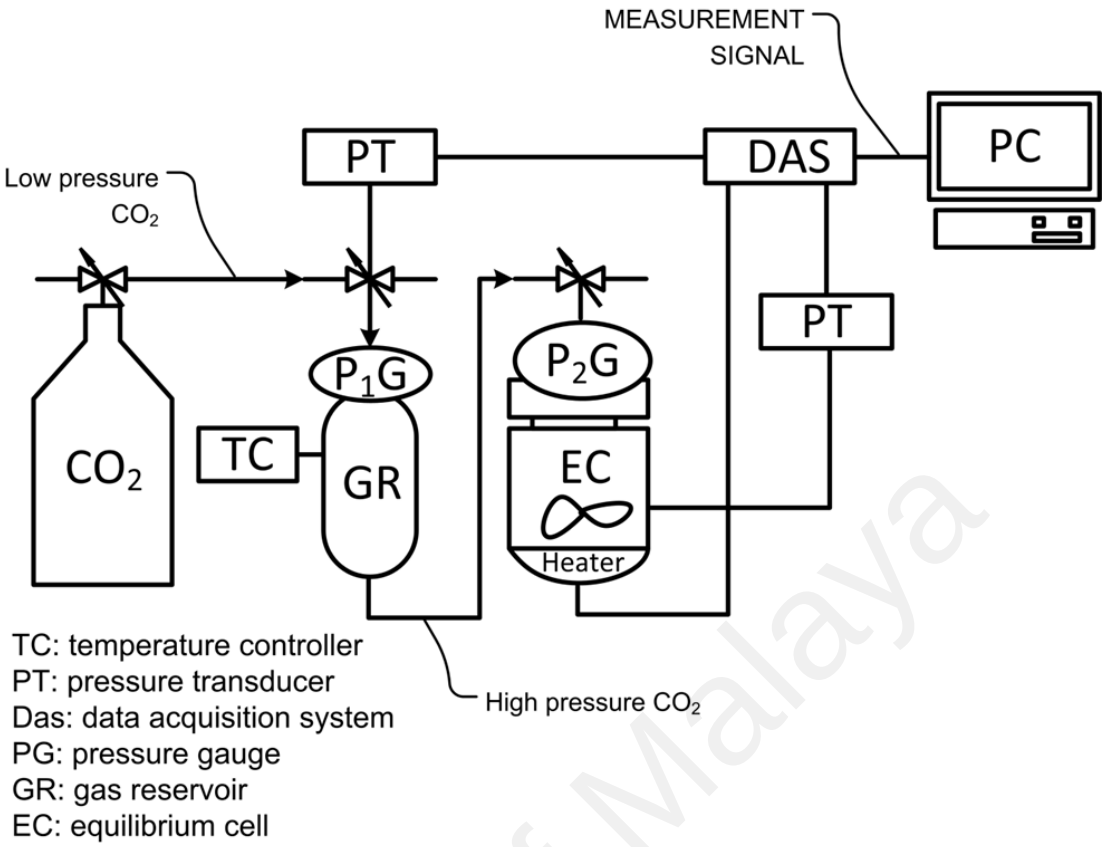

Figure 3.9: Schematic diagram of the experiment set-up for CO_2 absorption

3.9.1 CO_2 Loading Calculation Techniques

The following equations were used for calculating the amount of CO_2 absorbed in the solution (n_{CO2}). The volume of gas in the equilibrium cell, V_{EC} was attained from Equation 3-2 as follows:

$$\mathbf{V_{EC} = V_{EC,t} - V_L} \tag{3-2}$$

With an accuracy of ±0.1 ml. $V_{EC,\,t}$ is the total volume of the equilibrium cell and V_L is the volume of existing solution in the cell. The amount of CO_2 absorbed was obtained using Equation 3-3:

$$n_{CO_2} = \frac{V_{GR}}{RT}\left(\frac{P_{GR,1}}{Z_{R,1}} - \frac{P_{GR,2}}{Z_{R,2}}\right) + \frac{V_{EC}}{RT}\left(\frac{P_{EC,1}}{Z_{C,1}} - \frac{P_{EC,2}}{Z_{C,2}}\right) \quad (3\text{-}3)$$

Where, V_{GR} is the volume, $P_{GR,\,1}$ and $P_{GR,\,2}$ are the initial and final pressures of the gas reservoir respectively, Z_R is compressibility factor of the gas and $P_{EC,\,1}$ and $P_{EC,\,2}$ are the initial and final pressures of the equilibrium cell. The CO_2 loading in the liquid phase is calculated using Equation 3-4:

$$n_{CO_2} = \frac{n_{CO_2}}{m} \quad (3\text{-}4)$$

Where m is the mole of PEG (400-600)-$(ChCl)_2$ and PEG (400-600)-$(mImidI)_2$ that was charged into the cell, n_{CO_2} is loading which is the moles of CO_2 per mole of PEG (400-600)-$(ChCl)_2$ and PEG (400-600)-$(mImidI)_2$.

3.9.2 Physical CO_2 Absorption Based on Henry's Constant (H)

In this study, we present Henry's constant, as a thermo physical concept, which is related to gas solubility in aqueous solution. Henry's constant, a thermo physical property that is related to gas solubility in liquid, for the system CO_2-aqueous PEG (400-600)-$(ChCl)_2$ and CO_2-aqueous PEG (400-600)-$(mImidI)_2$ was obtained in this work. The CO_2 loading capacities for physical solvents are directed by their ability to dissolve gas at given gas phase partial pressure (Henry's law constant).

Based on the absorption results for PEG (400-600)-$(ChCl)_2$, PEG (400-600)-$(mImidI)_2$ and PEG (400-600), the corresponding Henry's constant (H) values were obtained. The Henry's constant (H) values were obtained using Equation 3-5:

$$\mathbf{K_H = \frac{L_{solution} \cdot bar}{mole_{gas}}} \quad (3\text{-}5)$$

In the above equation which is K= P/C, P is the partial pressure of the solute in the gas above and K is a constant with the dimensions of pressure divided by concentration.

Based on Equation 3-5, the Henry's constants increase as pressure raises, but decrease as the concentration of the CO_2 in the solution increases, so, it can be said that Henry's constant has reverse relation with CO_2 concentration in the aqueous solutions.

3.9.3 Enthalpy of Absorption

A major value for the evaluation of the energy for CO_2 capture is the enthalpy of absorption which includes the enthalpy of CO_2 dissolution (CO_2, g CO_2, l). The enthalpy of dissolution is exothermic and the heat of absorption is released in the absorber (Wappel, Gronald, Kalb, & Draxler, 2010). Moreover, the same amount of energy is needed to release the CO_2 from the loaded solvent. Enthalpy of absorption can be directly calculated using the van't Hoff Equation as follows:

$$\left(\frac{\mathbf{d\ ln}\, K_H}{\mathbf{d}(1/\mathbf{T})}\right) = \frac{\mathbf{\Delta H}}{\mathbf{R}} \quad (3\text{-}6)$$

Where K_H is Henry's constant , T is temperature and R is gas constant (Kim, Hoff, & Mejdell, 2014). By measuring the equilibrium Henry constant, K_H, at different temperature the van't Hoff plot can be used to assess a reaction when temperature changes. Heat of absorption of CO_2 in systems (PIL + H_2O) were calculated at temperatures ranging from 30 °C to 70 °C for four synthesized PILs using the Equation 3-6.

3.10 Regeneration of Synthesized PILs

Regeneration of solvents was carried out to reduce costs and material consumption, improving work efficiency and minimizing the negative effect on environment. The regeneration process was performed at atmospheric pressure after each cycle of CO_2 absorption into the aqueous PILs were completed. The regeneration temperature and duration were 90-100 ºC and 20 min, respectively. The CO_2 loaded solvent was heated at temperature between 90-100 ^oC in the beaker while stirring continuously to ensure all the CO_2 was removed. As desorption of CO_2 is much faster than the CO_2 absorption process, desorption duration of 20 min was found to be sufficient to ensure all CO_2 to be removed from the aqueous PILs. In this study, the absorption and desorption of the similar sample of PILs were carried out repeatedly for three cycles.

CHAPTER 4: RESULTS AND DISCUSSION

4.1 Introduction

This chapter is aimed to discuss the results on the synthesis and characterization of PEG based PILs which are PEG (400-600)-$(ChCl)_2$ and PEG (400-600)-$(mImidI)_2$ and also to evaluate the performance of the aqueous solution of these synthesized PILs for CO_2 capture. The CO_2 solubility was measured at various temperatures (30 ˚C, 50 ˚C, 70 ˚C) and pressure range of (5 to 13 bar). Data are reported as loading capacity (mol CO_2/mol PIL). In addition, the densities and viscosities of aqueous solution of PIL were determined. The Henry's law constants were also calculated and compared to other works. Enthalpy of CO_2 absorption using synthesized PILs were also obtained. Furthermore, a study on the regeneration of the aqueous PEG (400-600)-$(ChCl)_2$ and PEG (400-600)-$(mImidI)_2$ after CO_2 absorption were also performed.

4.2 Synthesis Procedure for Tosylation Reaction

As previously mentioned in the methodology chapter, tosylation method was applied for the synthesis of PEG (400-600)-di ts using 4-toluensulfonyl chloride (TsCl) to achieve good intermediate as good leaving group. Figure 4.1 shows the reaction of PEG (400-600) with TsCl. These reaction conditions require vigorous stirring. At the end, -OHs of PEG were replaced with -OTs and the PEG (400-600)-di tosylate was obtained as a product with high yield.

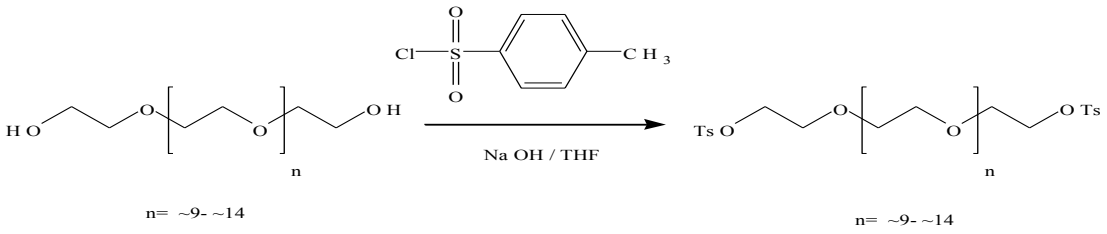

Figure 4.1: Reaction of PEG (400-600) with TsCl

4.2.1 Synthesis and ^{1}H NMR Results of PEG 400-di tosylate

Figure 4.2 Shows the substitution reactions for both PEG 400 and PEG 600 which were successfully converted to tosylate products; TsO- CH_2 (O-CH_2-CH_2-O)$_n$ CH_2 –OTs. The structure and ^{1}H NMR spectra for PEG 400- di tosylate are shown in Figure 4.2. The conversion and the amount of product obtained was determined to be 76% and 2.8 g respectively. ($CDCl_3$, 400 MHz, 25 $^{\circ}$C): δ 7.35, 7.8 (m, 8H aromatic ring), 4.2 (m, 4H, 2 CH_2-OTs), 3.6 (m, 32H, -CH_2 (O-CH_2-CH_2-O)n CH_2-), 2.44 (s, 6H, CH_3). In addition, conversion of the starting materials was confirmed with thin layer chromatography (TLC). TLC confirmed the conversion of starting materials to tosylated product as shown in Figure 4.3. As can be seen in this Figure (a, b, c), there is a spot at the left hand side which indicates the presence of tosylate (non-polar). Whereas, the spot on the right hand side confirmed the presence of tosylate in a new compound which was polar.

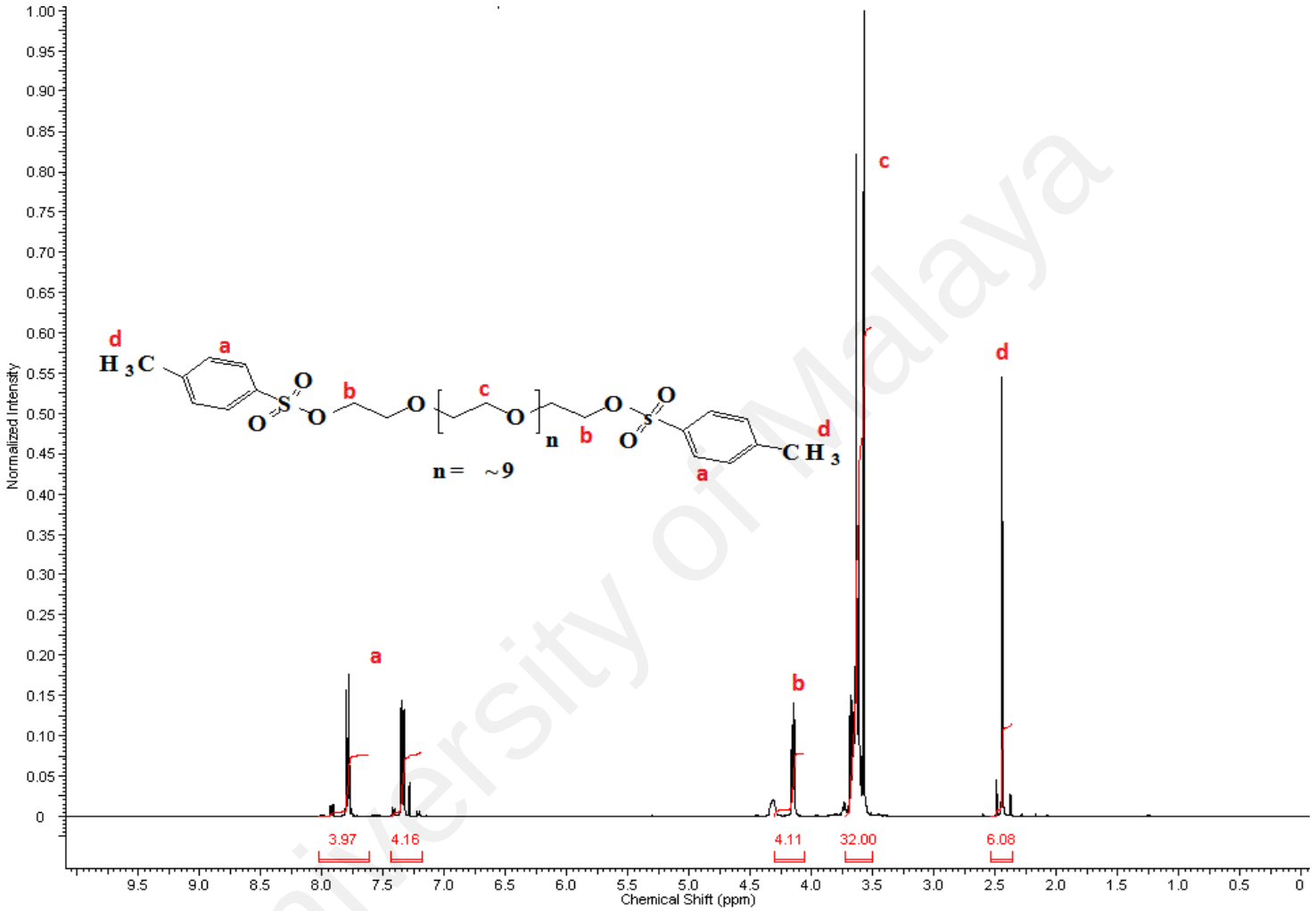

Figure 4.2: ^{1}H NMR spectra of PEG 400-di tosylate

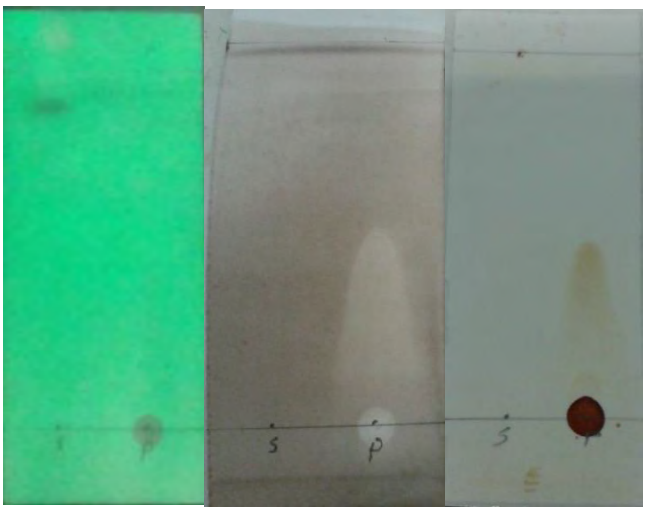

Figure 4.3: TLC analysis with different indicators a) UV indicator, b) with sulphuric acid indicator, c) with Iodide indicator

4.2.2 Synthesis and ^{1}H NMR Results of PEG 600-di tosylate

For production of PEG 600-$(OTs)_2$, the solution was added to 50 ml THF in a 100-mL flask and stirred for one (1) hour, followed by the addition of TsCl. The process was left overnight at room temperature. The ^{1}H NMR spectra and related structure for PEG 600-di tosylate are shown in Figure 4.4. The yield of reaction was 81% and the product obtained was 2.55 g. ^{1}H NMR ($CDCl_3$, 400 MHz, 25 $^{\circ}$C): δ 7.35, 7.8 (m, 8H aromatic ring), 4.2 (m, 4H, $2CH_2$-OTs), 3.6 (m, 52H, -CH_2 (O-CH_2-CH_2-O)$_n$ CH_2-), 2.45 (s, 6H, CH_3). ^{1}H NMR of the product confirmed tosyl rings features at 7.35 ppm and 7.8 ppm for both PEG (400-600)-di tosylate. The spectras are identical except the PEG backbone numbers, which are 36 for PEG 400-di tosylate and 56 for PEG 600-di tosylate.

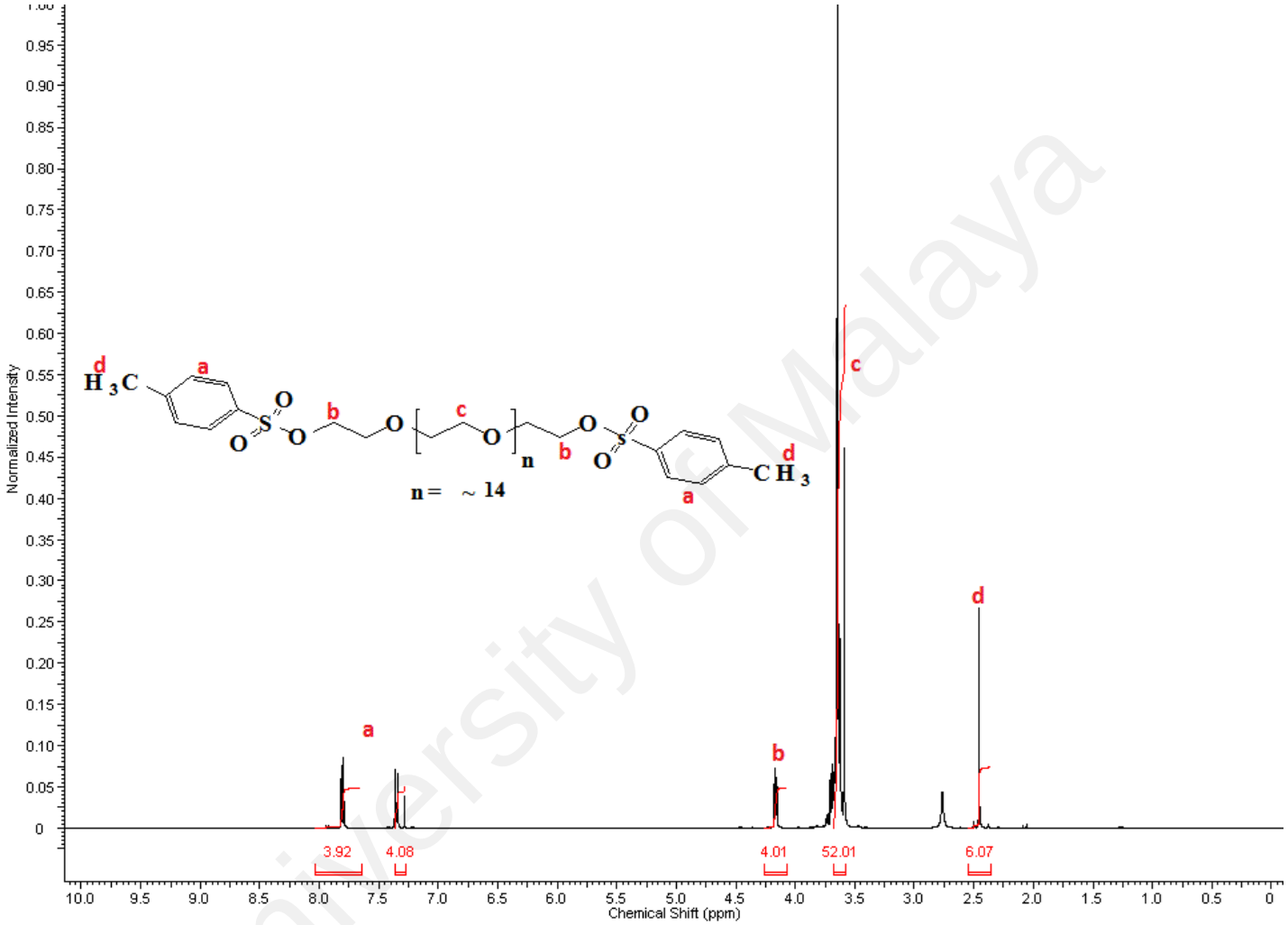

Figure 4.4: ^{1}H NMR spectra of PEG 600-di tosylate

4.3 Synthesis Procedure of PEG (400-600)-di choline chloride

PEG (400-600)-di choline chloride were synthesized from PEG (400-600)-di ts through reaction with choline chloride. A strong base (NaH) is used to attain high conversion of product. DMF was employed as a solvent for high solubility of starting materials.

4.3.1 Synthesis and ^{1}H NMR Results of PEG 400-di choline chloride

PEG 400-di choline chloride was further synthesized by adding choline chloride and sodium hydride into 50 ml DMF containing flask and was mixed thoroughly. After one (1) hour the reaction was followed by adding PEG 400-$(OTs)_2$ to the mixture. The reaction was carried out in stirring condition overnight. The residue was then removed by filtration and the solvent was evaporated to remove the DMF completely. The amount of 0.71 g of highly viscous yellow colour liquid product was collected and the yield of reaction was 82%. Progress of the polymerization can be monitored using ^{1}H NMR. A series of ^{1}H NMR spectra (in DMSO) was used to identify the reaction completion. The structure and ^{1}H NMR PEG 400-di choline chloride are shown in Figure 4.5. ^{1}H NMR (DMSO, 400 MHz, 25 $^{\circ}$C): δ 3.6 (m, 18H CH_3, 8 CH_2-CH_2-N, 36 -CH_2 (O-CH_2-CH_2-O)n CH_2-). Total numbers of 62 H was obtained from 26 H in choline chloride and 36 H in PEG backbone. The chemical shift from 3.5 to 4 confirmed the presence of the product.

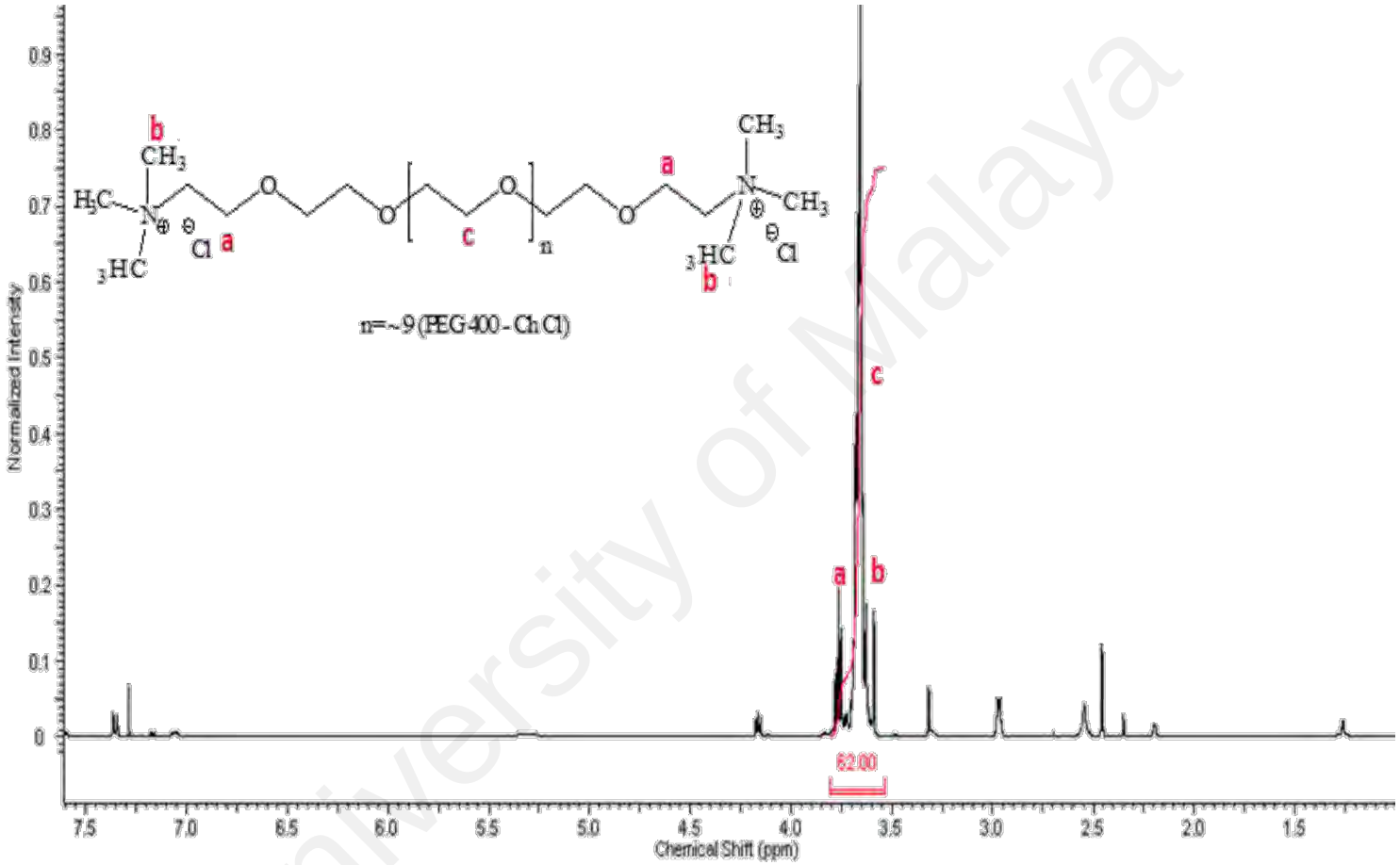

Figure 4.5: ^{1}H NMR spectra of PEG 400-di choline chloride

4.3.2 Synthesis and ^{1}H NMR Results of PEG 600- di choline chloride

A similar procedure was repeated for the synthesis PEG 600-$(ChCl)_2$ with a different amount of chemicals which were mentioned earlier in the Methodology chapter. Initially, choline chloride, sodium hydride and DMF were placed in the reaction flask and stirred vigorously for an hour, the reaction followed by the addition PEG 600-$(OTs)_2$ to the mixtures. The reaction was carried out overnight. After the residue filtered, then the solvent was evaporated, 0.67 g highly viscous liquid obtained as product a yield of 75%. Structure and ^{1}H NMR PEG 600-di choline chloride are shown in Figure 4.6. ^{1}H NMR (DMSO, 400 MHz, 25 $^{\circ}C$): δ 3.65 (m, 18H CH_3, 8 CH_2-CH_2-N, 56 -CH_2 (O-CH_2-CH_2-O)n CH_2-). The only difference between PEG 400-$(ChCl)_2$ and PEG 600-$(ChCl)_2$ was the number of hydrogens in the backbone, which were 56 for PEG 600-$(ChCl)_2$ and 36 for PEG 400-$(ChCl)_2$.

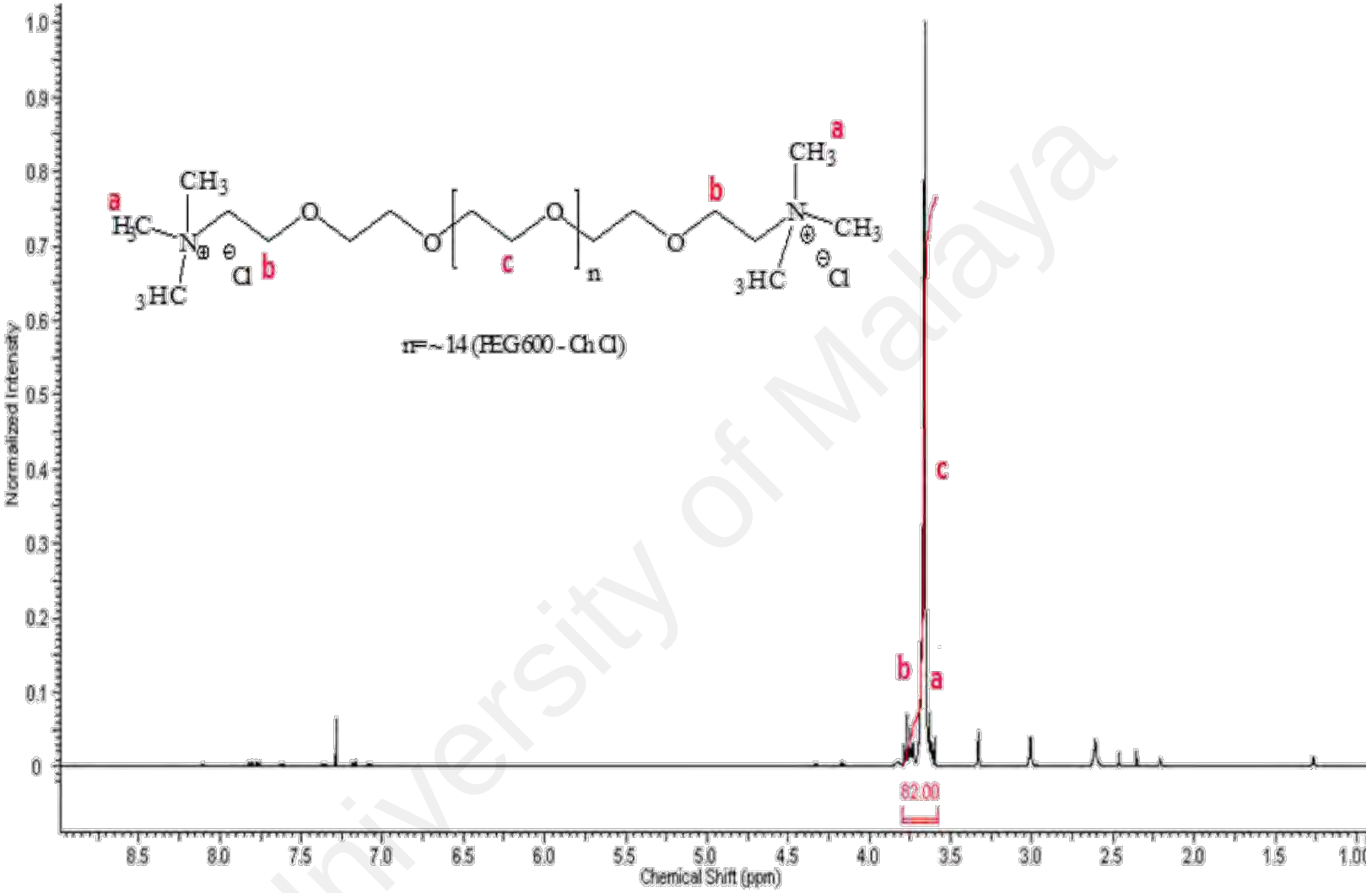

Figure 4.6: ^{1}H NMR spectra of PEG 600-di choline chloride

4.4 Synthesis of PEG (400-600)-di methyl imidazolium iodide

There were two steps in the syntheses of PEG (400-600)-(mImidI)$_2$. After preparing the PEG (400-600)-di ts, the tosylate intermediate undergone the substitution reaction with iodide. Thus, the reaction proceeds through iodination process to give iodide intermediate. The iodide intermediate at that time reacted with 1-methyl imidazole to attain a final product which was PEG (400-600)-(mImidI)$_2$.

4.4.1 Synthesis and ^{1}H NMR Results of PEG 400-di iodide

To attain the iodine intermediate, a pre-determined amount of PEG 400-(OTs)$_2$ was dissolved in acetone in a 100-mL round bottom flask in stirring condition. It was treated by sodium iodide for 8 hours. TLC confirmed the completion of reaction. The organic solvent was evaporated. Residue was taken up in DCM and washed with water. The excess iodine was removed by adding thiosulfate solution and lastly, the solution was washed with brine to clear the organic phase. $MgSO_4$ was utilized to dry the DCM. At the end, without further purification, 3.8 g of clean yellowish liquid was obtained with the yield of 81%. The ^{1}H NMR spectra fully confirmed the expected structures of PEG 400-di iodide. ^{1}H NMR ($CDCl_3$, 400 MHz, 25 $^{\circ}$C): δ 3.75 (t, 4H-CH_2O), δ3.65 (m, 36H, -CH_2 (O-CH_2-CH_2-O)$_n$ CH_2-), δ 3.25(t, 4H CH_2-I). Figure 4.7 shows the structure and ^{1}H NMR spectra for PEG 400-di iodide. Four hydrogens belong to CH_2-O are appeared at δ 3.75 and four hydrogens for CH_2-I are appeared at lower δ 3.25. Moreover, since the picks from δ 7 to 8 were not detected it was confirmed that the aromatic rings are not exist in product.

Figure 4.7: ^{1}H NMR spectra of PEG 400-di iodide

4.4.2 Synthesis and ^{1}H NMR Results of PEG 600-di iodide

As mentioned earlier, to synthesize PEG 600-di iodide, a pre-determined amount of PEG 600-$(OTs)_2$ was treated with sodium iodide in acetone under stirring condition for 8 hours. The procedure was identical to PEG 400-di iodide synthesis. TLC confirmed the completion of reaction. Purification of product involved seven stages. The solvent was vacuumed completely. DCM and water extraction occurred for further purification followed by sodium thiosulfate solution and brine respectively. DCM then dried with $MgSO_4$ and vacuumed until complete removal. Finally, 3.1 g yellowish viscous liquid product was obtained and the yield of reaction was 82%. ^{1}H NMR ($CDCl_3$, 400 MHz, 25 $^{\circ}$C): δ 3.75 (t, 4H CH_2-O), δ3.65 (m, 56H, -CH_2 (O-CH_2-CH_2-O)$_n$ CH_2-), δ 3.25(t, 4H CH_2-I). The structure and ^{1}H NMR spectra for PEG 600-di iodide are shown in Figure 4.8.

Figure 4.8: ^{1}H NMR spectra of PEG 600-di iodide

4.4.3 Synthesis and ^{1}H NMR Results of PEG 400-di methyl imidazolium iodide

The final synthesis of PEG 400-(mImidI)$_2$ was conducted by adding PEG 400-di iodide and 1-methyl imidazole in 40 mL of toluene. The amounts of chemicals were pre-determined earlier. The reaction was carried out under reflux condition for 12 hours. Formation of ionic liquid layer indicates the complete reaction. The residue was washed using 10 mL toluene (3 times). The pure PEG 400-(mImidI)$_2$ was collected after evaporation of solvent under pressure. The amount and the yield of product were 4.35 g and 87%, respectively. Figure 4.9 shows the final products structure and ^{1}H NMR spectra for PEG 400-(mImidI)$_2$. ^{1}H NMR (CD_3OD, 400 MHz, 25 $^{\circ}$C): δ 9 (s, 2H, N=CH-N), δ 7.70(s, 2H N-CH=CH-N), δ 7.60(s, 2H, N-CH=CH-N), δ 4.7(t, 4H, CH_2-O), δ 4(s, 6H, CH_3-N), δ 3.9(t, 4H, N-CH_2), δ 3.6(m, 36 -CH_2 (O-CH_2-CH_2-O)$_n$ CH_2-). The presence of the imidazole was confirmed with the appearance of aromatic hydrogens at δ 9, 7.70 and 7.60. In addition, it was confirmed with 6 hydrogens of methyl which were appeared at δ 3.9.

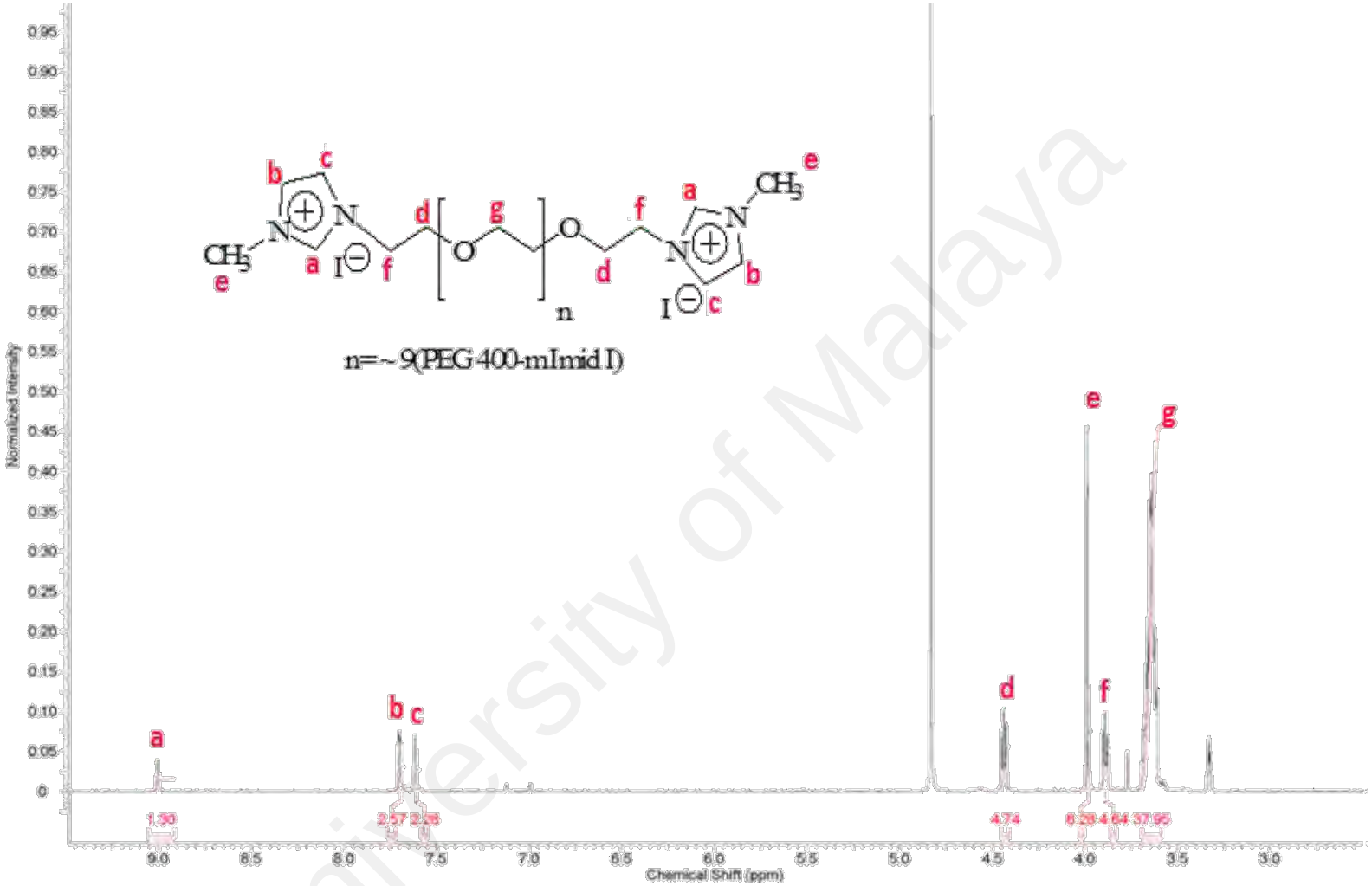

Figure 4.9: ^{1}H NMR spectra of PEG 400-(mImidI)$_2$

4.4.4 Synthesis and ^{1}H NMR Results of PEG 600-di methyl imidazolium iodide

The synthesis procedure for PEG 600-(mImidI)$_2$ was similar to PEG 400-(mImidI)$_2$. PEG 600-(mImidI)$_2$ and 1-methyl imidazole were reacted in 20 mL toluene for 12 hours. The completion of the reaction was confirmed through the presence of ionic liquid layer. The ionic liquid layer was then separated, where the residue was being washed by 10 mL toluene, and this process was repeated for 3 times. Solvent was evaporated and 3.3 g product with 89% yield was obtained as pure PEG 600-(mImidI)$_2$. The structure and ^{1}H NMR spectra for of PEG 600-(mImidI)$_2$ are shown in Figure 4.10. ^{1}H NMR (CD_3OD, 400 MHz, 25 $^{\circ}$C): δ 9(s, 2H, N=CH-N), δ 7.70(s, 2H N-CH=CH-N), δ 7.60(s, 2H, N-CH=CH-N), δ 4.4(t, 4H, CH_2-O), δ 4(s, 6H, CH_3-N), δ 3.9(t, 4H, N-CH_2), δ 3.6(m, 56 -CH_2 (O-CH_2-CH_2-O)n CH_2-).

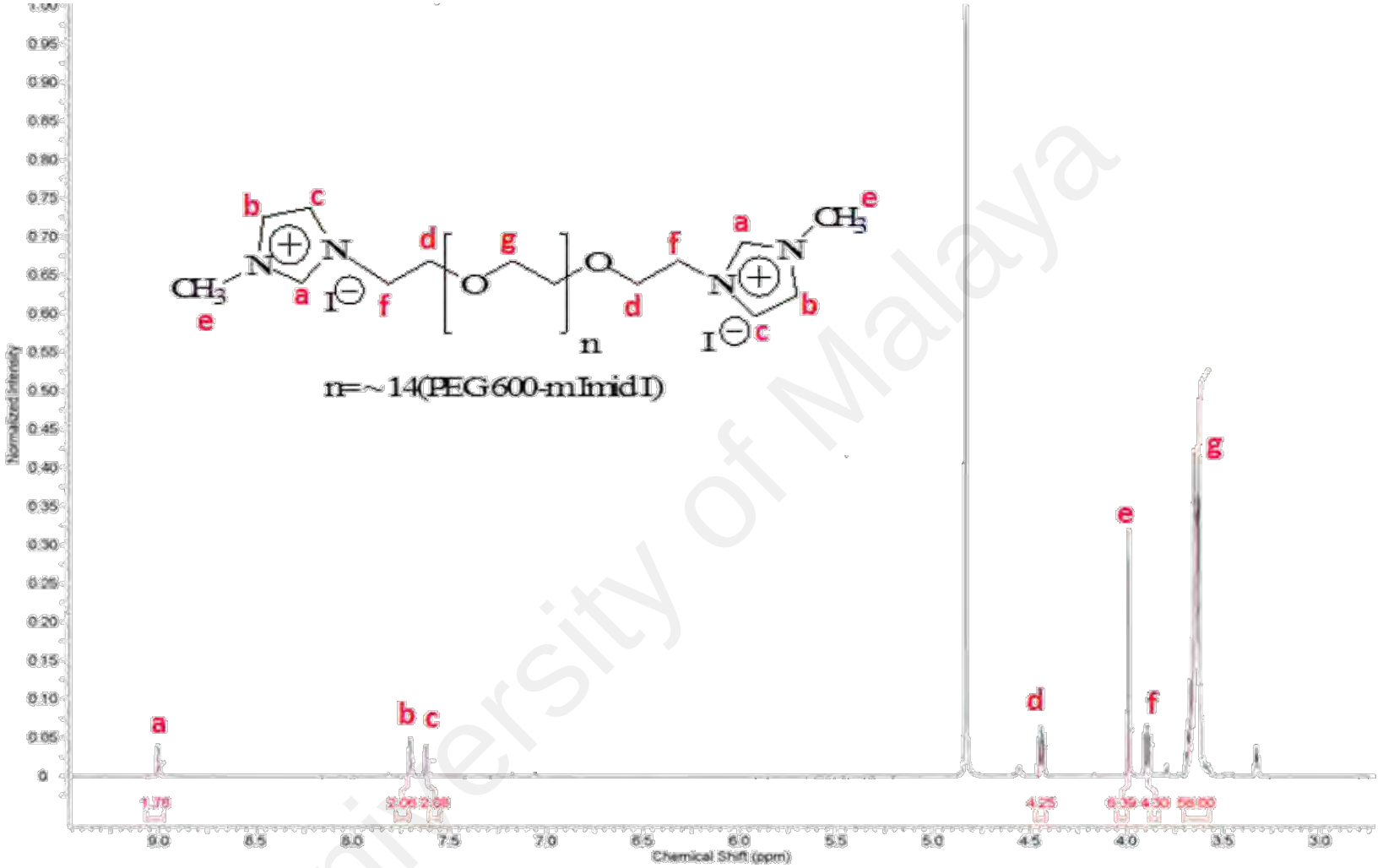

Figure 4.10: ^{1}H NMR spectra of PEG 600-(mImidI)$_2$

4.5 Polymer Characterization

The proton nuclear magnetic resonance (^{1}H-NMR), and fourier-transform infrared spectroscopy (FT-IR) were employed to characterize the synthesized PILs which are shown in Figure 4.11 and Figure 4.12. The ^{1}H NMR, and FT-IR spectra of PEG (400-600)-di tosylate and PEG (400-600)-di choline chloride fully confirmed the expected structure. Moreover, the structure of PEG (400-600)-di methyl imidazolium iodide were confirmed with ^{1}H-NMR completely.

Figure 4.11: PEG-di choline chloride

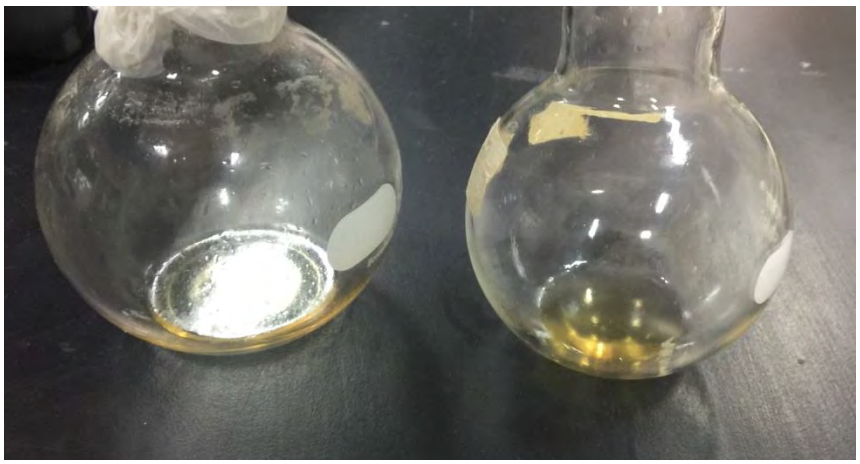

Figure 4.12: PEG (400-600)-di methyl imidazolium iodide

4.5.1 FT-IR Characterization

Measurements were conducted using FT-IR instrument. Figure 4.13 shows an example of ATR-FT-IR spectra of both PEG-di chcl and PEG. It can be seen from this figure that there are no OH groups in PEG-di chcl at 3200-3700 cm^{-1} and this confirmed the replacement of the OH group by choline chloride. It is important to mention that the synthesized PILs are hydrophilic. Thus, the existence of a flat curve in 3200-3700 cm^{-1} is inevitable due to the presence of water. Furthermore, the presence of chloride is confirmed with Cl bond in 800 cm^{-1}.

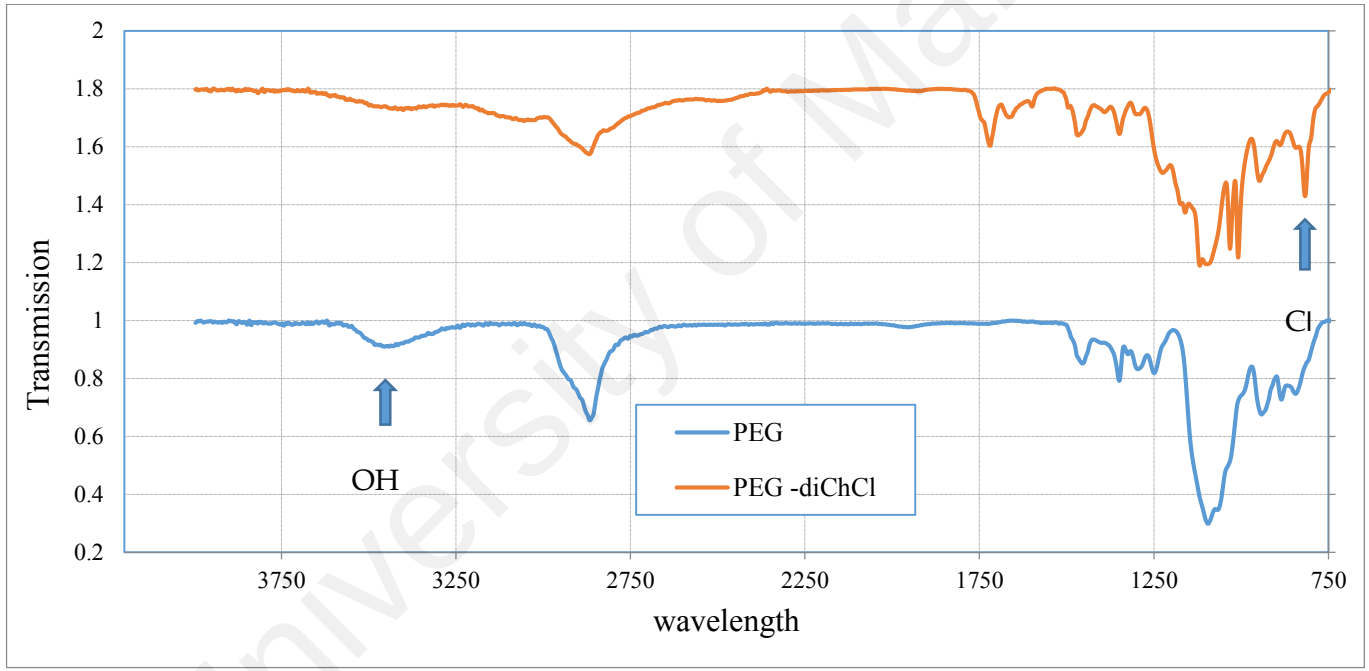

Figure 4.13: ATR-FT-IR spectra of a) PEG-di ChCl (above) b) PEG (below)

4.6 Physical Properties

The density and viscosity of aqueous mixtures of synthesized PILs are reported in this section. The resistance of a fluid to flow is a fundamental concept to understand viscosity and liquid characterization. The density and viscosity of a substance can be used to define the substance and its performance character.

4.6.1 Density and Viscosity Results for Aqueous Solutions of PEG (400-600)-$(ChCl)_2$ and PEG (400-600)-$(mImidI)_2$

The densities for aqueous solutions of synthesized polymers were obtained for 0.03 M samples in different temperatures. The results are presented in Table 4.1 and Figure 4.14. The results show a decrease in values with the increase in temperature. In addition, the experimental viscosity values of the 0.03 M concentration of aqueous solutions were determined and are tabulated in Table 4.3. The densities and viscosities of synthesized PILs were similar to the aqueous solvents which were used for CO_2 capture. For instance, the density and viscosity for aqueous solution of 2-Amino-2-hydroxymethyl-1,3-propanediol (AHPD) are 1.0084 g/cm^3 and 0.0905 mPa.s, respectively. These values are almost similar to the density and viscosity of synthesized PILs in this work. For the accuracy of experimental measurements, as PILs used in this study are new and literature data is not available for the comparison but density data for PEG 400 is available. The Table 4-2 shows that the results look in agreement with the reported data in literature.

Table 4.1: Density (ρ) results for synthesized PILs

PIL	Density at various temperatures (g/cm^3)							Ref
	25 ºC	30 ºC	40 ºC	50 ºC	60 ºC	70 ºC	80 ºC	
PEG 400	0.9987	0.9974	0.9939	0.9892	0.9846	0.9797	0.9756	This work
PEG 600	0.9992	0.9980	0.9944	0.9901	0.9852	0.9802	0.9778	This work
PEG 400-$(ChCl)_2$	0.9996	0.9984	0.9949	0.9907	0.9858	0.9802	0.9635	This work
PEG 600-$(ChCl)_2$	1.0003	0.9992	0.9956	0.9912	0.9863	0.9809	0.97091	This work
PEG 400-$(mImidI)_2$	1.0027	1.0014	0.9978	0.9936	0.9887	0.9832	0.9771	This work
PEG 600-$(mImidI)_2$	1.0052	1.0040	1.0004	0.9961	0.9911	0.9855	0.9794	This work
AHPD		1.0084	1.0003	1.0047	0.9951	0.99		(Park, 2002)

Table 4-2: Comparison of measured density (ρ) with literature value

	Exp. PEG 400 (g/cm^3)			Lit. PEG 400 (g/cm^3) (Han, Zhang, Chen, & Wei, 2008) (Trivedi, Bhanot, & Pandey, 2010)		Lit. PEG 400 (g/cm^3) (Eliassi, Modarress, & Mansoori, 1998)	
T/°C	ρ (g/cm^3)	Mass fraction	Mole fraction	ρ (g/cm^3)	Mole fraction	ρ (g/cm3)	Mass fraction
25	0.9987	0.01	0.0005	1.0126	0.005		
27						1.0035	0.05
30	0.9974	0.01	0.0005	1.0114	0.005		
37						1.0006	0.05
40	0.9939	0.01	0.0005	1.0075	0.005	0.9992	0.05
50	0.9892	0.01	0.0005	1.0025	0.005	0.9951	0.05
60	0.9846	0.01	0.0005				
70	0.9797	0.01	0.0005				
80	0.9756	0.01	0.0005				

In Figure 4.14 the density results clearly show that density of all the samples decreases with the increase in temperature. The density of PEG 600-$(mImidI)_2$ is the highest and the PEG 400-$(ChCl)_2$ is the least. It also shows that the imidazolium containing PILs have higher density as compared to choline chloride containing PILs.

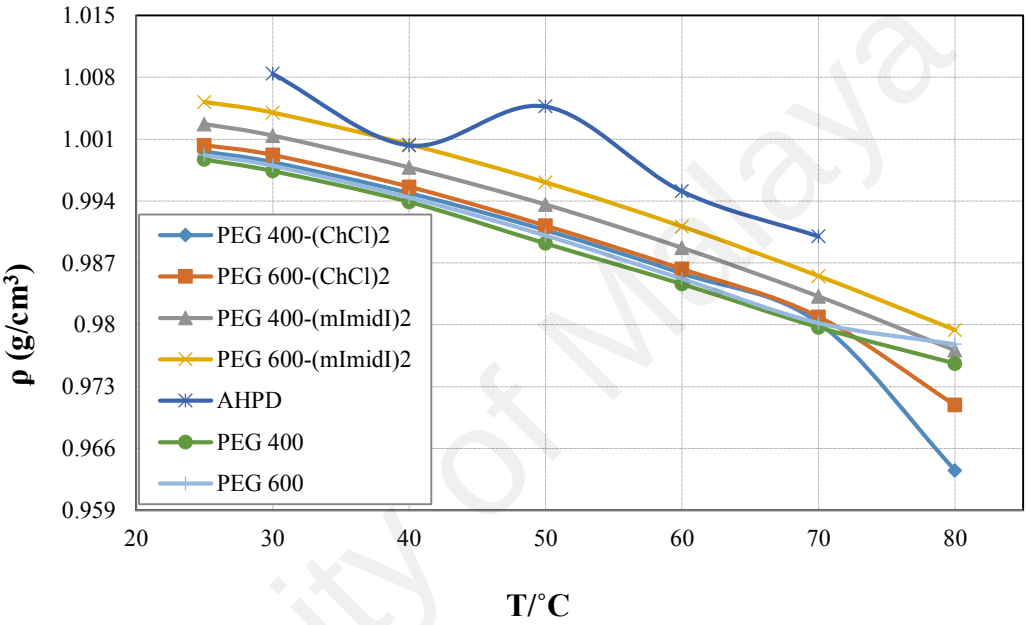

Figure 4.14: Comparison of density for aqueous PILs with literature.

Table 4.3 shows that the PEG 600 and PEG 600 containing PILs have slightly higher viscosity as compared to PEG 400 and PEG 400 containing PILs. This is because of high molecular weight of PEG 600 as compared to PEG 400.

Table 4.3: Viscosity (η) results for aqueous solutions of PEG (400-600)-$(ChCl)_2$ and PEG (400-600)-$(mImidI)_2$-(0.03 M)

PIL	η (mPa.s)	PIL	η (mPa.s)
PEG 400	1.13	PEG 600	1.15
PEG 400-$(ChCl)_2$	1.085	PEG 600-$(ChCl)_2$	1.11
PEG 400-$(mImidI)_2$	1.085	PEG 600-$(mImidI)_2$	1.11

To verify reliability of the data, the viscosity of PEG 400 (0.03 M) was compared with experimental values given by other author in literature as shown in Table 4.4.

Table 4.4: Comparison of measured viscosity (η) with literature values for PEG 400

Exp.		Lit. (Han, 2008)	
η (mPa.s)	**Mole fraction**	**η (mPa.s)**	**Mole fraction**
1.13	0.0005	1.16	0.005

4.7 Thermogravimetric Analysis (TGA)

TGA were performed with a sample weight of approximately 10 mg, between 25 °C to 500 °C for 45 min, with a heating ramp rate of 15 °Cmin^{-1} in a nitrogen atmosphere. Thermo-gravimetric weight loss curve was plotted against temperature. Figure 4.15 and Figure 4.16 show that the weight loss of synthesized polymers occurs at almost 250 °C, which indicates good thermal stability. This suggested that the polymer is stable at relatively high temperatures.

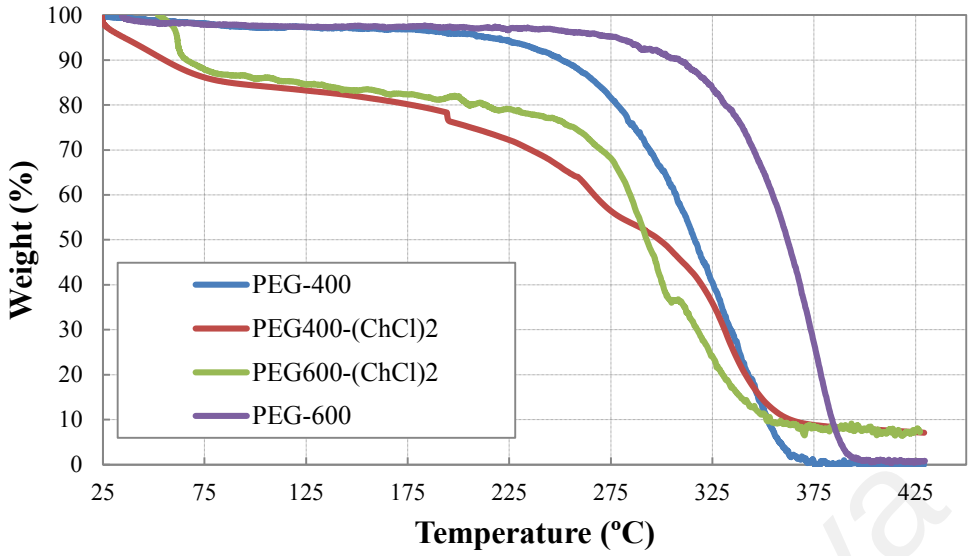

Figure 4.15: TGA curve of PEG (400-600)-$(ChCl)_2$ and PEG (400-600)

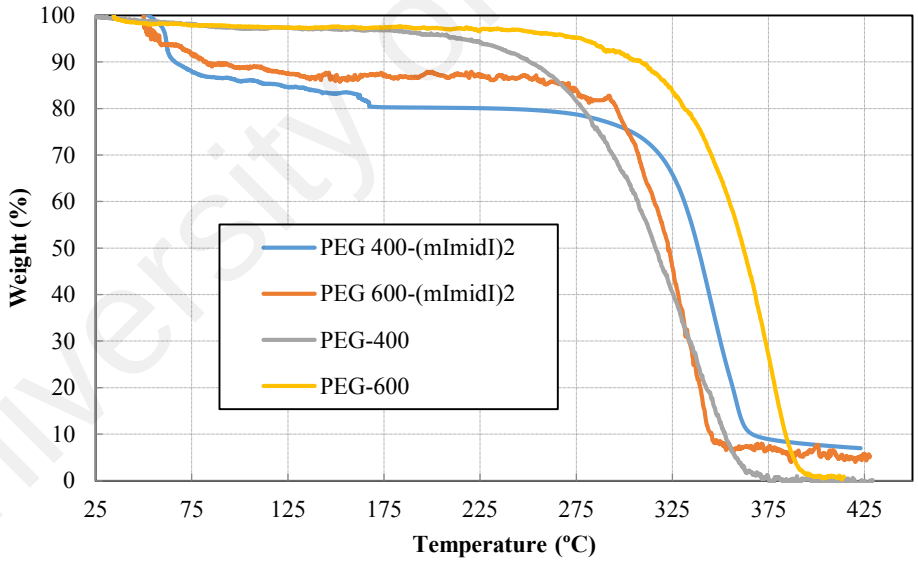

Figure 4.16: TGA curve of PEG (400-600)-$(mImidI)_2$ and PEG (400-600)

4.8 CO_2 Solubility in PEG (400-600)-$(ChCl)_2$ and PEG (400-600)-$(mImidI)_2$ at Various Temperatures and Pressures

CO_2 loading was measured at high pressures range of 10 to 13 bar, with a fixed concentration of the solvent (0.03 mol/L). During the experiment, all parameters were kept constant except for the pressure. The results are tabulated in Table 4.5. PILs show higher CO_2 loading at low temperatures. However, in order to investigate the effect of temperatures on CO_2 loading, various temperatures were used from 30 °C to 70 °C. Figure 4.17 and Figure 4.18 show the CO_2 loading (α) of PEG (400-600)-$(ChCl)_2$ and PEG (400-600)-$(mImidI)_2$ which are plotted against CO_2 partial pressure along with the CO_2 loading of the original PEGs at 30 °C. The effects of different factors are studied. By increasing the pressure, more gas absorbed in PEG and PEG containing PILs, due to large driving force available, this is because of the plasticization effect of CO_2 by pressure rise, which forces the CO_2 molecules to enter the chain (Simons, Nijmeijer, Bara, Noble, & Wessling, 2010). In terms of molecular weight; lower molecular weight PIL has higher mobility in the liquid phase, thus, significantly higher mobility and better distribution in aqueous solvent resulted in higher solubility. In terms of functional groups, for the PEG 400-$(mImidI)_2$ gave the best CO_2 solubility, it can be said that the presence of the N reactive center in the imidazole can be the key of CO_2 sorption. On the other hand, PILs have less viscosity as compared to original PEGs thus; diffusivity of CO_2 in PILs will be higher which will result in higher CO_2 solubility. Moreover, to investigate on higher concentration and lower pressure effect on sorbent, another experiment was performed at the pressure range from 5 to 13 bar with two new concentration of 0.055 M and 0.01 M of the best performance PIL in terms of CO_2 solubility which in this case was PEG 400-$(mImidI)_2$. The results are shown in Table 4.6. From Figure 4.17 and Figure 4.18, it can be seen that by increasing the temperature, the CO_2 loading decreases. Results show that PEG 400-$(mImidI)_2$ with 18.89 CO_2 loading at the pressure of 13.4 bar and 30 ºC has

higher CO_2 capacity as compared to its original PEG and PEG (400-600)-$(ChCl)_2$ and PEG 600-$(mImidI)_2$.

Table 4.5: CO_2 loading of PEG (400-600) and PEG (400-600)-$(ChCl)_2$ at different pressures (9.8 to 13.4 bar) and fixed temperature (30°C)

Absorbent (0.03M)	Loading (α)		
	9.8 (bar)	10.3 (bar)	13.4 (bar)
Choline Chloride	7.97	8.39	8.97
Choline Chloride + PEG 400	8.32	8.71	11.98
Methyl Imidazole	8.05	8.48	9.69
Methyl Imidazole + PEG 400	8.75	9.01	12.06
PEG 400	8.34	9.08	12.98
PEG 400-$(ChCl)_2$	10.45	10.82	16.33
PEG 600	8.70	9.04	12.69
PEG 600-$(ChCl)_2$	10.53	11.55	15.53
PEG 400-$(mImidI)_2$	13.36	14.31	18.89
PEG 600-$(mImidI)_2$	13.20	14.25	18.38

By increasing the concentration of the PEG 400-$(mImidI)_2$ from 0.03 M to 0.1 M, the CO_2 loading in aqueous solution of PEG 400-$(mImidI)_2$ has decreased and the results are tabulated in Table 4.6

Table 4.6: CO_2 loading of PEG 400-(mImidI)$_2$ at different pressures (5 to 13.4 bar) and fixed temperature (30 °C)

Absorbent	Loading (α)			
	5 (bar)	9.8(bar)	10.3(bar)	13.4(bar)
PEG 400-(mImidI)$_2$ (0.3M)	6.04	13.36	14.31	18.89
PEG 400-(mImidI)$_2$ (0.05M)	3.65	7.79	8.34	11.17
PEG 400-(mImidI)$_2$ (0.1M)	2.19	4.51	4.88	6.67

CO_2 loading results are plotted against CO_2 pressure in Figure 4.17 and Figure 4.18. It can be seen that by increasing the pressure the CO_2 loading in aqueous solution of original PEG (400-600) and PILs are also increased. The graph also presents that at higher pressures, there are bigger gaps between PILs loading. It shows that pressure has a significant effect on CO_2 loading for physical sorbents.

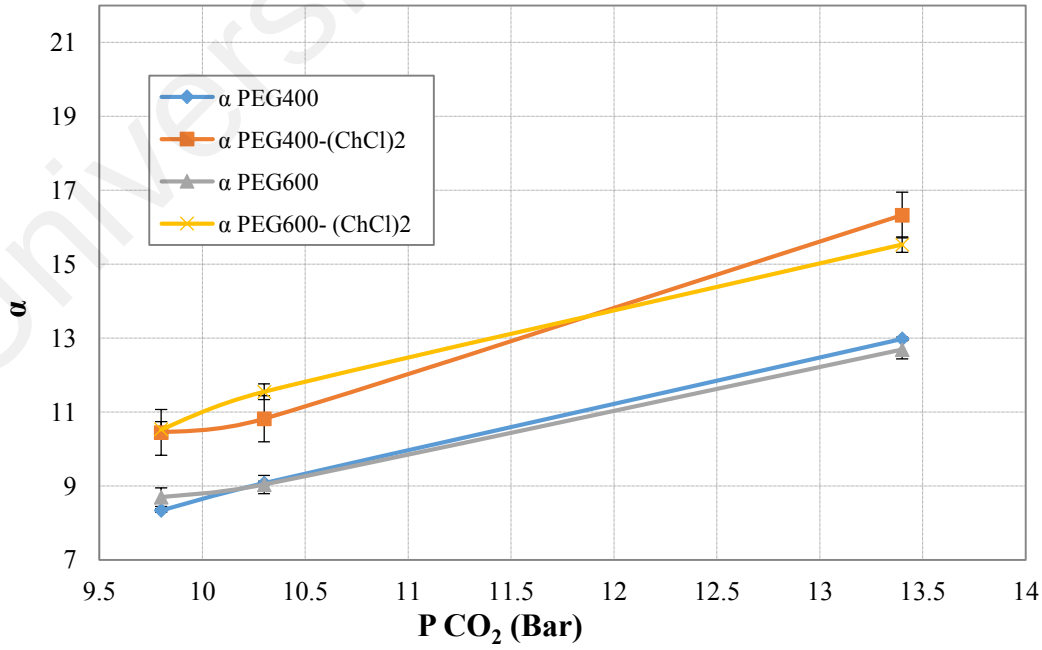

Figure 4.17: CO_2 loading of PEG (400-600) and PEG (400-600)-(ChCl)$_2$ at various pressures (9.8-13.4 bar)

Figure 4.17 and Figure 4.18 show that, the absorption of original PEGs and synthesized PILs have an approximate linear relationship of CO_2 loading as a function of pressure. This confirms that, the mechanism of CO_2 capture by PEG and PEG containing PILs are physical absorption.

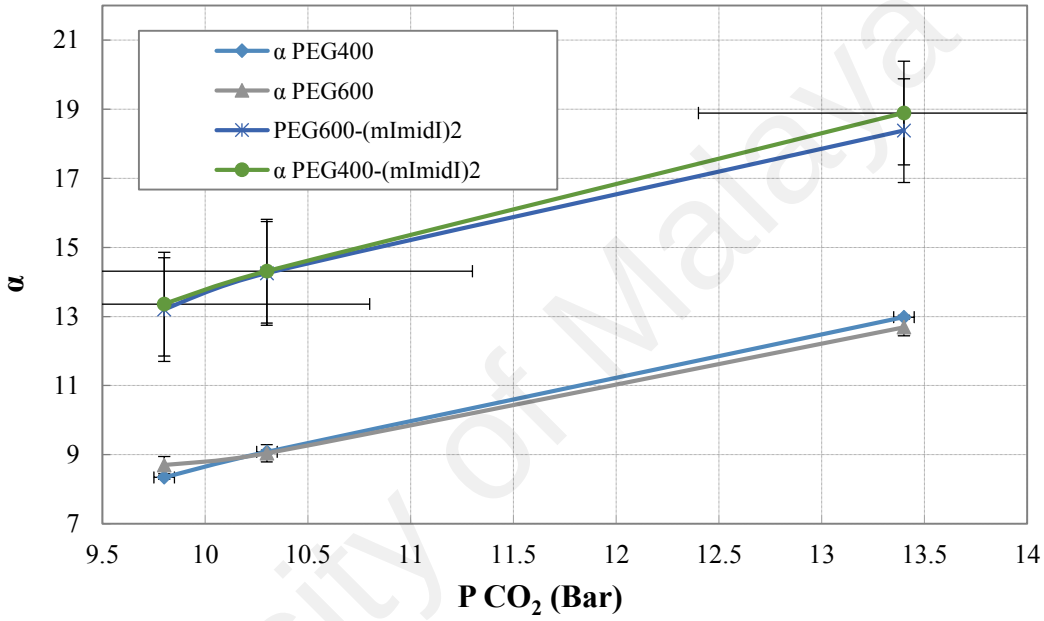

Figure 4.18: CO_2 loading of PEG (400-600) and PEG (400-600)-(mImidI)$_2$ at various pressures (9.8-13.4 bar)

CO_2 loading for three different concentration of PEG 400-(mImidI)$_2$ (0.03 M, 0.055 M and 0.1 M) at the pressure range of 5 to 13 bar are shown in Figure 4.19. It can be seen that by increasing the pressure, CO_2 loading have increased in PILs aqueous solutions.

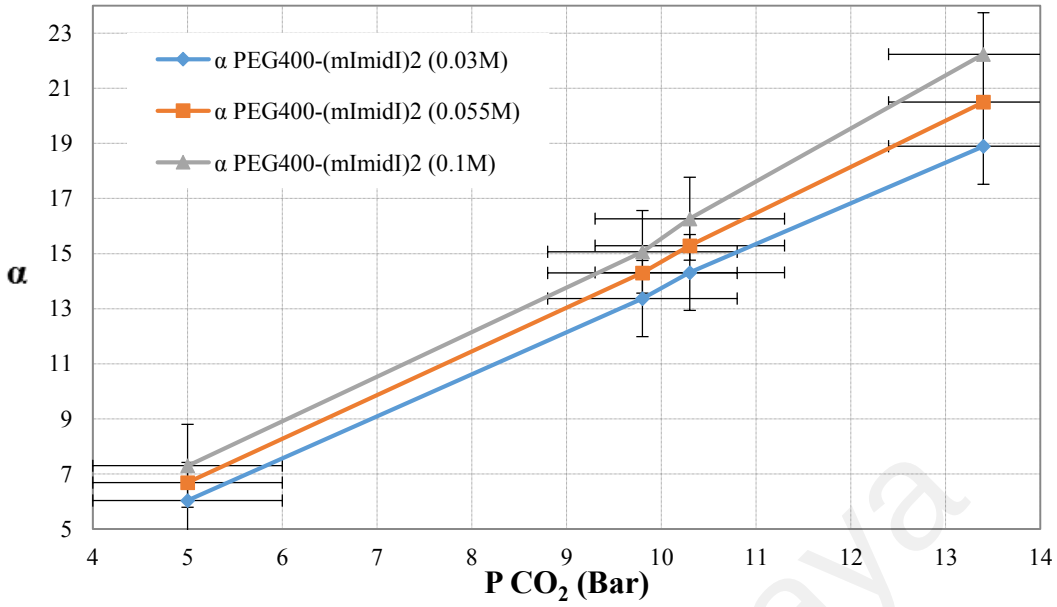

Figure 4.19: CO_2 loading of PEG (400-600)-(mImidI)$_2$ at different concentration (0.03-0.1 M) and at various pressures (5-13.4 bar).

Temperature effects in aqueous PILs CO_2 loading are plotted in Figure 4.20, Figure 4.21, Figure 4.22 and Figure 4.23. It can be observed that up to 70% decrease in PILs CO_2 loading by increasing the temperature from 30 ºC to 70 ºC.

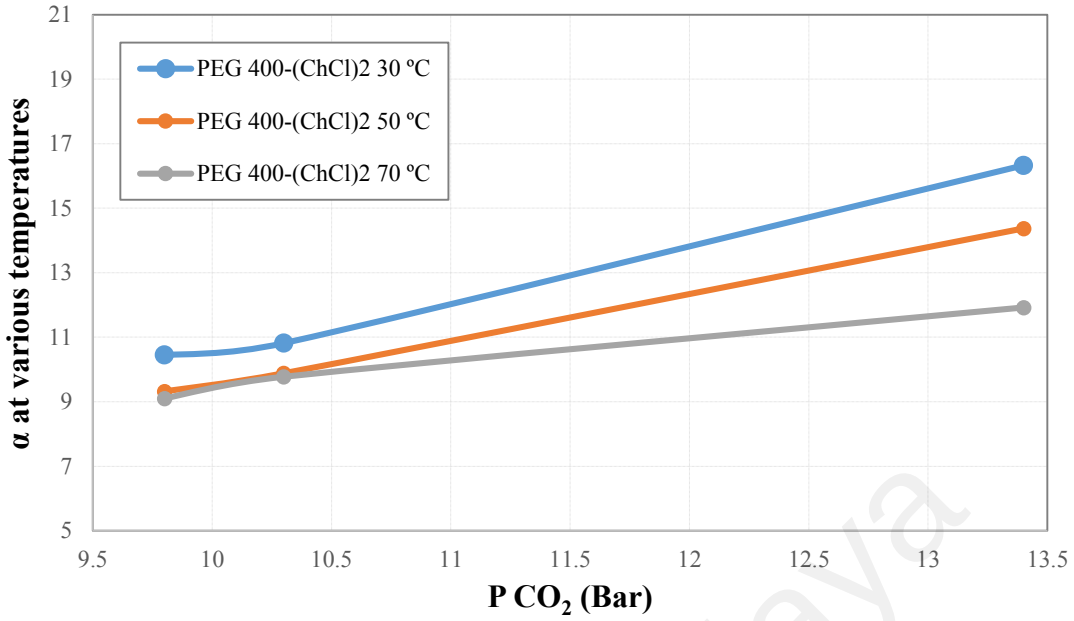

Figure 4.20: CO_2 loading of PEG 400-$(ChCl)_2$ at different pressures (9.8-13.4 bar) and temperatures (30 ˚C-70 ˚C)

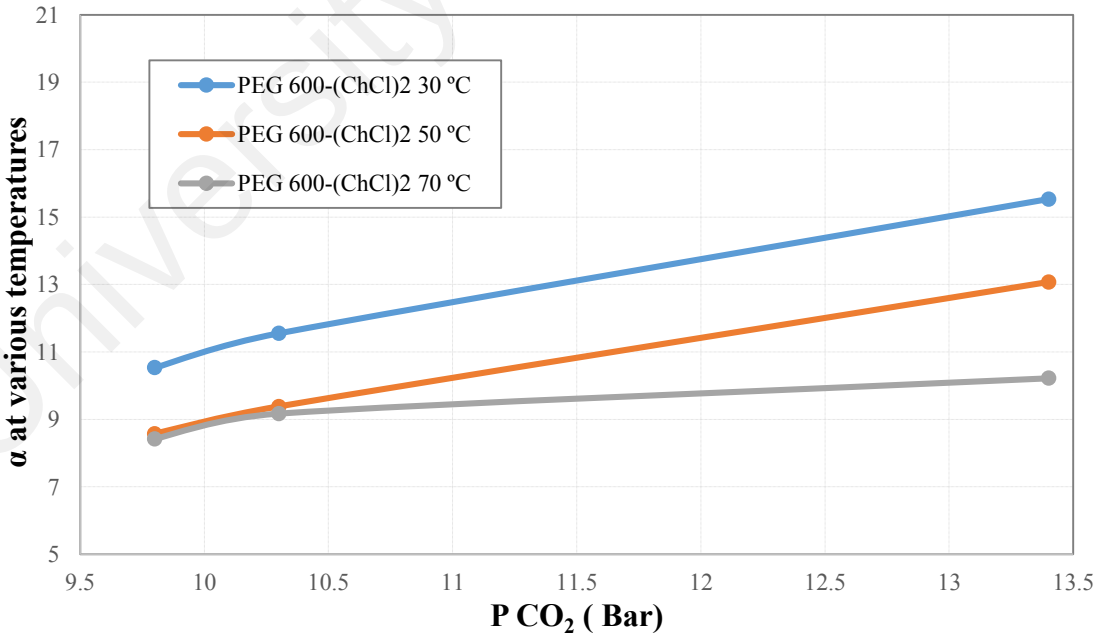

Figure 4.21: CO_2 loading of PEG 600-$(ChCl)_2$ at different pressures (9.8-13.4 bar) and temperatures (30 ˚C-70 ˚C)

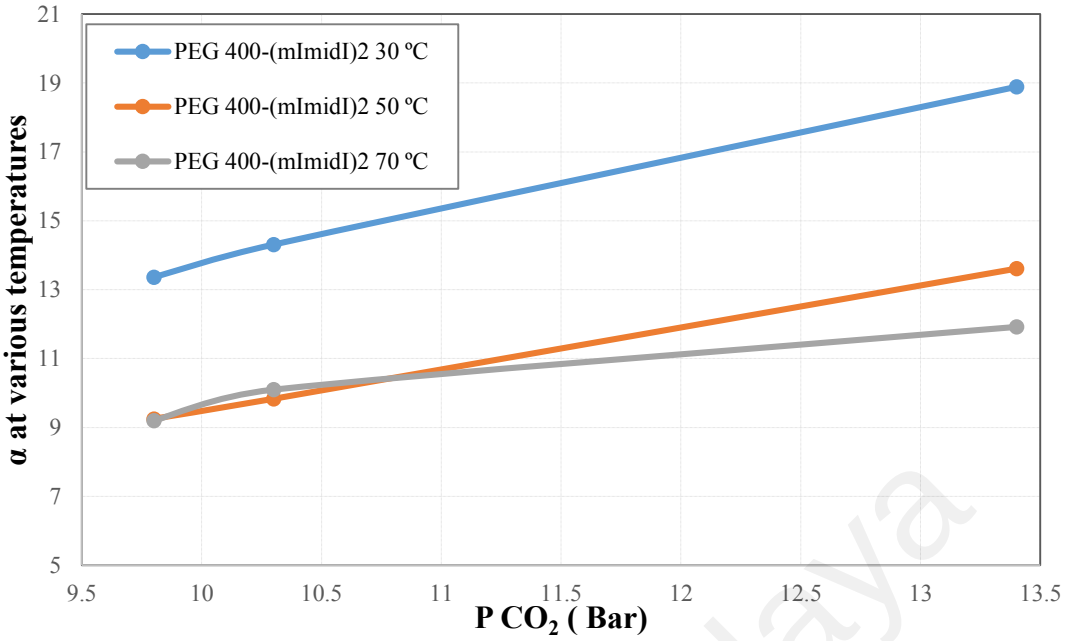

Figure 4.22: CO_2 loading of PEG 400-(mImidI)$_2$ at different pressures (9.8-13.4 bar) and temperatures (30 ˚C-70 ˚C)

From Figure 4.20, Figure 4.21 and Figure 4.22 it can be seen that, the increasing temperature from 30 ˚C to 50 ˚C has considerable impact on reducing the CO_2 loading for synthesized PILs. The CO_2 loading from 9.8 to 10.3 bar at temperature range from 50 ˚C to 70 ˚C was very close for PEG (400-600)-(ChCl)$_2$ and PEG 400-(mImidI)$_2$. However, for PEG 600-(mImidI)$_2$ the loading drop was considerable at the same temperature range. In addition, with increasing the pressure from 10.3 to 13.4 bar the loading rise gap was greater for synthesized PILs which is due to physical CO_2 absorption mechanism.

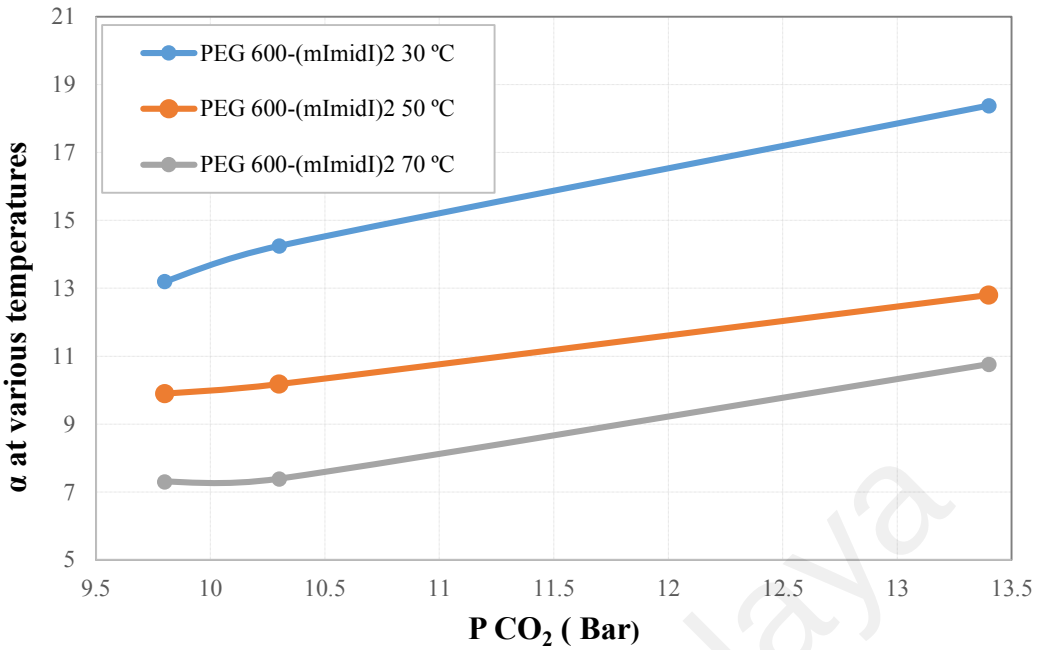

Figure 4.23: CO_2 loading of PEG 600-(mImidI)$_2$ at different pressures (9.8-13.4 bar) and temperatures (30 ˚C-70 ˚C)

The results clearly show that CO_2 solubility is reduced with increasing the temperature and more gas will be absorbed at high pressure due to the large driving force available. In addition, the strong linearity shows that the absorption process is dominated by physical absorption.

4.8.1 Determination of Henry's constant (H)

At high pressure, the CO_2 sorption in PEG (400-600)-(ChCl)$_2$ and PEG (400-600)-(mImidI)$_2$ solutions is considered as a physical absorption. The most important property of physical solvents are their unlimited absorption capacity which increases with the pressure rise. Another aspect which makes physical solvents promising is their sorption mechanism. The mechanism in physical solvents is based on van der waals attraction among the compounds in the liquid phase which are CO_2/PEG (400-600)-(ChCl)$_2$ and CO_2/PEG (400-600)-(mImidI)$_2$. The Henry's constant (H) values were obtained using

Equation 3-5. From the Equation 3-5 it can be seen that increasing number of gas mole has reversed effect on Henry's constant (H). Thus, higher Henry's constant (H) indicates lower CO_2 solubility in compounds. H values of other ionic liquids at similar temperature are also listed for comparison as shown in Table 4.7. The results show that the modification of PEG with choline chloride decreased the Henry's constant (H) for PEG 400-$(ChCl)_2$ and PEG 600-$(ChCl)_2$ from 36.75 to 30.11 and from 36.89 to 28.89 respectively and for PEG 400-$(mImidI)_2$ and PEG 600-$(mImidI)_2$ from 36.75 to 24.02 and 36.89 to 24.38 respectively at 30 ºC. Moreover, from the Table 4.9, it can be seen that the 4 M monodiethanolamine (MDEA) and its mixtures with [bmim][BF_4] up to 1 M have higher Henry's constant (H) than PEG (400-600)-$(ChCl)_2$ and PEG (400-600)-$(mImidI)_2$. It is worth mentioning that ILs and mixtures in the Table 4.9, Table 4.10 and Table 4.11 were utilized as pure or at high concentration as compared to 0.03 M of PEG (400-600)-$(ChCl)_2$ and PEG (400-600)-$(mImidI)_2$. This indicates that the proposed PEG (400-600)-$(ChCl)_2$ and PEG (400-600)-$(mImidI)_2$ solutions have better CO_2 capacity as compared to the other ionic liquids listed in Table 4.9, Table 4.10 and Table 4.11.

Table 4.7: Henry's constant of PEG (400-600)-$(ChCl)_2$ and PEG (400-600)-$(mImidI)_2$ at different temperature (30 ˚C- 70 ˚C) and concentration of (0.03 M).

T (˚C)	H (bar. L/mol)			
	PEG400-$(ChCl)_2$	**PEG600-$(ChCl)_2$**	**PEG400-$(mImidI)_2$**	**PEG600-$(mImidI)_2$**
30	30.11	28.89	24.02	24.38
50	33.61	36.31	34.33	33.85
70	36.09	39.99	34.16	44.23

Table 4.8: Comparison Henry's constant of PEG 400 with literature

T/°C	Exp. H (bar. L/mol)	Lit. H (bar. L/mol) (Li , 2012)	(mol/L)
25 °C		47.8 ± 0.12	Pure
30 °C	36.75 ± 0.05		0.03
40 °C		56.6 ± 0.12	Pure

According to Table 4.8, the Henry's constant of this work is smaller than the available literature value. This difference in values is because of different ranges of temperatures, pressures and concentration of applied solution for CO_2 sorption.

Table 4.9: Henry's constant for PEG (400-600), PEG (400-600)-$(ChCl)_2$ and PEG (400-600)-$(mImidI)_2$ at 30 °C.

Sorbent	(mol/L)	H (bar. L/mol)	Ref
PEG 400	0.03	36.75 ± 0.05	This work
PEG 400-$(ChCl)_2$	0.03	30.11 ± 0.6	This work
PEG 600	0.03	36.89 ± 0.2	This work
PEG 600-$(ChCl)_2$	0.03	28.89 ± 0.2	This work
PEG 400-$(mImidI)_2$	0.03	24.02 ± 1.5	This work
PEG 600-$(mImidI)_2$	0.03	24.38 ± 1.5	This work
[Bmim][Tf_2N]		42 ± 2	(Hou & Baltus, 2007)
[Pmmim][Tf_2N]		40.4 ± 0.6	(Hou & Baltus, 2007)
[Bmpy][Tf_2N]		35 ± 2	(Hou & Baltus, 2007)
[Perfluoro-hmim][Tf_2N]		32 ± 2	(Hou & Baltus, 2007)
[Bmim][BF_4]		63 ± 2	(Hou & Baltus, 2007)
[C_2mim][Tf_2N]		37	(Pinto, Rodríguez, Arce, & Soto, 2013)
[emim][Tf_2N]		39.5 ± 0.6	(Camper, Becker, Koval, & Nob 2006)
MDEA	4	40.6	(Ahmady, Hashim, & Aroua, 2011b)
MDEA + [bmim][BF_4]	4+ 0.2	39.5	(Ahmady, 2011b)
MDEA + [bmim][BF_4]	4+ 0.5	36.8	(Ahmady, 2011b)
MDEA + [bmim][BF_4]	4+ 1	29.1	(Ahmady, 2011b)
MDEA + [bmim][BF_4]	4+ 1.5	25.4	(Ahmady, 2011b)
MDEA + [bmim][BF_4]	4+ 2	19.9	(Ahmady, 2011b)

According to Table 4.9, the result of this work gave a smaller Henry's constant than literature value indicating a potentially large absorption amount using the synthesized PILs.

Table 4.10: Henry's constant of PEG (400-600), PEG (400-600)-$(ChCl)_2$ and PEG (400-600)-$(mImidI)_2$, at 50 ºC.

Sorbent	(mol/L)	H (bar. L/mol)	Ref
PEG 400-$(ChCl)_2$	0.03	33.61	This work
PEG 600-$(ChCl)_2$	0.03	36.31	This work
PEG 400-$(mImidI)_2$	0.03	34.33	This work
PEG 600-$(mImidI)_2$	0.03	33.85	This work
[emim][Tf_2N]		57.2 ± 0.8	(Camper, 2006)
Water + [bmim][BF_4]	2	31.7	(Ahmady, 2011b)
MDEA	4	57.2	(Ahmady, 2011b)
MDEA + [bmim][BF_4]	4+ 0.2	52	(Ahmady, 2011b)
MDEA + [bmim][BF_4]	4+ 1	36.6	(Ahmady, 2011b)
MDEA + [bmim][BF_4]	4+ 1.5	29.3	(Ahmady, 2011b)
MDEA + [bmim][BF_4]	4+ 2	23.7	(Ahmady, 2011b)
[Bmim][Tf_2N]		51± 2	(Hou & Baltus, 2007)
[Pmmim][Tf_2N]		53± 2	(Hou & Baltus, 2007)
[Bmpy][Tf_2N]		46± 1	(Hou & Baltus, 2007)
[Perfluoro-hmim][Tf_2N]		42± 2	(Hou & Baltus, 2007)
[Bmim][BF_4]		84± 4	(Hou & Baltus, 2007)

Table 4.11: Henry's constant of PEG (400-600), PEG (400-600)-$(ChCl)_2$ and PEG (400-600)-$(mImidI)_2$, at 70 ºC.

Sorbent	(mol/L)	H (bar. L/mol)	Ref
PEG 400-$(ChCl)_2$	0.03	36.09	This work
PEG 600-$(ChCl)_2$	0.03	39.99	This work
PEG 400-$(mImidI)_2$	0.03	34.16	This work
PEG 600-$(mImidI)_2$	0.03	44.23	This work
[emim][Tf_2N]		76 ± 1.2	(Camper, 2006)

4.8.2 Enthalpy of Absorption

The heat of absorption was calculated for PEG (400-600)-$(ChCl)_2$ and PEG (400-600)-$(mImidI)_2$ using van't Hoff equation. Results are plotted in Figure 4.24. For the synthesized PILs the enthalpy of the reaction are tabulated in Table 4.12. The low value enthalpies confirm the physical CO_2 sorption. For instance, the enthalpy of CO_2 absorption in aqueous for PEG 400-$(mImidI)_2$ is -9.19 KJ/mol. Based on literature, the enthalpy of absorption for the [perfluoro-hmim][Tf_2N] is -9 KJ/mol at 25 °C which is similar to the enthalpies obtained in this work. The enthalpy for %30 wt of MDEA solution is reported to be 59.171 KJ/mol which is considerably higher enthalpy which confirms a chemical sorption for MDEA solution (Kim, Hoff, Hessen, Haug-Warberg, & Svendsen, 2009). According to this, lowering the enthalpy of absorption might be one of the suggested options to reduce the energy demand for CO_2 capture.

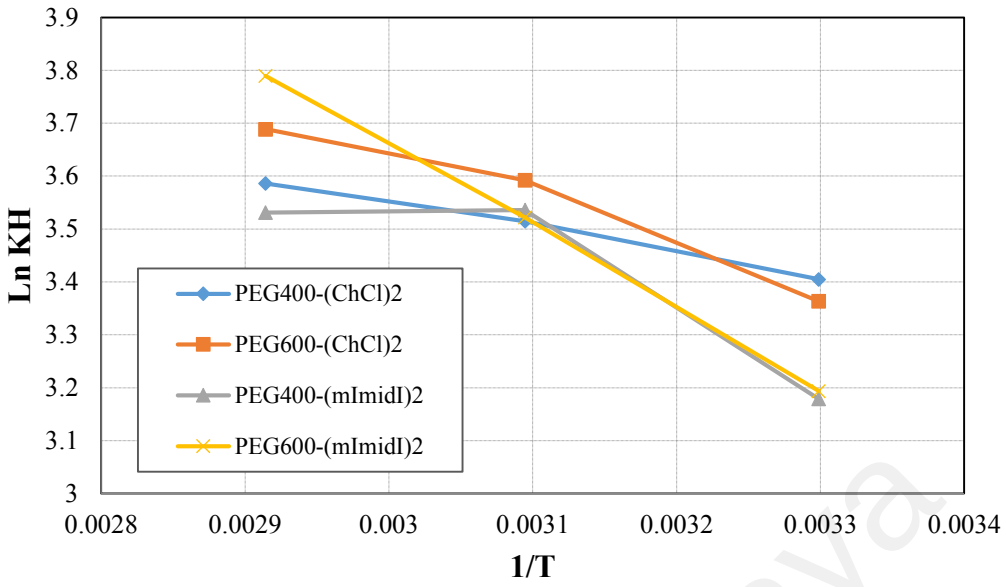

Figure 4.24: Van't Hoff plot for synthesized PILs

Table 4.12: Enthalpies of CO_2 absorption with synthesized PILs

Sorbent	ΔH (KJ/mol)	Ref
PEG 400-$(ChCl)_2$	-9.42	This work
PEG 600-$(ChCl)_2$	-9.55	This work
PEG 400-$(mImidI)_2$	-9.19	This work
PEG 600-$(mImidI)_2$	-9.44	This work
[perfluoro-hmim][Tf_2N]	-9	(Hou & Baltus, 2007)
PEG 400	−11.18	(Li, 2012)

4.9 Effect of Regeneration Cycles on CO_2 Capture of PEG (400-600)-$(ChCl)_2$ and PEG (400-600)-$(mImidI)_2$

Regeneration of the synthesized PILs showed that the absorbed CO_2 were released before the boiling point. Results obtained are tabulated in Table 4.13. Results confirmed that the synthesized PILs have a high stability on their sorption capacity even after three

cycles of regeneration, where there is only 15% decrease in CO_2 absorption capacity as compared with 14% ammonia solution, which reduced to 43% after three cycle test (Yeh, Pennline, Resnik, & Rygle, 2004).

Table 4.13: Regeneration results of PEG (400-600)-$(ChCl)_2$ and PEG (400-600)-$(mImidI)_2$ in three cycles

PIL	CO_2 Loading (mol/mol)		
	First cycle	Second cycle	Third cycle
PEG 400-$(ChCl)_2$	16.33	15.39	14.66
PEG 600-$(ChCl)_2$	15.53	15.32	15.00
PEG 400-$(mImidI)_2$	18.89	16.31	16.07
PEG 600-$(mImidI)_2$	18.38	16.5	15.56

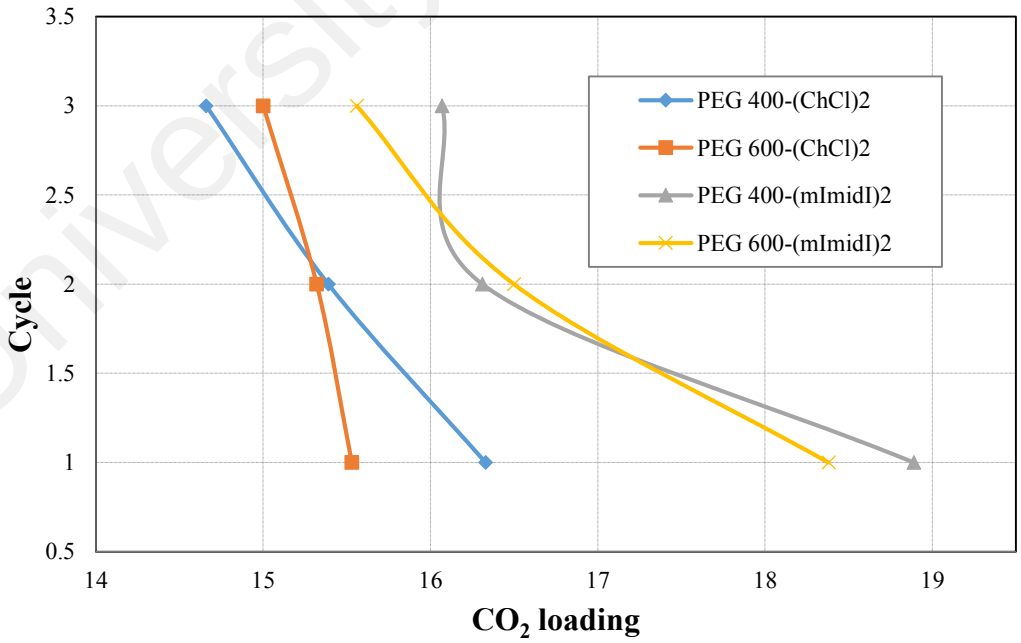

Figure 4.25: Cyclic regeneration of CO_2 loading for synthesized PILs

CHAPTER 5: CONCLUSIONS AND RECOMMENDATIONS

5.1 Conclusions

In this work, two novel materials with new established methods were successfully synthesized and utilized for CO_2 absorption. PEG as a potential sorbent in CO_2 capture is selected as back-bone. Two different molecular weight of PEG were chosen to study on the molecular effect. In terms of cation, choline chloride and methyl imidazole were chosen because of their impact on CO_2 sorption. Modified PEGs were characterized with FT-IR and ^{1}H-NMR. FT-IR characterization results confirmed the elimination of –OH and its replacement with choline chloride. Moreover, the ^{1}H-NMR characterization results showed the right number of hydrogen for PEG (400-600)-$(ChCl)_2$ and PEG (400-600)-$(mImid)_2$.

Physical properties for synthesized PILs were also studied. Thermal stability of the synthesized PILs were analyzed by TGA. TGA results showed high thermal stability for modified PEGs. Polymers weight loss occurs at approximately 250°C, which indicates the ability for the PILs to remain stable at high temperature. Densities and viscosities were attained for 0.03 M of aqueous solution of synthesized PILs. Results for density showed that the density of aqueous PILs are very close the PILs reported in literatures. Density results showed that PEG 600 and PEG 600 containing PILs have higher density as compared to PEG 400 and PEG 400 containing PILs and the highest density was belong to PEG 600-$(mImidI)_2$ with the amount of 1.0052 (g/cm^3) at 25 ˚C. Results for viscosity also confirmed that the PEG and PILs with higher molecular weight have shown higher viscosity as compared to PEG and PILs with less molecular weight.

CO_2 absorption using modified PEG (400-600) namely PEG (400-600)-$(ChCl)_2$ and PEG (400-600)-$(mImid)_2$ were carry-out at high pressures reactor (10 to 13 bar) and different temperatures (30 to 70 ºC). The results showed that using the modified PEG (400-600)- di choline chlorides with PEG (400-600) gave a considerable increase in CO_2 loading by 20% as compared to the original PEGs. Furthermore, the modified PEGs with methyl imidazole PEG (400-600)-$(mImidI)_2$ performed the best as a solvent with 30% increase in CO_2 loading as compared to original PEGs. The concentration impact of the sorbent was also investigated for the best performance PILs in terms of CO_2 solubility which was PEG 400-$(mImidI)_2$. In this case, three concentrations were used (0.03 M, 0.055 M and 0.1 M) at pressure ranging from 5-13 bar. The results showed reduction in CO_2 loading by increasing the concentration of the sorbent almost to double (for both concentrations). In terms of molecular weight, PEG 400-$(ChCl)_2$ gave higher CO_2 loading than PEG 600-$(ChCl)_2$ and PEG 400-$(mImidI)_2$ gave higher CO_2 loading than PEG 600-$(mImidI)_2$. This is due to PEG 400-$(ChCl)_2$ and PEG 400-$(mImidI)_2$ have shorter chain, and this gives higher mobility for PILs in the solution to be in contact with CO_2. Furthermore, PEG as the backbone is a physical sorbent where, the sorption mechanism is physical, due to attractive van der waals forces associated with compounds in liquid phase.

Henry's constant, was investigated for the CO_2-aqueouse PILs system. Results showed that modifying PEGs with choline chloride and methyl imidazole have positive impact on their CO_2 loading and Henry's constant. Results showed that modification of PEG (400-600) with choline chloride has decreased Henry's constant from 36.75 to 30.11 for PEG 400, from 36.89 to 28.89 for PEG 600 and this amount for modified PEG (400-600) with methyl imidazole were from 36.75 to 24.02 for PEG 400 and 36.89 to 24.38 for PEG 600 respectively at 30 ˚C.

The enthalpies for the CO_2 absorption were obtained through van't Hoff equation. Small values for heat of absorption confirmed the physical CO_2 absorption. The small values for enthalpy confirmed physical CO_2 absorption in aqueous synthesized PILs system. Where, the lowest amount is -9.19 KJ/mol for PEG 400-$(mImidI)_2$.

Moreover, stability of the PILs were also studied through pressure and temperature swing. Regeneration of the PILs confirmed their high stability after three cycles with only 15% reduction in their CO_2 loading capacity.

5.2 Future Work

This work focused on the exploration of PILs in terms of cation and the backbone effect. For future work, it is important to investigate the anion effect on PILs CO_2 sorption. Anion can be replaced with other potential anion using anion exchange methods to obtain PEG-grafted ILs for high CO_2 absorption capability.

REFERENCES

Ahmady, A., Hashim, M. A., & Aroua, M. K. (2011a). Absorption of carbon dioxide in the aqueous mixtures of methyldiethanolamine with three types of imidazolium-based ionic liquids. *Fluid phase equilibria, 309*(1), 76-82.

Ahmady, A., Hashim, M. A., & Aroua, M. K. (2011b). Density, viscosity, physical solubility and diffusivity of CO_2 in aqueous MDEA + [bmim][BF4] solutions from 303 to 333 K. *Chemical Engineering Journal, 172*(2–3), 763-770. doi: http://dx.doi.org/10.1016/j.cej.2011.06.059

Alothman, Z., Unsal, Y., Habila, M., Tuzen, M., & Soylak, M. (2015). A membrane filtration procedure for the enrichment, separation, and flame atomic absorption spectrometric determinations of some metals in water, hair, urine, and fish samples. *Desalination and Water Treatment, 53*(13), 3457-3465.

Amooghin, A. E., Sanaeepur, H., Moghadassi, A., Kargari, A., Ghanbari, D., & Mehrabadi, Z. S. (2010). Modification of ABS membrane by PEG for capturing carbon dioxide from CO_2/N_2 streams. *Separation Science and Technology, 45*(10), 1385-1394.

An, D., Wu, L., Li, B.-G., & Zhu, S. (2007). Synthesis and SO_2 absorption/desorption properties of poly (1, 1, 3, 3-tetramethylguanidine acrylate). *Macromolecules, 40*(9), 3388-3393.

Anthony, J. L., Anderson, J. L., Maginn, E. J., & Brennecke, J. F. (2005). Anion effects on gas solubility in ionic liquids. *The Journal of Physical Chemistry B, 109*(13), 6366-6374.

Aschenbrenner, O., & Styring, P. (2010). Comparative study of solvent properties for carbon dioxide absorption. *Energy & Environmental Science, 3*(8), 1106-1113.

Aziz, N., Yusoff, R., & Aroua, M. K. (2012). Absorption of CO_2 in aqueous mixtures of N-methyldiethanolamine and guanidinium tris (pentafluoroethyl) trifluorophosphate ionic liquid at high-pressure. *Fluid Phase Equilibria, 322*, 120-125.

Bahukudumbi, P., & Ford, D. M. (2006). Molecular modeling study of the permeability-selectivity trade-off in polymeric and microporous membranes. *Industrial & engineering chemistry research, 45*(16), 5640-5648.

Bai, H., & Ho, W. W. (2008). New carbon dioxide-selective membranes based on sulfonated polybenzimidazole (SPBI) copolymer matrix for fuel cell applications. *Industrial & engineering chemistry research, 48*(5), 2344-2354.

Bara, J. E., Gabriel, C. J., Hatakeyama, E. S., Carlisle, T. K., Lessmann, S., Noble, R. D., & Gin, D. L. (2008). Improving CO_2 selectivity in polymerized room-temperature ionic liquid gas separation membranes through incorporation of polar substituents. *Journal of Membrane Science, 321*(1), 3-7.

Bara, J. E., Gin, D. L., & Noble, R. D. (2008). Effect of anion on gas separation performance of polymer− room-temperature ionic liquid composite membranes. *Industrial & Engineering Chemistry Research, 47*(24), 9919-9924.

Bara, J. E., Hatakeyama, E. S., Gabriel, C. J., Zeng, X., Lessmann, S., Gin, D. L., & Noble, R. D. (2008). Synthesis and light gas separations in cross-linked gemini room temperature ionic liquid polymer membranes. *Journal of Membrane Science, 316*(1), 186-191.

Bara, J. E., Hatakeyama, E. S., Gin, D. L., & Noble, R. D. (2008). Improving CO_2 permeability in polymerized room-temperature ionic liquid gas separation membranes through the formation of a solid composite with a room-temperature ionic liquid. *Polymers for Advanced Technologies, 19*(10), 1415-1420.

Bara, J. E., Lessmann, S., Gabriel, C. J., Hatakeyama, E. S., Noble, R. D., & Gin, D. L. (2007). Synthesis and performance of polymerizable room-temperature ionic liquids as gas separation membranes. *Industrial & engineering chemistry research, 46*(16), 5397-5404.

Bara, J. E., Noble, R. D., & Gin, D. L. (2009). Effect of "free" cation substituent on gas separation performance of polymer− room-temperature ionic liquid composite membranes. *Industrial & engineering chemistry research, 48*(9), 4607-4610.

Ben Hamouda, S., Nguyen, Q. T., Langevin, D., & Roudesli, S. (2010). Poly (vinylalcohol)/poly (ethyleneglycol)/poly (ethyleneimine) blend membranes-structure and CO_2 facilitated transport. *Comptes Rendus Chimie, 13*(3), 372-379.

Bhavsar, R. S., Kumbharkar, S. C., & Kharul, U. K. (2012a). Polymeric ionic liquids (PILs): effect of anion variation on their CO_2 sorption. *Journal of Membrane Science, 389*, 305-315.

Bhavsar, R. S., Kumbharkar, S. C., & Kharul, U. K. (2012b). Polymeric ionic liquids (PILs): Effect of anion variation on their CO_2 sorption. *Journal of Membrane Science, 389*, 305-315.

Blanchard, L. A., Hancu, D., Beckman, E. J., & Brennecke, J. F. (1999). Green processing using ionic liquids and CO_2. *Nature, 399*(6731), 28-29.

Blasig, A., Tang, J., Hu, X., Shen, Y., & Radosz, M. (2007a). Magnetic suspension balance study of carbon dioxide solubility in ammonium-based polymerized ionic liquids: poly (p-vinylbenzyltrimethyl ammonium tetrafluoroborate) and poly ([2-(methacryloyloxy) ethyl] trimethyl ammonium tetrafluoroborate). *Fluid phase equilibria, 256*(1), 75-80.

Blasig, A., Tang, J., Hu, X., Shen, Y., & Radosz, M. (2007b). Magnetic suspension balance study of carbon dioxide solubility in ammonium-based polymerized ionic liquids: poly (p-vinylbenzyltrimethyl ammonium tetrafluoroborate) and poly ([2-(methacryloyloxy) ethyl] trimethyl ammonium tetrafluoroborate). *Fluid phase equilibria, 256*(1-2), 75-80.

Brunetti, A., Scura, F., Barbieri, G., & Drioli, E. (2010). Membrane technologies for CO_2 separation. *Journal of Membrane Science, 359*(1), 115-125.

Budzien, J. L., McCoy, J. D., Weinkauf, D. H., LaViolette, R. A., & Peterson, E. S. (1998). Solubility of gases in amorphous polyethylene. *Macromolecules, 31*(10), 3368-3371.

Cadena, C., Anthony, J. L., Shah, J. K., Morrow, T. I., Brennecke, J. F., & Maginn, E. J. (2004). Why is CO_2 so soluble in imidazolium-based ionic liquids? *Journal of the American Chemical Society, 126*(16), 5300-5308.

Camper, D., Bara, J. E., Gin, D. L., & Noble, R. D. (2008). Room-temperature ionic liquid− amine solutions: Tunable solvents for efficient and reversible capture of CO2. *Industrial & engineering chemistry research, 47*(21), 8496-8498.

Camper, D., Becker, C., Koval, C., & Noble, R. (2006). Diffusion and solubility measurements in room temperature ionic liquids. *Industrial & Engineering Chemistry Research, 45*(1), 445-450.

Car, A., Stropnik, C., Yave, W., & Peinemann, K.-V. (2008). PEG modified poly(amide-b-ethylene oxide) membranes for CO2 separation. *Journal of Membrane Science, 307*(1), 88-95. doi: https://doi.org/10.1016/j.memsci.2007.09.023

Carlisle, T. K., Bara, J. E., Lafrate, A. L., Gin, D. L., & Noble, R. D. (2010). Main-chain imidazolium polymer membranes for CO_2 separations: An initial study of a new ionic liquid-inspired platform. *Journal of Membrane Science, 359*(1), 37-43.

Carlisle, T. K., Nicodemus, G. D., Gin, D. L., & Noble, R. D. (2012). CO_2 light gas separation performance of cross-linked poly (vinylimidazolium) gel membranes as a function of ionic liquid loading and cross-linker content. *Journal of Membrane Science, 397*, 24-37.

Chakraborty, A. K., Astarita, G., & Bischoff, K. B. (1986). CO_2absorption in aqueous solutions of hindered amines. *Chemical Engineering Science, 41*(4), 997-1003. doi: https://doi.org/10.1016/0009-2509(86)87185-8

Change, I. P. o. C. (2015). *Climate change 2014: mitigation of climate change* (Vol. 3): Cambridge University Press.

Chen, H., Choi, J.-H., Salas-de la Cruz, D., Winey, K. I., & Elabd, Y. A. (2009). Polymerized ionic liquids: the effect of random copolymer composition on ion conduction. *Macromolecules, 42*(13), 4809-4816.

Chi, W. S., Hong, S. U., Jung, B., Kang, S. W., Kang, Y. S., & Kim, J. H. (2013). Synthesis, structure and gas permeation of polymerized ionic liquid graft copolymer membranes. *Journal of Membrane Science, 443*, 54-61.

Choi, W.-J., Seo, J.-B., Jang, S.-Y., Jung, J.-H., & Oh, K.-J. (2009). Removal characteristics of CO_2 using aqueous MEA/AMP solutions in the absorption and regeneration process. *Journal of Environmental Sciences, 21*(7), 907-913.

Eliassi, A., Modarress, H., & Mansoori, G. A. (1998). Densities of poly (ethylene glycol)+ water mixtures in the 298.15− 328.15 K temperature range. *Journal of Chemical & Engineering Data, 43*(5), 719-721.

Fahrenkamp-Uppenbrink, J. (2015). Whither carbon capture and storage? *Science, 349*(6248), 599-600.

Farzaneh, H., McLellan, B., & Ishihara, K. N. (2016). Toward a CO_2zero emissions energy system in the Middle East region. *International Journal of Green Energy, 13*(7), 682-694.

Feng, S., Ren, J., Li, Z., Li, H., Hua, K., Li, X., & Deng, M. (2013). Poly (amide-12-b-ethylene oxide)/glycerol triacetate blend membranes for CO_2 separation. *International Journal of Greenhouse Gas Control, 19*, 41-48.

Feng, Z., Cheng-Gang, F., You-Ting, W., Yuan-Tao, W., Ai-Min, L., & Zhi-Bing, Z. (2010). Absorption of CO_2 in the aqueous solutions of functionalized ionic liquids and MDEA. *Chemical Engineering Journal, 160*(2), 691-697.

Filburn, T., Helble, J., & Weiss, R. (2005). Development of supported ethanolamines and modified ethanolamines for CO_2 capture. *Industrial & Engineering Chemistry Research, 44*(5), 1542-1546.

Freeman, B. D. (1999). Basis of Permeability/Selectivity Tradeoff Relations in Polymeric Gas Separation Membranes. *Macromolecules, 32*(2), 375-380. doi: 10.1021/ma9814548

Fu, S., Sanders, E. S., Kulkarni, S. S., Wenz, G. B., & Koros, W. J. (2015). Temperature dependence of gas transport and sorption in carbon molecular sieve membranes derived from four 6FDA based polyimides: Entropic selectivity evaluation. *Carbon, 95*, 995-1006.

González-Álvarez, J., Blanco-Gomis, D., Arias-Abrodo, P., Díaz-Llorente, D., Ríos-Lombardía, N., Busto, E., . . . Gutiérrez-Álvarez, M. D. (2012). Polymeric imidazolium ionic liquids as valuable stationary phases in gas chromatography: Chemical synthesis and full characterization. *Analytica chimica acta, 721*, 173-181.

González-Álvarez, J., Blanco-Gomis, D., Arias-Abrodo, P., Pello-Palma, J., Ríos-Lombardía, N., Busto, E., . . . Gutiérrez-Álvarez, M. D. (2013). Analysis of beer volatiles by polymeric imidazolium-solid phase microextraction coatings: Synthesis and characterization of polymeric imidazolium ionic liquids. *Journal of Chromatography A, 1305*, 35-40.

Gupta, M., Coyle, I., & Thambimuthu, K. (2003). *CO_2 capture technologies and opportunities in Canada.* Paper presented at the 1st Canadian CC&S Technology Roadmap Workshop.

Gurkan, B. E., de la Fuente, J. C., Mindrup, E. M., Ficke, L. E., Goodrich, B. F., Price, E. A., . . . Brennecke, J. F. (2010). Equimolar CO_2 absorption by anion-functionalized ionic liquids. *Journal of the American Chemical Society, 132*(7), 2116-2117.

Hagewiesche, D. P., Ashour, S. S., Al-Ghawas, H. A., & Sandall, O. C. (1995). Absorption of carbon dioxide into aqueous blends of monoethanolamine and N-methyldiethanolamine. *Chemical Engineering Science, 50*(7), 1071-1079.

Hall, J. E. (2015). *Guyton and Hall textbook of medical physiology e-Book*: Elsevier Health Sciences.

Han, F., Zhang, J., Chen, G., & Wei, X. (2008). Density, viscosity, and excess properties for aqueous poly (ethylene glycol) solutions from (298.15 to 323.15) K. *Journal of Chemical & Engineering Data, 53*(11), 2598-2601.

Hasib-ur-Rahman, M., Siaj, M., & Larachi, F. (2010a). Ionic liquids for CO_2 capture—development and progress. *Chemical Engineering and Processing: Process Intensification, 49*(4), 313-322.

Hasib-ur-Rahman, M., Siaj, M., & Larachi, F. (2010b). Ionic liquids for CO_2 capture—Development and progress. *Chemical Engineering and Processing: Process Intensification, 49*(4), 313-322.

Hasib-ur-Rahman, M., Siaj, M., & Larachi, F. (2012). CO_2 capture in alkanolamine/room-temperature ionic liquid emulsions: A viable approach with carbamate crystallization and curbed corrosion behavior. *International Journal of Greenhouse Gas Control, 6*, 246-252.

Hirao, M., Ito, K., & Ohno, H. (2000a). Preparation and polymerization of new organic molten salts; N-alkylimidazolium salt derivatives. *Electrochimica Acta, 45*(8-9), 1291-1294.

Hirao, M., Ito, K., & Ohno, H. (2000b). Preparation and polymerization of new organic molten salts; N-alkylimidazolium salt derivatives. *Electrochimica Acta, 45*(8), 1291-1294.

Hong, S. U., Park, D., Ko, Y., & Baek, I. (2009). Polymer-ionic liquid gels for enhanced gas transport. *Chemical Communications*(46), 7227-7229.

Hosseini, S. S., Teoh, M. M., & Chung, T. S. (2008). Hydrogen separation and purification in membranes of miscible polymer blends with interpenetration networks. *Polymer, 49*(6), 1594-1603. doi: http://dx.doi.org/10.1016/j.polymer.2008.01.052

Hou, Y., & Baltus, R. E. (2007). Experimental measurement of the solubility and diffusivity of CO2 in room-temperature ionic liquids using a transient thin-liquid-film method. *Industrial & Engineering Chemistry Research, 46*(24), 8166-8175.

Hu, X., Tang, J., Blasig, A., Shen, Y., & Radosz, M. (2006a). CO_2 permeability, diffusivity and solubility in polyethylene glycol-grafted polyionic membranes and their CO_2 selectivity relative to methane and nitrogen. *Journal of Membrane Science, 281*(1-2), 130-138.

Hu, X., Tang, J., Blasig, A., Shen, Y., & Radosz, M. (2006b). CO_2 permeability, diffusivity and solubility in polyethylene glycol-grafted polyionic membranes and their CO_2 selectivity relative to methane and nitrogen. *Journal of Membrane Science, 281*(1), 130-138.

Hudiono, Y. C., Carlisle, T. K., LaFrate, A. L., Gin, D. L., & Noble, R. D. (2011). Novel mixed matrix membranes based on polymerizable room-temperature ionic liquids

and SAPO-34 particles to improve CO_2 separation. *Journal of Membrane Science, 370*(1), 141-148.

Isik, M., Gracia, R., Kollnus, L. C., Tomé, L. C., Marrucho, I. M., & Mecerreyes, D. (2013). Cholinium-based poly (ionic liquid) s: synthesis, characterization, and application as biocompatible ion gels and cellulose coatings. *ACS Macro Letters, 2*(11), 975-979.

Jansen, J. C., Friess, K., Clarizia, G., Schauer, J., & Izak, P. (2010). High ionic liquid content polymeric gel membranes: preparation and performance. *Macromolecules, 44*(1), 39-45.

Kabalka, G. W., Varma, M., Varma, R. S., Srivastava, P. C., & Knapp Jr, F. F. (1986). The tosylation of alcohols. *The Journal of Organic Chemistry, 51*(12), 2386-2388.

Kato, S., Tsujita, Y., Yoshimizu, H., Kinoshita, T., & Higgins, J. (1997). Characterization and CO_2 sorption behaviour of polystyrene/polycarbonate blend system. *Polymer, 38*(11), 2807-2811.

Kim, I., Hoff, K. A., Hessen, E. T., Haug-Warberg, T., & Svendsen, H. F. (2009). Enthalpy of absorption of CO_2 with alkanolamine solutions predicted from reaction equilibrium constants. *Chemical Engineering Science, 64*(9), 2027-2038.

Kim, I., Hoff, K. A., & Mejdell, T. (2014). Heat of absorption of CO_2 with aqueous solutions of MEA: new experimental data. *Energy Procedia, 63*, 1446-1455.

Kumbharkar, S. C., Bhavsar, R. S., & Kharul, U. K. (2014). Film forming polymeric ionic liquids (PILs) based on polybenzimidazoles for CO_2 separation. *RSC Advances, 4*(9), 4500-4503.

Leung, D. Y. C., Caramanna, G., & Maroto-Valer, M. M. (2014). An overview of current status of carbon dioxide capture and storage technologies. *Renewable and Sustainable Energy Reviews, 39*(Supplement C), 426-443. doi: https://doi.org/10.1016/j.rser.2014.07.093

Li, J.-R., Ma, Y., McCarthy, M. C., Sculley, J., Yu, J., Jeong, H.-K., . . . Zhou, H.-C. (2011). Carbon dioxide capture-related gas adsorption and separation in metal-organic frameworks. *Coordination Chemistry Reviews, 255*(15), 1791-1823.

Li, J., Ye, Y., Chen, L., & Qi, Z. (2012). Solubilities of CO2 in Poly(ethylene glycols) from (303.15 to 333.15) K. *Journal of Chemical & Engineering Data, 57*(2), 610-616. doi: 10.1021/je201197m

Li, P., Ge, B., Zhang, S., Chen, S., Zhang, Q., & Zhao, Y. (2008). CO_2 capture by polyethylenimine-modified fibrous adsorbent. *Langmuir, 24*(13), 6567-6574.

Li, P., Paul, D., & Chung, T.-S. (2012a). High performance membranes based on ionic liquid polymers for CO_2 separation from the flue gas. *Green Chemistry, 14*(4), 1052-1063.

Li, P., Paul, D., & Chung, T.-S. (2012b). High performance membranes based on ionic liquid polymers for CO_2 separation from the flue gas. *Green Chemistry, 14*(4), 1052-1063.

Li, P., Pramoda, K., & Chung, T.-S. (2011). CO_2 separation from flue gas using polyvinyl-(room temperature ionic liquid)–room temperature ionic liquid composite membranes. *Industrial & Engineering Chemistry Research, 50*(15), 9344-9353.

Li, X., Hou, M., Zhang, Z., Han, B., Yang, G., Wang, X., & Zou, L. (2008). Absorption of CO_2 by ionic liquid/polyethylene glycol mixture and the thermodynamic parameters. *Green Chemistry, 10*(8), 879-884.

Li, Y., Yang, L., Zhu, X., Hu, J., & Liu, H. (2017). Post-synthesis modification of porous organic polymers with amine: a task-specific microenvironment for CO_2 capture. *International Journal of Coal Science & Technology, 4*(1), 50-59.

Liang, Z., Fu, K., Idem, R., & Tontiwachwuthikul, P. (2016). Review on current advances, future challenges and consideration issues for post-combustion CO_2 capture using amine-based absorbents. *Chinese Journal of Chemical Engineering, 24*(2), 278-288.

Liang, Z. H., Rongwong, W., Liu, H., Fu, K., Gao, H., Cao, F., . . . Sumon, K. (2015). Recent progress and new developments in post-combustion carbon-capture technology with amine based solvents. *International Journal of Greenhouse Gas Control, 40*, 26-54.

Low, W., & White, E. (1943). A Study of Polysaccharide Hydroxylation Using p-Toluenesulfonyl Chloride and Triphenylchloromethane1a. *Journal of the American Chemical Society, 65*(12), 2430-2432.

Lu, J., Yan, F., & Texter, J. (2009). Advanced applications of ionic liquids in polymer science. *Progress in Polymer Science, 34*(5), 431-448.

Luis, P., Van Gerven, T., & Van der Bruggen, B. (2012). Recent developments in membrane-based technologies for CO_2 capture. *Progress in Energy and Combustion Science, 38*(3), 419-448.

Lutz, J. F. (2008). Polymerization of oligo (ethylene glycol)(meth) acrylates: toward new generations of smart biocompatible materials. *Journal of Polymer Science Part A: Polymer Chemistry, 46*(11), 3459-3470.

Magalhaes, T., Aquino, A., Dalla Vecchia, F., Bernard, F., Seferin, M., Menezes, S., . . . Einloft, S. (2014). Syntheses and characterization of new poly (ionic liquid) s designed for CO_2 capture. *RSC Advances, 4*(35), 18164-18170.

Marcilla, R., Blazquez, J. A., Fernandez, R., Grande, H., Pomposo, J. A., & Mecerreyes, D. (2005). Synthesis of novel polycations using the chemistry of ionic liquids. *Macromolecular Chemistry and Physics, 206*(2), 299-304.

Meisen, A., & Shuai, X. (1997). Research and development issues in CO_2 capture. *Energy Conversion and Management, 38*, S37-S42.

Mirzaei, S., Shamiri, A., & Aroua, M. K. (2015). A review of different solvents, mass transfer, and hydrodynamics for postcombustion CO_2 capture. *Reviews in Chemical Engineering, 31*(6), 521-561.

Mogri, Z., & Paul, D. (2001). Gas sorption and transport in poly (alkyl (meth) acrylate) s. II. Sorption and diffusion properties. *Polymer, 42*(18), 7781-7789.

Mondal, M. K., Balsora, H. K., & Varshney, P. (2012). Progress and trends in CO_2 capture/separation technologies: A review. *Energy, 46*(1), 431-441.

Olivier, J., Bouwman, A., Van der Maas, C., & Berdowski, J. (1994). Emission database for global atmospheric research (EDGAR). *Environmental Monitoring and Assessment, 31*(1-2), 93-106.

Orme, C. J., Klaehn, J. R., Harrup, M. K., Luther, T. A., Peterson, E. S., & Stewart, F. F. (2006). Gas permeability in rubbery polyphosphazene membranes. *Journal of Membrane Science, 280*(1), 175-184.

Ouchi, M., Inoue, Y., Liu, Y., Nagamune, S., Nakamura, S., Wada, K., & Hakushi, T. (1990). Convenient and efficient tosylation of oligoethylene glycols and the related alcohols in tetrahydrofuran–water in the presence of sodium hydroxide. *Bulletin of the Chemical Society of Japan, 63*(4), 1260-1262.

Park, J.-y., Yoon, S. J., Lee, H., Yoon, J.-H., Shim, J.-G., Lee, J. K., . . . Eum, H.-M. (2002). Density, Viscosity, and Solubility of CO2 in Aqueous Solutions of 2-Amino-2-hydroxymethyl-1,3-propanediol. *Journal of Chemical & Engineering Data, 47*(4), 970-973. doi: 10.1021/je0200012

Petersen, M. A., Yin, L., Kokkoli, E., & Hillmyer, M. A. (2010). Synthesis and characterization of reactive PEO–PMCL polymersomes. *Polymer Chemistry, 1*(8), 1281-1290.

Petkovic, M., Seddon, K. R., Rebelo, L. P. N., & Pereira, C. S. (2011). Ionic liquids: a pathway to environmental acceptability. *Chemical Society Reviews, 40*(3), 1383-1403.

Pinto, A. M., Rodríguez, H., Arce, A., & Soto, A. (2013). Carbon dioxide absorption in the ionic liquid 1-ethylpyridinium ethylsulfate and in its mixtures with another ionic liquid. *International Journal of Greenhouse Gas Control, 18*, 296-304.

Pont, A.-L., Marcilla, R., De Meatza, I., Grande, H., & Mecerreyes, D. (2009). Pyrrolidinium-based polymeric ionic liquids as mechanically and electrochemically stable polymer electrolytes. *Journal of Power Sources, 188*(2), 558-563.

Raeissi, S., & Peters, C. J. (2008). Carbon dioxide solubility in the homologous 1-alkyl-3-methylimidazolium bis (trifluoromethylsulfonyl) imide family†. *Journal of Chemical & Engineering Data, 54*(2), 382-386.

Reijerkerk, S. R., Knoef, M. H., Nijmeijer, K., & Wessling, M. (2010). Poly (ethylene glycol) and poly (dimethyl siloxane): Combining their advantages into efficient CO_2 gas separation membranes. *Journal of Membrane Science, 352*(1), 126-135.

Robeson, L. M. (1991). Correlation of separation factor versus permeability for polymeric membranes. *Journal of Membrane Science, 62*(2), 165-185.

Robeson, L. M. (2008). The upper bound revisited. *Journal of Membrane Science, 320*(1-2), 390-400.

Robinson, K., McCluskey, A., & Attalla, M. (2011). The effect molecular structural variations has on the CO_2 absorption characteristics of heterocyclic amines. *Energy Procedia, 4*, 224-231.

Rochelle, G., Bishnoi, S., Chi, S., Dang, H., & Santos, J. (2001). Research needs for CO_2 capture from flue gas by aqueous absorption. *Stripping, US Department of Energy, Pittsburgh, PA, USA*.

Sadeghpour, M., Yusoff, R., & Aroua, M. K. Polymeric ionic liquids (PILs) for CO.

Salamone, J., Israel, S., Taylor, P., & Snider, B. (1973). Synthesis and homopolymerization studies of vinylimidazolium salts. *Polymer, 14*(12), 639-644.

Samadi, A., Kemmerlin, R. K., & Husson, S. M. (2010). Polymerized ionic liquid sorbents for CO_2 separation. *Energy & Fuels, 24*(10), 5797-5804.

Samanta, A., & Bandyopadhyay, S. S. (2009). Absorption of carbon dioxide into aqueous solutions of piperazine activated 2-amino-2-methyl-1-propanol. *Chemical Engineering Science, 64*(6), 1185-1194. doi: https://doi.org/10.1016/j.ces.2008.10.049

Sánchez, L. G., Meindersma, G., & De Haan, A. (2007). Solvent properties of functionalized ionic liquids for CO_2 absorption. *Chemical Engineering Research and Design, 85*(1), 31-39.

Scovazzo, P. (2009). Determination of the upper limits, benchmarks, and critical properties for gas separations using stabilized room temperature ionic liquid membranes (SILMs) for the purpose of guiding future research. *Journal of Membrane Science, 343*(1-2), 199-211.

Sema, T., Naami, A., Fu, K., Edali, M., Liu, H., Shi, H., . . . Tontiwachwuthikul, P. (2012). Comprehensive mass transfer and reaction kinetics studies of CO_2 absorption into aqueous solutions of blended MDEA–MEA. *Chemical Engineering Journal, 209*, 501-512.

Sigma Aldrich (2018) Polyethylene glycol price were retrieved from https://www.sigmaaldrich.com/malaysia.html dated 21 April 2018.

Shaplov, A. S., Lozinskaya, E. I., Ponkratov, D. O., Malyshkina, I. A., Vidal, F., Aubert, P.-H., . . . Wandrey, C. (2011). Bis (trifluoromethylsulfonyl) amide based "polymeric ionic liquids": Synthesis, purification and peculiarities of structure–properties relationships. *Electrochimica Acta, 57*, 74-90.

Shaplov, A. S., Marcilla, R., & Mecerreyes, D. (2015). Recent Advances in Innovative Polymer Electrolytes based on Poly(ionic liquid)s. *Electrochimica Acta, 175*, 18-34. doi: http://dx.doi.org/10.1016/j.electacta.2015.03.038

Simons, K. (2010). *Membrane technologies for CO_2 capture*: University of Twente.

Simons, K., Nijmeijer, K., Bara, J. E., Noble, R. D., & Wessling, M. (2010). How do polymerized room-temperature ionic liquid membranes plasticize during high pressure CO_2 permeation? *Journal of Membrane Science, 360*(1-2), 202-209.

Soosaiprakasam, I. R., & Veawab, A. (2008). Corrosion and polarization behavior of carbon steel in MEA-based CO_2 capture process. *International Journal of Greenhouse Gas Control, 2*(4), 553-562.

Su, F., Lu, C., Kuo, S.-C., & Zeng, W. (2010). Adsorption of CO_2 on amine-functionalized Y-type zeolites. *Energy & Fuels, 24*(2), 1441-1448.

Supasitmongkol, S., & Styring, P. (2010). High CO_2 solubility in ionic liquids and a tetraalkylammonium-based poly (ionic liquid). *Energy & Environmental Science, 3*(12), 1961-1972.

Swaidan, R., Ghanem, B., & Pinnau, I. (2015a). Fine-tuned intrinsically ultramicroporous polymers redefine the permeability/selectivity upper bounds of membrane-based air and hydrogen separations. *ACS Macro Letters, 4*(9), 947-951.

Swaidan, R., Ghanem, B., & Pinnau, I. (2015b). Fine-tuned intrinsically ultramicroporous polymers redefine the permeability/selectivity upper bounds of membrane-based air and hydrogen separations: ACS Publications.

Tang, H., Tang, J., Ding, S., Radosz, M., & Shen, Y. (2005). Atom transfer radical polymerization of styrenic ionic liquid monomers and carbon dioxide absorption of the polymerized ionic liquids. *Journal of Polymer Science Part A: Polymer Chemistry, 43*(7), 1432-1443.

Tang, J., Radosz, M., & Shen, Y. (2008). Poly (ionic liquid) s as optically transparent microwave-absorbing materials. *Macromolecules, 41*(2), 493-496.

Tang, J., Shen, Y., Radosz, M., & Sun, W. (2009). Isothermal carbon dioxide sorption in poly (ionic liquid) s. *Industrial & engineering chemistry research, 48*(20), 9113-9118.

Tang, J., Sun, W., Tang, H., Radosz, M., & Shen, Y. (2005). Enhanced CO_2 absorption of poly (ionic liquid) s. *Macromolecules, 38*(6), 2037-2039.

Tang, J., Tang, H., Sun, W., Plancher, H., Radosz, M., & Shen, Y. (2005a). Poly (ionic liquid) s: a new material with enhanced and fast CO_2 absorption. *Chem. Commun.*(26), 3325-3327.

Tang, J., Tang, H., Sun, W., Plancher, H., Radosz, M., & Shen, Y. (2005b). Poly (ionic liquid) s: a new material with enhanced and fast CO_2 absorption. *Chemical Communications*(26), 3325-3327.

Tang, J., Tang, H., Sun, W., Radosz, M., & Shen, Y. (2005a). Low-pressure CO_2 sorption in ammonium-based poly (ionic liquid) s. *Polymer, 46*(26), 12460-12467.

Tang, J., Tang, H., Sun, W., Radosz, M., & Shen, Y. (2005b). Low-pressure CO_2 sorption in ammonium-based poly (ionic liquid) s. *Polymer, 46*(26), 12460-12467.

Tang, J., Tang, H., Sun, W., Radosz, M., & Shen, Y. (2005c). Poly (ionic liquid) s as new materials for CO_2 absorption. *Journal of Polymer Science Part A: Polymer Chemistry, 43*(22), 5477-5489.

Tomé, L. C., Gouveia, A. S., Freire, C. S., Mecerreyes, D., & Marrucho, I. M. (2015). Polymeric ionic liquid-based membranes: Influence of polycation variation on gas transport and CO_2 selectivity properties. *Journal of Membrane Science, 486*, 40-48.

Tomé, L. C., Isik, M., Freire, C. S. R., Mecerreyes, D., & Marrucho, I. M. (2015). Novel pyrrolidinium-based polymeric ionic liquids with cyano counter-anions: High performance membrane materials for post-combustion CO_2 separation. *Journal of Membrane Science, 483*, 155-165. doi: http://dx.doi.org/10.1016/j.memsci.2015.02.020

Tomé, L. C., Mecerreyes, D., Freire, C. S., Rebelo, L. P. N., & Marrucho, I. M. (2013a). Pyrrolidinium-based polymeric ionic liquid materials: New perspectives for CO_2 separation membranes. *Journal of Membrane Science, 428*, 260-266.

Tomé, L. C., Mecerreyes, D., Freire, C. S., Rebelo, L. P. N., & Marrucho, I. M. (2013b). Pyrrolidinium-based polymeric ionic liquid materials: New perspectives for CO_2 separation membranes. *Journal of Membrane Science, 428*, 260-266.

Trivedi, S., Bhanot, C., & Pandey, S. (2010). Densities of {poly (ethylene glycol)+ water} over the temperature range (283.15 to 363.15) K. *The Journal of Chemical Thermodynamics, 42*(11), 1367-1371.

Uchytil, P., Schauer, J., Petrychkovych, R., Setnickova, K., & Suen, S. (2011). Ionic liquid membranes for carbon dioxide–methane separation. *Journal of Membrane Science, 383*(1), 262-271.

Wang, Y., Lang, X., & Fan, S. (2013). Hydrate capture CO 2 from shifted synthesis gas, flue gas and sour natural gas or biogas. *Journal of Energy Chemistry, 22*(1), 39-47.

Wappel, D., Gronald, G., Kalb, R., & Draxler, J. (2010). Ionic liquids for post-combustion CO_2 absorption. *International Journal of Greenhouse Gas Control, 4*(3), 486-494.

Weber, C., Czaplewska, J. A., Baumgaertel, A., Altuntas, E., Gottschaldt, M., Hoogenboom, R., & Schubert, U. S. (2012). A sugar decorated macromolecular bottle brush by carbohydrate-initiated cationic ring-opening polymerization. *Macromolecules, 45*(1), 46-55.

Wilke, A., Yuan, J., Antonietti, M., & Weber, J. (2012). Enhanced carbon dioxide adsorption by a mesoporous poly (ionic liquid). *ACS Macro Letters, 1*(8), 1028-1031.

Xiong, Y., Wang, Y., Wang, H., & Wang, R. (2011). A facile one-step synthesis to ionic liquid-based cross-linked polymeric nanoparticles and their application for CO_2 fixation. *Polymer Chemistry, 2*(10), 2306-2315.

Xu, X., Song, C., Andresen, J. M., Miller, B. G., & Scaroni, A. W. (2002). Novel polyethylenimine-modified mesoporous molecular sieve of MCM-41 type as high-capacity adsorbent for CO_2 capture. *Energy & Fuels, 16*(6), 1463-1469.

Yang, H., Xu, Z., Fan, M., Gupta, R., Slimane, R. B., Bland, A. E., & Wright, I. (2008). Progress in carbon dioxide separation and capture: A review. *Journal of Environmental Sciences, 20*(1), 14-27. doi: https://doi.org/10.1016/S1001-0742(08)60002-9

Yeh, J. T., Pennline, H. W., Resnik, K. P., & Rygle, K. (2004). *Absorption and regeneration studies for CO_2 capture by aqueous ammonia.* Paper presented at the Third Annual Conference on Carbon Capture & Sequestration, Alexndria, VA.

Yu, G., Li, Q., Li, N., Man, Z., Pu, C., Asumana, C., & Chen, X. (2014). Synthesis of new crosslinked porous ammonium-based poly (ionic liquid) and application in CO2 adsorption. *Polymer Engineering & Science, 54*(1), 59-63.

Yu, X., Yang, J., Yan, J., & Tu, S. T. Membrane Technologies for CO_2 Capture. *Handbook of Clean Energy Systems*.

Yuan, J., & Antonietti, M. (2011). Poly (ionic liquid) s: Polymers expanding classical property profiles. *Polymer, 52*(7), 1469-1482.

Yuan, J., Mecerreyes, D., & Antonietti, M. (2013). Poly (ionic liquid) s: An update. *Progress in Polymer Science, 38*(7), 1009-1036.

Zhang, G.-J., Zhou, X., Zang, X.-H., Li, Z., Wang, C., & Wang, Z. (2014). Original article Analysis of nitrobenzene compounds in water and soil samples by graphene composite-based solid-phase microextraction coupled with gas chromatography-mass spectrometry. *Chinese Chemical Letters*.

Zhang, L., Qu, R., Sha, Y., Wang, X., & Yang, L. (2015). Membrane gas absorption for CO_2 capture from flue gas containing fine particles and gaseous contaminants. *International Journal of Greenhouse Gas Control, 33*, 10-17.

Zhang, Y., Sunarso, J., Liu, S., & Wang, R. (2013). Current status and development of membranes for CO_2/CH_4 separation: A review. *International Journal of Greenhouse Gas Control, 12*, 84-107.

Zhao, Q., & Anderson, J. L. (2010). Selective extraction of CO_2 from simulated flue gas using polymeric ionic liquid sorbent coatings in solid-phase microextraction gas chromatography. *Journal of Chromatography A, 1217*(27), 4517-4522.

ZHAO, Z., DONG, H., & ZHANG, X. (2012). The Research Progress of CO_2 Capture with Ionic Liquids. *Chinese Journal of Chemical Engineering, 20*(1), 120-129.

Zhijun, Z., Haifeng, D., & ZHANG, X. (2012). The research progress of CO2 capture with ionic liquids. *Chinese Journal of Chemical Engineering, 20*(1), 120-129.

Zhu, D., Fang, M., Lv, Z., Wang, Z., & Luo, Z. (2011). Selection of blended solvents for CO_2 absorption from coal-fired flue gas. Part 1: Monoethanolamine (MEA)-based solvents. *Energy & Fuels, 26*(1), 147-153.

Zulfiqar, S., Sarwar, M. I., & Mecerreyes, D. (2015). Polymeric ionic liquids for CO_2 capture and separation: potential, progress and challenges. *Polymer Chemistry, 6*(36), 6435-6451. doi: 10.1039/C5PY00842E